The *Skyscraper Revolution*: Global Economic Development and Land Savings*

Gabriel M. Ahlfeldt † Nathaniel Baum-Snow ‡ Remi Jedwab §

December 21, 2024

Abstract

Tall buildings make up over 20% of real estate by value in the world's largest cities. Nonetheless, many governments constrain tall building construction, hindering urbanization and growth. Quantification for all cities worldwide using a canonical land use model disciplined with reduced form elasticity estimates indicates that eliminating existing height constraints would generate a global welfare gain of 6.4%. Aggregate land values would decline by 6.0%, incentivizing landowners to support height restrictions. Estimated elasticities of city population and built area with respect to aggregate city building heights are 0.13 and -0.16 in developing economies, reinforcing the quantitative evidence that tall buildings facilitate urban growth and compactness. Interactions between static demand factors and the geography of bedrock isolate 1975-2015 tall building construction driven by technology-induced reductions in the cost of height.

Key words: Urban Density; International Buildings Heights; Skyscrapers; Tall Buildings; Sustainable Urbanization; City Growth; Commercial Real Estate; Housing Supply; Urban Sprawl; Land Savings; Housing Affordability; Geographical Constraints; Environment

JEL: R11, R12, R14, R31, R33, O18, O13

*We thank David Albouy, Milena Almagro, Jason Barr, Adrien Bilal, Jan Brueckner, Filipe Campante, Donald Davis, Klaus Desmet, Rebecca Diamond, Jonathan Dingel, Gilles Duranton, Fernando Ferreira, Edward Glaeser, Marco Gonzalez-Navarro, Gabriel Kreindler, Jessie Handbury, Mariaflavia Harari, Matthew Kahn, Jeffrey Lin, John Morrow, David Nagy, Elias Papaioannou, Charly Porcher, Daniel Ramos-Menchelli, Lindsay Relihan, Tanner Regan, Frederic Robert-Nicoud, Jorge De la Roca, Stephen L. Ross, Alexander Rothenberg, Nick Tsivanidis, Matthew Turner, Tony Venables, C. Luke Watson, and numerous seminar audiences for helpful comments.

†London School of Economics and Humboldt University in Berlin. Email: g.ahlfeldt@lse.ac.uk

‡University of Toronto. Email: nate.baum.snow@rotman.utoronto.ca

§George Washington University and NYU Marron Institute of Urban Management. Email: jedwab@gwu.edu

1 Introduction

Chicago's ten-storey 42-meter tall Home Insurance Building, built in 1885 and often called the world's first "skyscraper" (Schleier, 1986), was an early example of the use of technologies that would prove to transform cities around the world. Since then, continued technological improvements that have lowered the cost of building tall have facilitated the construction of the more than 16,000 km of buildings of over 55 meters (∼13-14 floors) in cities worldwide, or about four times the Euclidean distance between Los Angeles and New York City. Most of this construction has occurred since 1975 for residential use, and much in developing economies. With the equivalent of almost 43,000 Empire State Buildings, the stock of tall buildings worldwide holds an aggregate asset value of more than 15 trillion dollars. Indeed, a look at many global cities today leaves no doubt that the *Skyscraper Revolution* has been transformative (Glaeser, 2012). The mean aggregate height of tall buildings across cities of over 5 million inhabitants is greater than 100 km. In cities of over 1 million people, tall buildings account for ∼10% of the physical stock and almost 20% of aggregate construction costs for existing structures.[1]

With structural change out of agriculture, many cities in the developing world face strong urbanization pressures and high demand for density (Bryan, Glaeser and Tsivanidis, 2020). Moreover, many developed economies face a housing crisis that is exacerbated by supply constraints (Knoll et al., 2017; Glaeser and Gyourko, 2018). Some nations and cities are laissez-faire about vertical development, or even "invest" in their skyline through direct subsidy, public-private partnerships, public land donations, or tax incentives.[2] Others restrict vertical development through floor area ratio caps, height limits, and land use planning restrictions (Brueckner et al., 2017). Given the considerable amount of government involvement in the tall building sector, it is essential to study the consequences of vertical development.

This paper evaluates the economic benefits of the skyscraper revolution and quantifies the economic costs of height restrictions that may have held back some of its potential transformative effects. In doing so, we depart from a literature that views tall buildings as a mere consequence of urbanization. Instead, we shed new light on the role tall buildings can play as catalysts of urbanization owing to ongoing technological progress that reduces the cost of building tall. Cities that expand vertically can accommodate more workers in more productive locations, fostering structural change, increasing output, and enhancing welfare. Land use regulations that prevent economically viable vertical growth may thus lead to spatial misallocation (Hsieh and Moretti, 2019) and delay economic development (Gechter and Tsivanidis, 2023; Anagol et al., 2024).

We quantify the benefits associated with 1975-2015 reductions in the "cost of height", the elasticity of tall building construction cost per unit of floor area with respect to height. Our empirical analysis recovers causal effects of the component of 1975-2015 tall building construction driven by reductions in the cost of height on urban population growth, urban form, and land use. Innovations to the tall building sector in the 1960s and 1970s, including the development of reinforced concrete, computer aided design and engineering, and improved crane technologies,

[1] Data on building volumes indicate that fractions of the building stock in buildings over 55 m tall are 80% in Hong Kong, 58% Seoul, 39% in Singapore, 35% in Mumbai, 32% in Taipei, 30% in Moscow, 29% in Dubai, 27% in Kuala Lumpur, 26% in Sao Paulo, 22% in Hanoi, 17% in Manila, 16% in Bogota, and 12% in New York.

[2] One World Trade Center cost $3.9 billion, one-third of which was covered by New York's Port Authority and the State of New York. The Clock Towers (Saudi Arabia), the Petronas Towers (Malaysia), the Iconic Tower (Egypt), the AD Plaza (Kazakhstan), the Burj Khalifa (UAE), Tour F (Ivory Coast) and Taipei 101 (Taiwan) cost governments 2.2%, 2.0%, 0.8%, 0.7%, 0.6%, 0.6% and 0.5% of national GDP, respectively.

reduced tall building construction costs in developing economies in particular, thereby facilitating their "Skyscraper Revolution". Using data from 11,257 urban agglomerations worldwide in developing economies, we find average elasticities of city population and built-up land area to total city tall building heights of 0.13 and -0.16, respectively. For cities of 1 million inhabitants, these map to semi-elasticities of population and built area with respect to the cost of height of -0.19 and 0.24, respectively, with magnitudes increasing in city population. Remarkably, we find similar population effects in developed countries for the historical 1850 to 1975 period.

To measure the realized and potential benefits of the skyscraper revolution, we confront a quantitative urban land use model with reduced-form moments from the data. As in the standard urban model (Brueckner, 1987), we assume a monocentric city structure with equilibrium rent and density falling in distance from an exogenous historic center. Unlike in the standard model, we allow for endogenous land use (Duranton and Puga, 2015) and wages, which are influenced by imperfectly elastic labor supply to the city. Residential and commercial real estate developers face costs that are convex in building height and depend on city characteristics. Each city's rural hinterland hosts potential in-migrants, with migration responses depending on idiosyncratic preference heterogeneity between rural and urban locations and the stock of potential migrants, with the heterogeneity parameter estimated by simulated method of moments.

Reductions in the cost of height increase welfare by allowing cities to accommodate greater populations in denser residential *and* work locations. Productivity and wages rise through agglomeration forces. Conditional on urban population, rents decline because of lower construction costs, though with sufficiently large endogenous population responses, rents may increase. Commuting costs decline because of greater urban compactness.

For each city worldwide, we quantify the model to rationalize the observed 2015 population conditional on local construction costs and a measure of the restrictiveness of height constraints. Calibration to an equilibrium constrained by height restrictions is novel to the literature and allows us to predict the aggregate effects of removing existing height constraints on labor and land markets. We infer height restrictions by comparing each city's 2015 aggregate height of tall buildings to that for the 95^{th} percentile city with similar observed characteristics. Counterfactual exercises indicate 5.3% greater average worker (consumer) welfare in developing economies in environments with no height restrictions relative to the 2015 equilibrium. Due to the positive net effects on real estate supply near city centers of relaxing height restrictions, cities become more compact. Increases in real wages, despite rent increases associated with population inflows and income growth, account for about half of the associated welfare gains. In contrast, banning existing buildings above 55 meters would reduce worker welfare by 1.8%. That is, absent negative height externalities, existing land use and height regulations mean that only about one-quarter of potential welfare gains from heights have been realized. Our analysis provides estimates against which the potential social and environmental costs of tall buildings can be compared.

Fully relaxing existing height constraints would reduce aggregate land values by 4.8% in developing economies, as higher central densities allow peripheral land to be taken out of urban use. Reducing height regulation redistributes welfare from land to labor. Landlords lose with the lower rents associated with the supply expansion that comes with new heights but workers gain more due to higher real wages and enhanced access to preferred locations. As in Ortalo-Magné and Prat (2014) and Duranton and Puga (2023), this result highlights incumbent landlords' incentives to enact land use restrictions to impede development, thereby restricting densification

and associated welfare gains. Because land use restrictions are more stringent in developed economies, their corresponding consequences of eliminating height restrictions are even greater. Impacts of height constraints are also increasing in city size and declining in the cost of height. Relatedly, given expected global urban population growth of 1.5% per year till 2050 (United Nations, 2018) and an annual rate of technological progress in the tall building sector of ∼2% (Ahlfeldt and Barr, 2022), the global cost of height restrictions will only increase in the future.

For identification of elasticities of population and built land area with respect to heights, we use an instrumental variables strategy that leverages both cross-sectional and time series variation in the cost of building tall. In the cross-section, we use variation in city mean bedrock depth as a key source of identifying variation. Descriptive analysis and building cost function estimates indicate that the elasticity of construction cost to height per building floor area is U-shaped in bedrock depth, which is consistent with engineering standards for foundation depth and the narrative in Barr et al. (2011). Bedrock that is too close to the surface must be blasted away at high cost to make room for building foundations. Foundations built above bedrock that is beyond the optimal depth must be reached with the costly installation of deep wide piles, placed on a costly raft, or engineered to be underpinned by many very long deeply bored piles.

As favorable bedrock depth acts as a cost shifter, cities with more favorable bedrock depths experienced more construction of tall buildings conditional on their levels of real estate demand. However, a sufficiently high level of demand, proxied for with 1975 city population, is needed for bedrock depth to matter for tall building construction. As a result, the elasticity of tall building construction with respect to 1975 city population is greater at more favorable bedrock depths. Differencing over the 1975-2015 period additionally leverages secular reductions in the cost of height for identification. Particularly in the developing world, costs were sufficiently prohibitive in 1975 to preclude the existence of many tall buildings. Put together, our identification strategy amounts to triple difference comparisons of historically (pre-1975) large versus small cities on more versus less favorable bedrock depths over time (between 1975 and 2015). Formal model comparative statics that follow the logic above justify this empirical approach.

We find no relationship between our instruments for 1975-2015 heights growth and pre-1975 population growth. The instruments are only activated once the Skyscraper Revolution begins. Likewise, we find no relationship between our instruments and population growth in countries that disproportionately constrain heights. Our identifying variation comes from bedrock depths in central areas of cities, which drive more tall building construction in these areas only. Bedrock depths in peripheral city areas, where demand conditions typically do not justify vertical construction, have no impact. In addition to these three aforementioned "placebo" tests, we verify that the effects are driven by cities that were relatively more populated pre-1975 and that cities that were historically small did not take advantage of, and did not benefit from, reductions in the cost of height post-1975. Lastly, we show robustness of our results to controls for a host of potential confounding factors that could be correlated with bedrock depth. Relatedly, in case shallow bedrock is correlated with relevant above-ground factors, results hold when drawing identification comparisons between moderately and very deep bedrock cities.

To implement the empirical strategy, we compile a unique data set of all 12,877 urban agglomerations with populations over 50,000 worldwide (in 182 countries), covering about 90% of the world's total urban population. For these cities, we organize census-based population and satellite-based area estimates going back to 1975, allowing us to measure population and land

use in and around these cities over time. To capture the vertical size of cities, we use a data set of 270 thousand tall buildings from *Emporis*. This data set has comprehensive information on the location, use, and construction year of all buildings over 55 meters tall worldwide.

A large literature assesses the extent to which various types of capital accumulation, and in particular infrastructure construction, drive urban change. However, this is the first paper to comprehensively study how declines in the costs of building tall have contributed to economic development around the world. Like highways and accessibility (Faber, 2014; Chiovelli, Michalopoulos and Papaioannou, 2018; Balboni, 2019; Morten and Oliveira, 2024), railroads/subways (Gonzalez-Navarro and Turner, 2018; Heblich et al., 2020; Balboni et al., 2021), airports/ports (Campante and Yanagizawa-Drott, 2018; Ducruet et al., 2020), and sewers (Coury et al., 2022), tall buildings form a central component of the capital stock globally.

Our estimates are of similar or greater magnitudes to those in the literature for impacts of other components of urban capital stocks. For example, Duranton and Turner (2012) estimates an elasticity of urban population growth with respect to urban highway stocks of 0.15 for the US, similar to our tall building elasticity estimate of 0.13 for the developing world. However, our estimated population density elasticity for tall buildings of 0.31 is about three times as large as those found for urban radial highways in the US and China (Baum-Snow, 2007; Baum-Snow et al., 2017) and much larger than for other types of infrastructure. These investigations of how infrastructure drives urban growth are grounded in the classic empirical literature going back to Glaeser et al. (1992), Henderson et al. (1995), and Ades and Glaeser (1995) that study the determinants of urban TFP growth and variation across locations in equilibrium city sizes.

Understanding how the skyscraper revolution fits into the process of urban development is all the more important as cities that do not develop vertically tend to sprawl (Brueckner and Fansler, 1983; Burchfield et al., 2006; Civelli et al., 2023) and/or become inefficiently spatially configured. Odd urban spatial structures impede growth (Harari, 2020), and associated sprawl typically occupies land that is particularly valuable in non-urban uses. According to World Bank (2022), urban areas occupied 3.6 million sq km in 2011, whereas 48.0 million sq km of land was in agriculture. As cities are more likely to be sited on agriculturally productive land (Henderson et al., 2018), land savings through increased urban compactness frees up more space for agriculture and tree canopy. Taller cities make us "greener" (Glaeser, 2012) by accommodating more people on less land. In that, the skyscraper revolution has parallels with the Green Revolution, whose goal was to use rural land more intensively in order to use less land globally (Gollin et al., 2021).

Our model incorporates insights from the land use and housing production literatures to accommodate height restrictions and linkages across labor and housing markets within and between residential and commercial sectors. As in Albouy et al. (2020), we employ the classical land use theory of Alonso (1964), Mills (1967), and Muth (1969), with additional elements from quantitative spatial models (Redding and Rossi-Hansberg, 2017). Qualitative conclusions mirror those from the more targeted modeling frameworks in Bertaud and Brueckner (2005) and Henderson et al. (2021), though we emphasize variation across cities in the cost of height. The use of the simple monocentric city structure allows our model to reasonably characterize cities of many different sizes and shapes, in part as captured by differences in fundamental productivities and amenities. While the flow of tall buildings reflects economic activity at the time they are built (Ahlfeldt and Barr, 2020; Harari and Wong, 2019), in our model skyscrapers also increase nearby densities and productivities (Curci, 2020; Liu et al., 2020).

Much research on the existence and implications of housing market regulation has been carried out for developed economies (Saiz, 2010; Gyourko and Molloy, 2015; D'Amico, Glaeser, Gyourko, Kerr and Ponzetto, 2024). The more limited work for the developing world comes to the same conclusion, that height regulations are broadly binding and have negative welfare consequences (Brueckner and Sridhar, 2012; Brueckner et al., 2017). We provide a comprehensive quantitative evaluation of the extent to which reductions in the cost of building high have influenced affordability, rural-urban migration, productivity, and welfare for all cities worldwide. Moreover, we quantify the prospects for further gains through relaxation of existing height regulations. In general equilibrium, vertical construction benefits workers over landowners.

2 Data and Descriptive Evidence

Here we explain the data assembly for the 11,257 cities in our main sample. We then describe the evolution of skyscraper technology, demonstrating how variation in bedrock depth is useful for identification. This leads to estimates of the relationship between bedrock depth and the cost of height. Finally, we specify first stage estimation equations and present these results.

2.1 Data Sources

City Level Outcomes: Using the *Global Human Settlements-Urban Centre Database* (GHS-UCDB) (Florczyk et al., 2019, v1.2), we obtain the GIS boundaries of all 12,877 2015 vintage agglomerations ("urban centres") worldwide, which we refer to as cities. The GHS-UCSB reports the built-up area and population of each city circa 1975, 1990, 2000 and 2015 within 2015 definition city geographies. It also reports land area, which is calculated separately for each year using common density thresholds. As built-up area is more consistently measured over time, this is our main measure of urbanized land.[3] The 12,877 cities account for ∼90% of the world's total urban population in 2015 (United Nations, 2018). We focus our analysis on the 11,257 cities in the 125 developing economies as defined by the World Bank in 2015.

As an alternative measure of growth, we use the radiance calibrated (not top-coded) version of night lights data (NGDC, 2015), which is available for select years 1996-2011. We calculate the total sum of lights at night across ≈ 1 km resolution pixels for each city in each year. Lastly, historical population data (Bairoch, 1988; Buringh and Hub, 2013) is used to study pre-trends.
Building Heights and Construction Costs: Emporis (2022) was a global provider of international skyscraper and high-rise building data. Emporis collected information about the full life-cycle of each building over 55 meters tall worldwide, and many shorter buildings. The database contains information for 693,855 "existing [completed]" buildings.[4] We observe geographic coordinates or locality, allowing us to assign each building to a GHS-UCDB city. For a select set of 1,053 buildings, Emporis also reports the construction cost and some attributes. Construction cost excludes land acquisition costs. As "soft" legal, regulatory and engineering costs tend to scale with building height, we consider our cost data to cover variable costs only.

[3]These cities are aggregates of 1 km square grid cells, each of which is above thresholds for built-up area or population per land area of 0.5 and 1500, respectively. These clusters must have at least 50,000 inhabitants in 2015 to be considered cities. As regions within which population is counted remains unchanged from 1975 to 2015, our data overstates the urban population in 1975, resulting in a cross city average 47% and cross-country average 36% of developing country populations in cities. Built-up area is calculated by aggregating the fractions of 80X80 m grid cells covered in building footprints, measured using satellites. Population is taken from censuses.

[4]We only use "buildings with towers", "high-rise buildings", "low-rise buildings", "multi-story buildings", and "skyscrapers" for our analysis. Since 2022, these data have been integrated into CoStar Group data products.

Inspection of the kernel density of 2015 building heights reveals a mode and large spike at 55 meters. Since cities are likely to have more buildings below than above 55 m and the observed distribution of building heights is relatively smooth above it, following Barr and Jedwab (2023) we infer that Emporis likely only captures the universe of buildings above this height. Using the year of construction (and demolition if demolished), we obtain the total *sum of heights* (m) of all buildings of at least 55 meters for each city-year from the 19th century to date.

Figure 1: Global Evolution of Aggregate Tall Building Heights (Km), 1895-2021

(a) All Tall Buildings

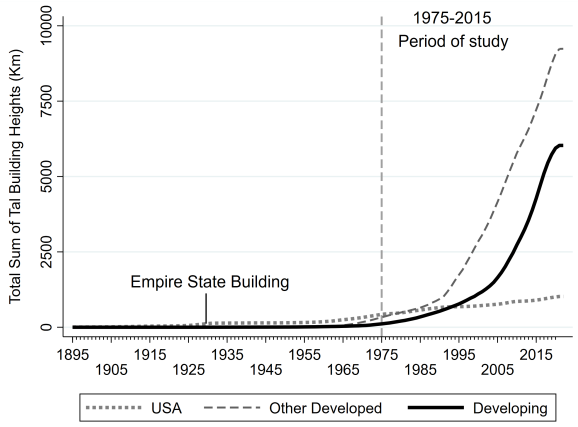

(b) Residential vs. Office Towers

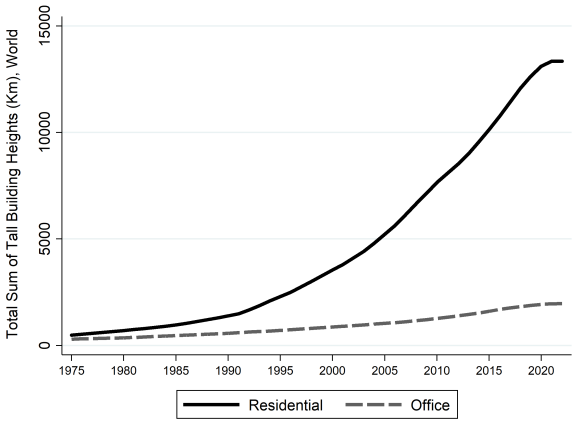

Notes: The left panel shows the evolution of the total stock of tall building heights (km) for cities in the U.S., other developed ("high-income") economies, and developing economies, all defined circa 2015. The right panel shows the evolution of the total world stock of tall building heights (km) separately for residential buildings and office buildings 1975-2021 (mixed use buildings are rare). Only tall buildings above 55 meters ($\approx$ 180 feet or 13-14 floors) are included in the calculations.

Patterns in the data support the logic of focusing our analysis on the developing world. As seen in Figure 1, until the 1960s, the vast majority of the world's tall buildings housed offices in large cities of high income countries, especially the US. Starting in the 1970s, the construction of tall buildings spread through many middle income countries and into medium sized and smaller cities worldwide. Most such construction was for residential rather than commercial use. During our primary study period of 1975-2015, the total stock of heights increased from a clean slate of near 0, with only 1% of cities having any heights, to over 6,000 km in developing economies.[5]

While tall buildings were concentrated in a few developed regions in 1975, one can observe the growth of tall buildings in the developing world by 2015 (see Figure 2 below.)

To account for the fact that many cities have no buildings above 55 m in some years, we use $\ln(\text{Heights} + 1)$ to measure the sum of heights in each city. While this is not the only way to aggregate intensive and extensive margin comparisons across cities, we show below that it provides results that are also consistent with examination of extensive margin comparisons and can be interpreted in the context of the model. Results are robust to using alternative scaling factors, the inverse hyperbolic sine transformation, an alternative minimum height threshold of 100 meters, or cross-sectional satellite-based building volume data (described below).

Bedrock Depth: Shangguan et al. (2017) reports bedrock depth in meters at an $\approx$1 km resolution for the world. To avoid introducing selection on tall building location decisions within cities, we use *mean bedrock depth* for each city within its 2015 boundary as our primary bedrock measure. Shangguan et al. (2017) indicates "this data set is based on observations extracted

[5]In 1975, 40% of developing economy heights are in Brazilian cities; Johannesburg, Mexico City, and Caracas each had an additional 10%. Our main results hold when excluding the few cities with heights in 1975 (unreported).

from a global compilation of soil profile data (about 1.3 million locations) and borehole data (about 1.6 million locations)." Looking across all pixels within our city boundaries, 80% of the variance in bedrock depth is between rather than within cities in our data.[6]

Figure 2: Sum of Tall Building Heights (Km), World Cities, 1975 and 2015

(a) 1975

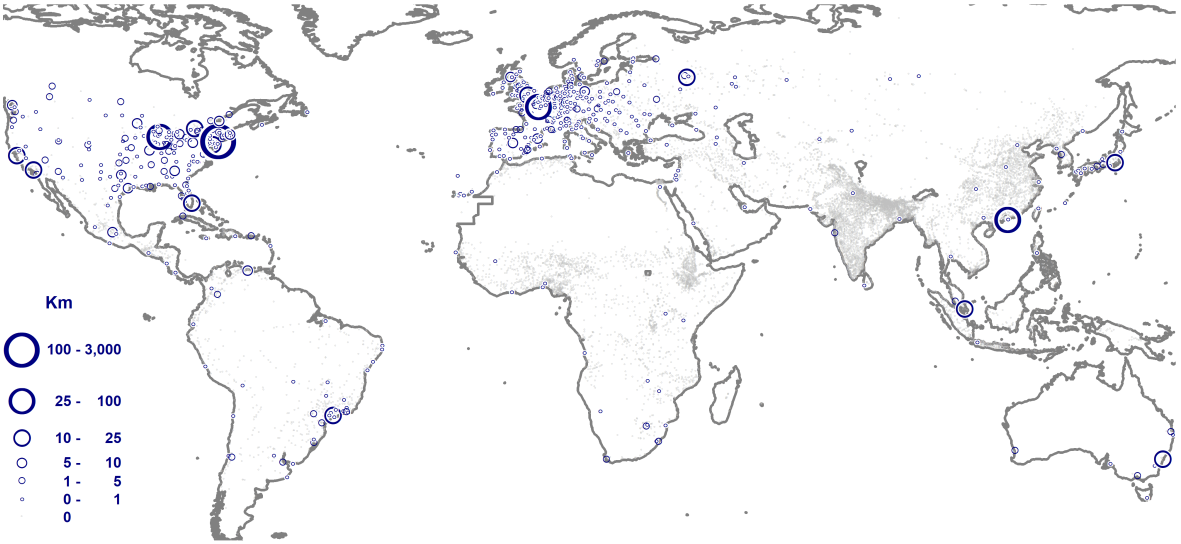

(b) 2015

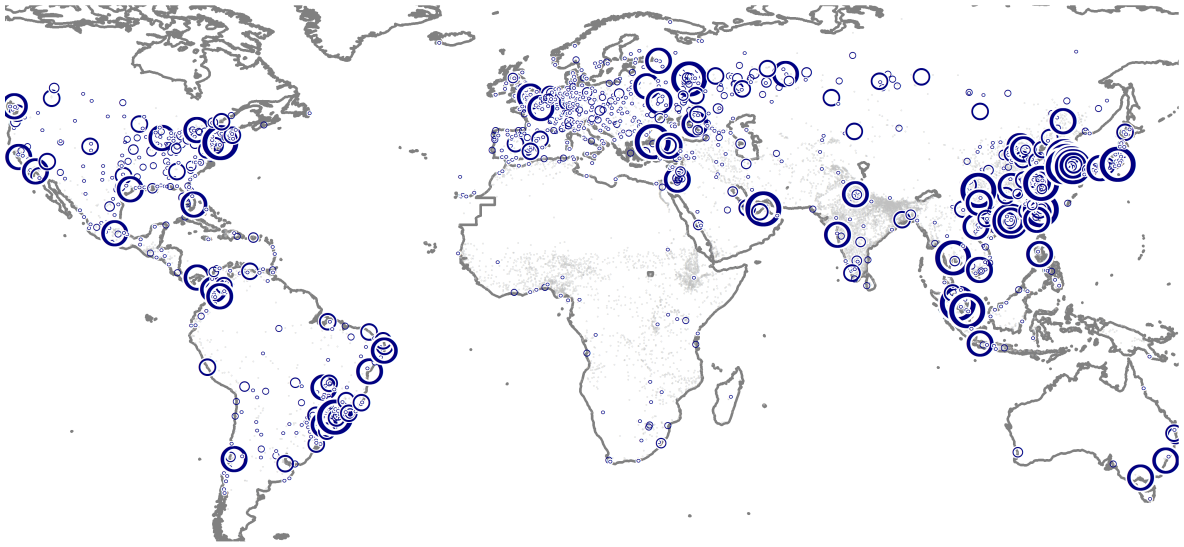

Notes: Bubble sizes indicate the total stock of tall building heights (km) for all 12,877 world cities of at least 50,000 residents circa 2015. The same legend applies to both panels, with tiny grey dots indicating cities with no tall buildings. Only buildings above 55 meters (≈ 180 feet or 13-14 floors) are included in the calculations.

Bedrock depths have been determined through slow-moving geological processes, including movements of glaciers during past ice ages and of tectonic plates. The main glaciation periods occurred millions of years ago and the last cold episode of the Last Glacial Period ended ∼10,000 years ago, millennia before urban settlements first appeared. Plate tectonics in the past 3-4 billion years have also shaped the earth's terrain. Weathering and erosion contribute to exposing or decomposing bedrock, thereby making it shallower or deeper. Overall, the importance of past ice ages and the ambiguous effects of weathering and erosion may explain the weak correlations (of less than 0.1) that we find between mean bedrock depth and various physical geographic

[6]Our results are not sensitive to the use of mean bedrock depth across all pixels or the bedrock depth at the centroid of each city's brightest 3X3 block of 9 pixels. Bedrock depth is uncorrelated with distance to this pixel.

features in and around city boundaries, including elevation, ruggedness, proximity to coasts and lakes, earthquake risk, soil quality, and wind speed. We find similarly weak correlations for subways and access to markets in nearby cities, mines, and oil and gas fields. Such physical and economic geographic variables are used as controls in robustness analysis. Appendix A.1 provides details on the sources and construction of these controls.

2.2 The Data Generating Process for Heights

Two attributes of the tall building cost function are central for our analysis. First, the cost of height has declined over time. Second, by 2015, construction costs were lower in cities with intermediate bedrock depths. Here we describe the history and engineering principles that generate these facts and then formally derive developers' profit maximizing choices of heights.

Until the mid-1950s, the vast majority of tall buildings were constructed by US firms in US cities using steel frame technology. Over the following two decades, concrete technology matured enough such that it was used to frame about half of new US tall buildings by 1975. Steel technology is capital and expertise intensive, whereas concrete construction requires more time to build but uses lower cost labor and materials. The advent of mainframe computing and standardized computer aided design and engineering, which expanded greatly into the 1970s and 1980s, complemented the move to concrete based construction. By automating the engineering calculations determining building specifications required to withstand collateral wind loads, this technology further reduced the cost of building tall. By 2005, over 80% of new construction tall buildings over 80 meters in the US were concrete (Council on Tall Buildings and Urban Habitat, 2022). Crane technology also improved, with tower cranes developed in the 1950s giving way to mobile cranes in the 1960s and climbing tower cranes in the 1970s. Based on the construction cost data in Emporis, this technical progress came with at least a 25% decline in the cost of height in the US over the 1975-2015 period (Appendix Figure A1). As this technical progress generated larger reductions in the engineering costs and complexity of constructing the tallest buildings, these structures experienced greater cost reductions.

While construction practices for tall buildings in the US transitioned slowly from steel to concrete, concrete construction dominated *from the beginning* in the developing world. Lower labor costs and higher shipping and production costs for steel than cement, which is mixed into concrete, justifies this choice. Even today, there are almost no steel-framed tall buildings in the developing world (Council on Tall Buildings and Urban Habitat, 2022). US firms were in charge of most tall building construction projects in the developing world through the 1970s. Diffusion of construction technologies over time meant that local builders managed most new construction by the 1990s. Moreover, the rise of tall building construction contributed to a 1975-1980 tripling of cement imports into developing economies (USGS, 2020; UN COMTRADE, 2020).

The relationship between the cost of height and bedrock depth is determined by the minimum building foundation depth required for stability. Rankine's Theory, a simple engineering rule of thumb, lays out a proportional relationship between building weight (which is roughly proportional to height conditional on construction materials) and required foundation depth, with the constant of proportionality differing as a function of soil conditions. According to this rule, optimal foundation depth is ∼10% of a building's height. In order for a building to be stable, the bottom of the foundation must either be anchored to bedrock, have a sufficiently wide base ("raft"), or incorporate many deeply bored piles. As rafts and numerous deeply bored piles

are more costly to install, builders prefer to anchor to bedrock if it is not too deep. However, if bedrock is within only a few meters of the surface, expensive blasting is required to install the foundation. Figure A2 provides a visualization. Figure A3 provides descriptive evidence showing that unit construction cost for tall buildings is minimized at intermediate bedrock depths.[7]

The engineering evidence thus suggests that a reasonable approximation of the cost function for developing a building of height S on bedrock depth B_{ac} in city a of country c at time t is

$$C_{act}(S) = q_{act} S^{1+\theta_t(B_{ac})}. \tag{1}$$

Consistent with our evidence of secular reductions in the cost of height conditional on bedrock depth, we allow θ to change over time.[8] As the elasticity of construction cost per square meter with respect to height is greater at low and high bedrock depths, θ is also U-shaped in B_{ac}.[9] As q is non-parameterically indexed by city and time, it incorporates differences in bedrock depth in addition to labor and materials costs that may change over time.

To corroborate the descriptive evidence that cost of height θ is U-shaped in bedrock B, we recover rough non-parametric estimates of the θ function with our limited (Emporis) construction cost data. We regress log construction cost per floor area on building height for each bedrock depth using a locally weighted regression approach.[10] The result, depicted in Figure A4, supports the engineering-based hypothesis that bedrock at intermediate depths is associated with lower costs of height. Estimates of θ range from 0.2 at intermediate bedrock depths to 0.8 at depth 0 and more than 1.0 at high depths. These results support the idea that cities with bedrock in an intermediate range accommodate high real estate demand at lower cost.

As construction cost differs by bedrock depth, the profit maximizing level of height also differs by bedrock depth conditional on demand conditions. We model unconstrained competitive building developers to have the following profit function associated with building to height $S(x)$ at location x in city a in country c at time t.

$$\pi_{act}(S, x) = \int_0^S p_{act}(x, s)ds - C_{act}(S) - r_{act}(x). \tag{2}$$

$p_{act}(x, s)$ is the sales price per unit of real estate services at location x and height s and $r_{act}(x)$ denotes the fixed cost component of development, which includes both the land price and any regulatory development costs at location x. The model in Section 4 lays out a demand structure that justifies the separable form $p_{act}(x, s) = p_{act}(x)s^{\omega}$, where ω is positive and close to 0. (For the model to be well-behaved, we need $\theta > \omega$.) A positive ω reflects the amenity value associated with views and reduced noise. In the model, we impose that the price per floor area of real estate declines in CBD distance x: $p_{act}(x) = p^0_{act} f(x), f'(x) \leq 0$. Each city a in country c at time t faces its own real estate demand conditions, leading us to index CBD rents by this triplet.

Profit maximization yields the following expression for optimal height, S^*.

$$\ln S^*(p_{act}(x), q_{act}, \theta_t(B_{ac})) = \frac{1}{\theta_t(B_{ac}) - \omega} \left(\ln \frac{p_{act}(x)}{q_{act}} - \ln \left[1 + \theta_t(B_{ac})\right] \right) \tag{3}$$

[7] Our construction cost data is dominated by steel construction buildings in the US. Due to their extra weight, concrete buildings would typically have greater optimal bedrock depths conditional on height.

[8] For Cobb-Douglas production with capital share α and fixed lot size, the cost of height θ equals $\frac{1-\alpha}{\alpha}$.

[9] While optimal bedrock depth is expected to be slightly greater for taller buildings, a result with weak evidence in the data, allowing θ to additionally depend on height would make the model intractably complex. Moreover, we do not have sufficient data to estimate the relationship between θ and height conditional on bedrock depth.

[10] Distance to the central business district (CBD) instruments for building height, conditional on included controls for city and country-decade fixed effects. See Appendix A.4 for details.

Developers' choices of log height depend on the interaction between bedrock depth, as included in $\theta_t(B_{ac})$, and the level of demand, as included in $p_{act}(x)$. That is, not only do developers build taller in locations with higher demand, the elasticity of profit-maximizing height with respect to price is greater in locations with more favorable bedrock depths. In the model section, we extend this framework to accommodate regulatory height limits.

Eq. (3) lays out the logic behind our triple difference empirical strategy. The first two differences are over time and for shallow relative to intermediate bedrock depths, both of which are associated with reductions in θ. In our primary empirical specification, the related direct changes in the impacts of bedrock depth on heights are controlled for instead of being used for identification. The third difference is the amplification that comes in higher demand relative to unit cost locations, where the level of $\ln \frac{p}{q}$ is greater, for which 1975 city population proxies for $\ln p$. Differentiating Eq. (3) with respect to time, bedrock depth B and then $\ln p$ leaves only this triple-interaction term.[11] The secular decline in the cost of height over time has facilitated more tall building construction in high demand locations, *and particularly so in cities with favorable bedrock*. In 1975, building tall was prohibitively costly throughout the developing world. As the cost of height declined for all cities, it is the locations with strong (pre-1975) demand conditions *and* favorable bedrock depths that are predicted to increase their heights the most (post-1975).

We are now in a position to characterize aggregate city building heights. As real estate prices decline in CBD distance, each city has a unique endogenous distance cutoff x_{act}^{55} within which buildings of over 55 m exist in each year. Aggregating differences in $\ln S^*$ in Eq. (3) for each location within x_{act}^{55} across cities delivers aggregates of location-specific height differences that follow the same profiles with respect to bedrock depth and demand conditions as those for each location x. Cities with greater heights at all locations must also have a greater aggregate stock of heights when adding up over the same range of x and a greater difference in stocks when comparing across cities of different bedrock depths and levels of demand.

2.3 Descriptive Evidence and Identification

Figure 3 below provides a descriptive visualization in support of our identification strategy using our primary estimation sample of 11,273 cities in 125 developing economies. The left panel is a heat map of average 1975-2015 city heights growth as a function of 1975 log city population (vertical axis) and bedrock depth (horizontal axis), residualized for population and bedrock depth bin fixed effects (and country fixed effects). Difference in difference (DiD) comparisons within this left panel make up our fundamental identifying variation. The right panel presents an analogous heat map for 1975-2015 average city population growth rates, similarly residualized.

The underlying regression used to generate these graphed residuals is

$$y_{ac} = \tilde{\phi}_{b(ac)} + \tilde{\rho}_{p(ac)} + \tilde{\kappa_c} + \tilde{\varepsilon}_{ac}. \tag{4}$$

y_{ac} is the 1975-2015 growth rate in either heights or population in city a of country c, $\tilde{\phi}_{b(ac)}$ are 31 five-meter wide bedrock depth bin fixed effects (0, 5, ..., 150+), $\tilde{\rho}_{p(ac)}$ are 15 fixed effects for log 1975 population bins (width = 0.38), and $\tilde{\kappa_c}$ are 125 country fixed effects. Figure 3 plots average estimates of $\tilde{\varepsilon}_{ac}$ for each population-bedrock depth bin combination. For the sake of simplicity, bedrock bins above 55 m (2% of the sample) are grouped together.

Residualization for bin fixed effects comes for both conceptual and practical reasons. Classical

[11] In particular, differentiation of Eq. (3) with respect to t, B and $\ln p$ yields $\frac{2}{(\theta-\omega)^3}\frac{d\theta}{dt}\frac{d\theta}{dB}d\ln p > 0$.

theory and evidence on local economic growth emphasizes convergence (Barro and Sala-i Martin, 1992; Glaeser et al., 1992), a phenomenon seen in our data. Low population cities tend to grow faster than high population cities at all bedrock depths. Such convergence is also seen in heights. Residualization for population category fixed effects forces identifying comparisons to be across bedrock depths within 1975 population size bins. It also facilitates easier visual comparisons across population bins within bedrock depths in Figure 3. Additional residualization for bedrock depth bins is done for symmetry and to focus identification on DiD type comparisons.

Figure 3: Descriptive Evidence for the Triple-Difference

(a) Residualized Heights Growth, 1975-2015 (b) Residualized Pop. Growth, 1975-2015

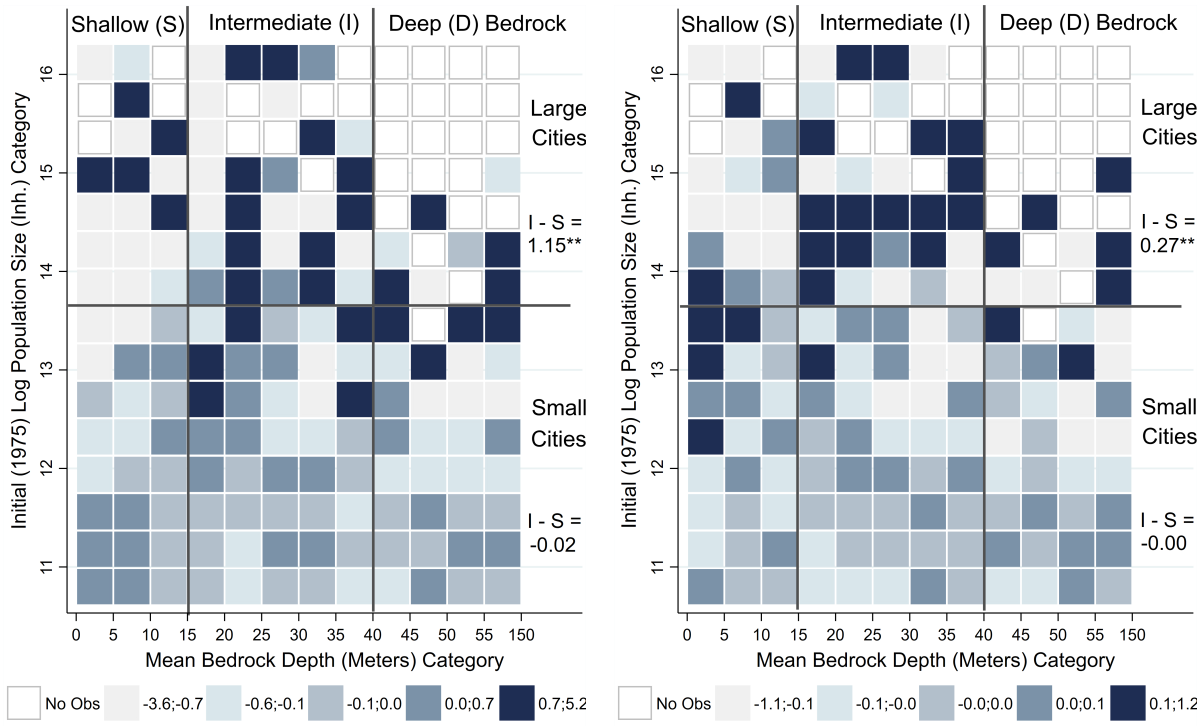

Notes: Tiles in the left panel are colored to show quintiles of average rates of 1975-2015 tall building heights growth across cities in each indicated population and bedrock tuple after residualizing for population group and bedrock group fixed effects. Tiles in the right panel are colored to show quintiles of average rates of 1975-2015 population growth for the same cities after the same residualization process. The sample includes all 11,273 cities in 125 developing economies. 1975 city population bins are each 0.38 log points wide. The horizontal line is at a population of 1 million, above which lie 168 "Large" cities. 59% of cities are on "Shallow" bedrock, less than 15 meters deep (≈ 49 ft). 35% of cities are on "Intermediate" bedrock, 15-39.99 meters deep (≈ 49-131 ft). The largest bedrock category (55-150 meters) includes 2% of cities.

Horizontal comparison across most pairs of tiles in the central "Intermediate" versus left "Shallow" regions across rows, or conditional on 1975 population, reveals greater heights and population growth at intermediate bedrock depths. This relationship is stronger for populations above the horizontal line (1 million inhabitants).[12] Likewise, vertically comparing heights or population growth rates within intermediate bedrock bins reveals a pattern of stronger growth rates in initially larger cities, or darker shaded tiles toward the top of the two graphs.

Aggregating across tiles within the black lines defines samples that can be used to implement formal DiD analyses. The estimated gap in heights growth in initially "large" (one-million-plus) cities in 1975 on intermediate (I) relative to shallow (S) bedrock is 1.15** (se=0.51; N = 155).

[12]Comparing "Deep Bedrock" with "Intermediate" cities is not as informative, as there are only 13 deep bedrock cities above 1 million. While the "Shallow", "Intermediate" and "Deep Bedrock" categorizations used here are somewhat arbitrary, we demonstrate below that results depend little on these category cutoffs.

The gap for population growth is 0.27** (se=0.12). Taking the ratio yields the implied Wald estimate of the elasticity of population with respect to heights of 0.23** (se=0.11). For initially "small" cities in 1975, no significant differences are observed between intermediate and shallow bedrock depths (-0.02 (se=0.02) for heights; -0.00 (se=0.01) for population; N = 10,433). As a result, estimates for large relative to small cities × intermediate relative to shallow bedrock are similar to the ones found for large cities only: 1.17** (se=0.51) for heights, 0.27** (se=0.12) for population, and 0.23** (se=0.11) for the Wald estimate (F-stat=5.3).[13] As these estimates only use some of the available identifying variation, and mask within population-bedrock group heterogeneity, they should be viewed as noisy measures of our headline population elasticity estimate of 0.13, which is explained in detail in the following section.

The visual evidence in Figure 3 indicates that more heights have been constructed in larger cities conditional on bedrock depth, with steeper gradients for cities on intermediate bedrock depths. A similar pattern holds for city population growth rates. We show that these facts hold systematically by graphing estimated coefficients γ_b from the following descriptive regression:

$$y_{ac} = \sum_b \gamma_b \left[\ln \text{Pop}_{ac75} \mathbb{1}(b \leq \text{Bedrock}_{ac} < b + 5)\right] + \delta \ln \text{Pop}_{ac75} + \kappa_c + \phi_{b(ac)} + \varepsilon_{ac}, \quad (5)$$

where b = {0,5,...}. This equation is a more parameterized version of Eq. (4). Rather than controlling for 1975 population category fixed effects, we simply control for log 1975 population (retaining bedrock bin and country fixed effects). This specification essentially projects the residual $\tilde{\varepsilon}_{ac}$ on log population separately by bedrock depth bin. The result is separate elasticities of height or population growth with respect to 1975 population for each bedrock bin b, conditional on bin and country fixed effects. As the regression controls for log 1975 population, all γ_b coefficients are of the bin-specific relationship between 1975 ln population and 1975-2015 growth relative to that for the the "0" (0-4.99) m bedrock depth bin. The γ_b estimates thus capture comparisons of the shading gradients across columns in Figure 3. These are graphed in Figure 4. Bubble sizes are proportional to the number of observations. Quadratic lines of fit are indicated.

Figure 4 Panel (a) below shows the inverse U shaped impact of city mean bedrock depth on the (residualized) 1975-2015 growth rate in aggregate heights in strong relative to weak demand cities. Such height elasticities are greater by up to 0.8 in cities at intermediate bedrock depths than in cities with bedrock at the surface. As seen in Panel (b), the elasticity of (residualized) population growth with respect to 1975 population is about 0.1 greater for cities in the same intermediate range of bedrock depth than the low or high ranges. Implied Wald statistics for population elasticities of aggregate heights are thus in the 0.10-0.15 range. As the quadratic function does a reasonable job of fitting coefficient patterns, most of the empirical work uses this parameterization.[14] With 90% of cities in the 0-30 bedrock depth range, cities in the upward-sloping portions of both panels of Figure 4 provide most of the identifying variation.[15]

[13] Without residualization, the Wald estimate is 0.20. Including deep bedrock cities raises estimates slightly. Results also hold when adjusting the bedrock categorization cutoffs by +/- 5 m. Lastly, the estimate is unchanged but standard errors decrease in a cell-based analysis weighting by the number of cities in each cell.

[14] These quadratic fits are generated by regressing the graphed bin coefficients on bedrock depth and bedrock depth-squared, weighting by the number of cities in each bin, and graphing the predicted values. More flexible partial polynomial fits look similar (not shown), though they peak at slightly smaller bedrock depths.

[15] We corroborate this descriptive evidence by examining estimates like those in Figure 4 Panel A but for buildings of different heights. As taller buildings require deeper foundations, the relative cost of construction at optimal bedrock depths versus that at the surface is predicted to be larger for taller buildings. Using results from regressions like Eq. (5) for aggregate city heights growth calculated only using buildings in each of 3 different height ranges (55-100, 100-200, and 200+ m), we find that the apexes of lines of best fit increase in height.

Figure 4: Relationships Between 1975-2015 Heights or 1975-2015 Population Growth and log 1975 Population by Bedrock Depth

(a) Heights Growth, 1975-2015

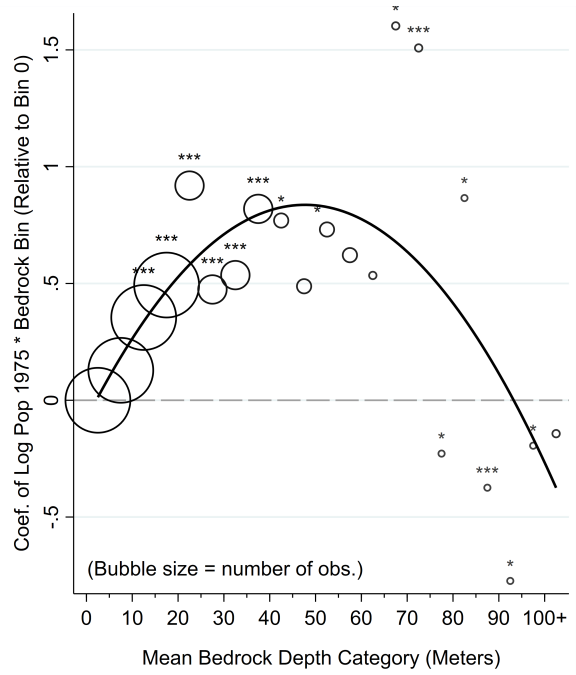

(b) Population Growth, 1975-2015

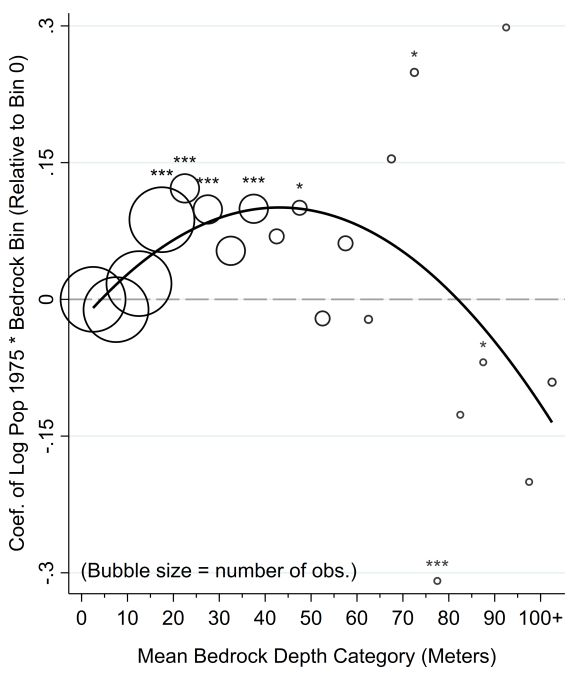

Notes: Panel A graphs coefficients on ln 1975 city population for each 5 meter bin of city-level mean bedrock depth in which the dependent variable is the 1975-2015 change in the log sum of heights plus one. Panel B is analogous but with the dependent variable the 1975-2015 change in log population. The size of the bubbles indicates the relative number of city observations in each mean bedrock depth bin. Stars indicate the statistical significance of each bin-specific coefficient on log 1975 city population. The quadratic fit is shown, weighting by the number of observations in each bin.

2.4 Predicting City Level Height Growth

We specify an aggregate heights supply equation that focuses on our comparisons of heights in initially large versus small cities with favorable relative to unfavorable depth bedrock. A specification that is linear in 1975 log population and quadratic in city mean bedrock depth follows the logic of Figure 4. Our first stage and reduced form regressions thus take the form:

$$\begin{aligned} y_{ac} = \gamma_1[\text{Bedrock}_{ac} \times \ln \text{Pop}_{ac75}] + \gamma_2[\text{Bedrock}_{ac}^2 \times \ln \text{Pop}_{ac75}] \\ + k_1 \text{Bedrock}_{ac} + k_2 \text{Bedrock}_{ac}^2 + \delta \ln \text{Pop}_{ac75} \\ + X_{ac75}\xi_1 + [X_{ac75} \times \ln \text{Pop}_{ac75}]\xi_2 + \kappa_c + \epsilon_{ac}. \end{aligned} \tag{6}$$

Dependent variables are 1975-2015 growth rates in city aggregate heights or population. The key components of this equation are the population-bedrock depth interactions, with coefficients γ_1 and γ_2. These terms capture how the relationships between tall building construction or population growth and bedrock depth differ by pre-Skyscraper Revolution 1975 city population. To verify that bedrock depths and not correlates drive identification, in robustness checks explored below we include a vector of control variables X_{ac75} and its interaction with $\ln \text{Pop}_{ac75}$.

Table 1 builds up to justify using the form in Eq. (6) as our primary specification. In doing so, we demonstrate emphasis on identifying variation across bedrock depths in large cities (relative to small cities) in 2015 but not 1975. Panels A and B present the coefficients on quadratics in city mean bedrock depth interacted with measures of 1975 city population. Panels A, B and C present first stage coefficients, reduced form coefficients, and resulting IV estimates, respectively.

Specifications (1)-(3) systematically progress through the logic of our identification strategy. Specification (1) replaces ln Pop_{ac75} in Eq. (6) with a dummy variable for the city having over 1 million residents in 1975 and a dummy for smaller cities. The left column shows interaction coefficients with the large city dummy and the right column shows interaction coefficients with the smaller city dummy. Coefficient magnitudes are much greater for large than for small cities, with stronger first stage power. Following the DiD logic in our discussion of Figure 3, bedrock depth is only a good predictor of heights growth, and hence population growth, in large cities. Specification (2) drops the small cities interaction and instead simply controls for ln Pop_{ac75}, yielding similar results. Specification (3) reports results of our primary specification in Eq. (6). First stage and reduced form interaction coefficients are between the "Large" and "Small" columns of (1) and first stage power is much greater, as (3) uses continuous variation across cities of all sizes for identification. However, the IV estimate of 0.13 is stable across specifications. In our primary specification, it just comes with a smaller standard error and greater first stage power.

Table 1: First Stage Estimates and Identification

Period for Dep. Var.:	1975-2015				1975	2015
	(1)		(2)	(3)	(4)	(5)
Interaction Variable =	1975 Large City Dummy	1975 Small City Dummy	1975 Large City Dummy	ln 1975 CityPop	ln 1975 CityPop	ln 1975 CityPop
Panel A: First Stage	Dependent Variable: Δ ln (Heights+1)				DepVar:ln(Heights+1)	
Bedrock*InteractionVariable	0.060**	0.001	0.059**	0.026***	0.003	0.029***
	[0.030]	[0.001]	[0.029]	[0.006]	[0.003]	[0.006]
Bedrock^2*InteractionVariable	-0.0001	-0.0000**	-0.0001	-0.0002**	-0.0000*	-0.0002**
	[0.0002]	[0.0000]	[0.0002]	[0.0001]	[0.0000]	[0.0001]
Panel B: Reduced Form	Dependent Variable: Δ ln Population				Dep Var: ln Pop	
Bedrock*InteractionVariable	0.014**	0.001***	0.012**	0.004***	-	0.004***
	[0.006]	[0.000]	[0.006]	[0.001]	-	[0.001]
Bedrock^2*InteractionVariable	-0.0001**	-0.0000	-0.0001*	-0.0000***	-	-0.0000***
	[0.0000]	[0.0000]	[0.0000]	[0.0000]	-	[0.0000]
Panel C: IV	Dependent Variable: Δ ln Population				Dep Var: ln Pop	
Δln(Heights+1)	0.13**	-0.06	0.12**	0.13***	-	0.13***
(ln(Heights+1) in (5))	[0.06]	[0.19]	[0.06]	[0.03]	-	[0.03]
(Partial) First Stage F	11.43	4.10	11.31	22.84	1.71	22.84
Observations (Cities)	11,258		11,258	11,258	11,258	11,258
1975 Large City Dummy	Yes	Yes	Yes	No	No	No
ln 1975 City Population	No	No	Yes	Yes	Yes	Yes
Bedrock, Bedrock^2	No	No	Yes	Yes	Yes	Yes
Country Fixed Effects	Yes	Yes	Yes	Yes	Yes	Yes

Notes: First stage, reduced form, and IV results of 5 different specifications are shown in the table. The interaction variable "1975 Large City" is a dummy variable for the city being over 1 million in 1975 and "1975 Small City" is a dummy variable for all other cities. Specification (1) has two endogenous heights variables, one for "large" cities and one for "small" cities. Each is instrumented with a quadratic in bedrock depth interacted with the city size interactions. Specification (2) instruments for heights growth in all cities with only the 1975 large city-bedrock depth quadratic interaction. Specification (3) is our primary specification which uses the ln Pop 1975-bedrock depth quadratic interaction instead. Specifications (4) and (5) are cross-sectional regressions for 1975 and 2015, respectively. All 11,258 cities in developing economies make up the sample. Remaining coefficients are reported in Appendix Table A2. Robust standard errors in brackets.

Results in the final two columns of Table 1 put 1975 or 2015 levels of dependent variables on the left hand side of regressions that otherwise have the same form as our primary specification.

Evident is no predictive power of the bedrock depth-population interaction in 1975 and strong predictive power in 2015. 1975 is indeed approximately a "clean slate" for cities in the developing world in our empirical context. As a result, it is almost the same to estimate regressions using 2015 levels or 1975-2015 changes. Table A2 reports remaining coefficients.

To relate these results to the supply model sketched above with some rough quantification, consider a comparison between a 16 meter bedrock depth city of 1 million in 1975 and one in which bedrock is at the surface. Estimates in Tables 1 and A2 Column (3) indicate that height growth is 82 log points greater in the favorable bedrock city. Recognizing that the cost of height θ has a range of 0.62 across these bedrock depths (Figure A4), this implies a partial elasticity of heights with respect to θ of 0.82/(-0.62) = -1.3 for cities of 1 million. It is -0.9 for cities of 500 thousand and -2.3 for cities of 5 million. These increases in magnitude with city population follow the logic of interactions between θ and $\ln p^0$ in Eq. (2).

2.5 Placebo Checks

Identification concerns would arise if bedrock depths more favorable for tall building construction, or unobserved correlates, allowed (pre-1975) large cities to have greater post-1975 growth potential through mechanisms other than reducing the cost of building tall. Any threats to identification could thus come from correlations between bedrock and latent city demand growth that was different for initially large and small cities. While our empirical analysis in the following section shows robustness to inclusion of some such potential omitted variables that could be correlated with bedrock depth, here we carry out three "placebo" checks to allay such potential identification concerns. The results of these checks are reported in Table 2 below.

The first check shows no differential pre-treatment trends in population when relying on the Clio-Infra database on settlement size (Buringh and Hub, 2013). We focus on the 560 cities with available historical population data in the 42 developing economies in 1975 for which at least two-thirds of the cities in our baseline sample have an available historical population estimate (the 560 cities account for 95% of the total city population of the 42 countries). The first two columns of Table 2 show reduced form relationships between bedrock depth interacted with population for the 1975-2015 and 1950-1975 periods, respectively. Results in Column (1) are consistent with results in Table 1 Specification (3). In contrast, we find a small insignificant relationship between bedrock depth and 1950-1975 population growth, especially considering its high mean of 41%. Similarly, we find no population pre-trends when using 1900-1975, 1900-1950, or 1850-1975 (unreported). Finally, as there were almost no heights in developing economy cities in 1975, there is no possibility of pre-trends in heights growth, a result that we verify (unreported).

The third and fourth sets of results in Table 2 present spatial placebo checks. These are separate regressions of heights growth near and far from centroids of cities' brightest 9X9 megapixels on mean bedrock depth and its square near these bright pixels ("Central") and in areas located farther away but where tall buildings are still typically found ("Peripheral"), both interacted with log 1975 population.[16] Central bedrock depths predict central heights growth but peripheral bedrock depths do not (Column (3)). Column (4) shows a lack of predictive power of both central and peripheral bedrock depths for peripheral heights growth. These results confirm that our identifying variation comes from bedrock depths in central areas of cities, which drive

[16] "Central" is the region within 10% of the Euclidean distance from the urban edge to the brightest pixel. "Peripheral" is the region between 10% and 50% of this distance. The two regions account for 82% of heights.

more vertical construction in these same areas only. Peripheral bedrock depths, which are more likely to be correlated with factors outside cities, do not predict such construction.

Table 2: Temporal and Spatial Placebo Checks

	(1)	(2)	(3)		(4)		(5)
Dependent Variable:	Δ ln Pop (Buringh et al)		Δ ln Central Heights (H)		Δ ln Peripheral H		Δ ln Pop
	1975-2015 Baseline	1950-1975 Pre-Trend	Central Bedrock	Periph. Bedrock	Central Bedrock	Periph. Bedrock	Constrained Countries
Bedrock*ln 1975 Pop	0.017***	0.004	0.035**	-0.015	0.022	-0.003	-0.001
	[0.006]	[0.014]	[0.017]	[0.018]	[0.022]	[0.023]	[0.002]
Bedrock^2*ln 1975 Pop	-0.0005***	0.0000	-0.000	-0.000	-0.000	-0.000	-0.0000
	[0.0001]	[0.0004]	[0.000]	[0.000]	[0.000]	[0.000]	[0.0001]
Partial First Stage F	-	-	7.54	2.16	1.54	0.29	-
Mean	0.042	0.414	0.195		0.282		0.602
Observations (Cities)	560	560	9,377		9,377		3,315

Notes: Specifications are similar to those in Table 1 Column (3), with controls for country fixed effects, ln 1975 city population, and a quadratic in city mean bedrock depth. (1) and (2) use all cities belonging to 42 countries that were considered "developing economies" as of 1975 and for which at least two thirds of the cities in our sample have an available historical (pre-1975) population estimate in the Buringh and Hub (2013) database. "Central" in (3) and (4) is defined as the region within 10% of the Euclidean distance to the city center. (Very small area cities are excluded from the sample.) "Peripheral" is the region located between the 10% and 50% of the Euclidean distance to the city center. (3) and (4) show the results of one regression each. In (5), we keep cities belonging to 47 height-constrained countries defined using the height gap methodology discussed in Section 3.4 with an aggregated residual below 0. Robust SEs in brackets.

Results in column (5) show that cities which we infer to be in the 47 most height constrained countries exhibit no relationship between bedrock depth and population growth. If the instruments had a direct impact on population growth, thus not satisfying the exclusion restriction, this relationship would appear in the sample of countries with few tall buildings. We defer further discussion of how we define height constrained countries to Section 3.4 below but note that we rely on the heights data and measures of city population and economic size to identify the countries whose cities have relatively little heights, *ceteris paribus*.

3 Empirical Analysis

Our central empirical interest is in estimating the causal effects of technology-induced changes in aggregate heights in tall buildings on city population and built area. As is clarified in the model in Section 4 below, we conceptualize these labor and land market responses to operate through the following causal chain. Identifying variation in heights is through cost of height (θ) induced variation in real estate supply. Holding local productivities and amenities constant, a positive real estate supply shock leads to lower real estate prices and a greater city equilibrium quantity of floorspace. The associated aggregate real estate demand response comes from a combination of greater floorspace use by existing residents and firms and in-migrants to the city from the hinterland. The lower cost of height disproportionately grows real estate supply near the center, where the level of real estate demand is greatest. This increases urban compactness, which enhances the average city productivity, amenity, and real wage. Demand for urban living shifts out, representing an additional in-migration force. With a finite migration elasticity from idiosyncratic location preferences, urban utility grows. An increase in equilibrium floor space near the center comes with depressed land demand near the urban fringe, manifesting as a negative built area response.

The following decomposition incorporates these relationships, where Y indicates city population or built area and H measures the quantity of real estate services in tall buildings.

$$\frac{d\ln Y}{d\ln H} \equiv \beta = \frac{d\ln Y}{d\ \text{MBD}} \Big/ \frac{d\ln H}{d\ \text{MBD}} = \frac{d\ln Y}{d\theta} \Big/ \frac{d\ln H}{d\theta}$$

The empirical work primarily uses city aggregate height in buildings of at least 55 m plus one to measure H. As seen from the estimates in Table 1 Column (3), $\frac{d\ln H}{d\ \text{MBD}}$ and $\frac{d\ln Y}{d\ \text{MBD}}$ both follow the same pattern of increasing in ln 1975 population at low to intermediate bedrock depths before declining in ln 1975 population at higher bedrock depths. Ratios are approximately constant for large cities of different populations, which provide the bulk of the identifying variation in heights, as is discussed in Section 2.3. While the model in Section 4 formally describes $\frac{d\ln Y}{d\theta}$ following the logic discussed above, with conversions from $\frac{d\ln Y}{d\ \text{MBD}}$ to $\frac{d\ln Y}{d\theta}$ possible using estimates of $\frac{d\ \text{MBD}}{d\theta}$ calculated from Figure A4, here we intentionally remain agnostic about the exact mechanisms behind the observed city population and built area responses and instead focus directly on using variation in bedrock depth to identify β.

We also use reduced form estimates of β to discipline the model. Height elasticity estimates for a sample of cities we infer to have relatively lax development restrictions are used to fit the parameter governing migration responses to urban utility, which is key for welfare calculations. In a closed city, this parameter is 0, and a lower cost of height manifests as lower floorspace rents and shorter commutes. Empirically, this scenario maps to a large negative built area elasticity and a zero population elasticity, both with respect to heights. As the migration elasticity grows, in-migration responds more, thereby bidding up rents and lengthening commute times. The result is smaller welfare gains for city residents but more opportunities for outsiders. Empirically, this means larger positive population responses and smaller magnitude negative built area responses.

Long difference regressions of the form in Eq. (7) make up the heart of our empirical analysis. Our primary dependent variables of interest $\Delta \ln Y_{ac}$ are the 1975-2015 growth rates of population or built-up area in agglomeration a of country c. Consistent with the first stage specification in Eq. (6), our baseline specification includes controls for a quadratic in mean city bedrock depth, log 1975 city population, and country fixed effects. Robustness checks additionally include controls for potential confounders X_{ac} interacted with log 1975 population.

$$\begin{aligned}\Delta \ln \text{Y}_{ac} = \beta \Delta \ln(\text{Heights}_{ac}+1) + \alpha_1 \text{Bedrock}_{ac} + \alpha_2 \text{Bedrock}_{ac}^2 + \alpha_3 \ln \text{Pop}_{ac75} \\ + X_{ac75}\eta_1 + [X_{ac75} \times \ln \text{Pop}_{ac75}]\eta_2 + k_c + e_{ac}\end{aligned} \tag{7}$$

We primarily examine IV versions of Eq. (7), in which log population in 1975 interacted with a quadratic in city mean bedrock depth enters as instruments for $\Delta\ln(\text{Heights}_{ac}+1)$.

Including the mean bedrock depth controls in Eq. (7) is not necessary for identification but makes it stronger. Without these controls, we would rely on their exclusion from the heights demand equation for identification. While we think it is reasonable that bedrock depth is not a demand factor, results in Section 2.4 show that bedrock depth does not provide much identifying variation in heights on its own except across large cities. Instead, we interact bedrock depth with a static demand factor (log 1975 city population) to generate heights supply shocks.

3.1 Main Empirical Results

Table 3 presents our headline empirical results. Reprising evidence in Table 1, Panel A Column 1 shows that a 100 log point increase in tall building heights leads to about a 13 percent increase in city population. This magnitude of height increase is the average for cities worldwide in the top tercile of 1975 population, while the average city in the developing world had 1975-2015 height growth of 27 log points. Column (2) shows that a 100 log point increase in heights caused the built-up land area of a city to decline by about 16 percent, which is similar to the 18 percent response for total city area (Col. 3). Putting the results in Columns 1 and 3 together, it is clear that exogenous height growth has substantially increased population density. When population density is explicitly put on the left-hand side of the regression, the coefficient is 0.31 (Col. 4). The final column shows results for the growth rate in the total sum of lights at night 1996-2011.[17]

Table 3: Main Empirical Results

Dep. Var.:	(1) Δ ln Pop. 1975-2015	(2) Δ ln Built Area 1975-2015	(3) Δ ln Urban Area 1975-2015	(4) Δ ln Pop Dens 1975-2015	(5) Δ ln Lights 1996-2011
			Panel A: IV Estimates		
Δ ln(Heights+1)	0.13***	-0.16***	-0.18**	0.31***	0.17***
	[0.03]	[0.04]	[0.08]	[0.08]	[0.06]
First Stage F	22.84	22.84	22.84	22.84	16.32
			Panel B: OLS Estimates		
Δ ln(Heights+1)	0.08***	-0.02***	0.10***	-0.02**	0.05***
	[0.00]	[0.01]	[0.01]	[0.01]	[0.01]

Notes: The sample consists of 11,257 cities in developing economies. Eq. (7) shows the specification used. Country fixed effects and controls for ln 1975 city population and a quadratic in city mean bedrock depth are included. (5) uses $\Delta \ln(\text{Heights} + 1)$ for 1990-2015 and ln 1990 city population to construct the instruments. Appendix Table A3 reports coefficients on control variables. Population density is defined using (total) urban area. Robust standard errors in brackets.

One potential concern is that trends in the amenity or productivity values of cities, or other demand factors, may be differentially correlated with bedrock depth in large versus small cities (as of 1975). However, inclusion of a large number of additional controls for physical and economic geographic factors that might be correlated with bedrock depth does not affect results. We select such robustness controls either because they could themselves drive urban change or because they may be correlated with other unobserved variables that do so.

Results of these robustness checks are reported in Figure 5. Row 1 graphs coefficients from the first two columns of Table 3 as benchmarks. Rows 2-6 and 8-11 report corresponding coefficients when additionally controlling for each indicated variable along with its square and interactions with 1975 log city population, thereby mimicking the functional form used for the IV based on bedrock depth. Rows 7, 12, and 13 report coefficients including all indicated controls simultaneously. Rows 14-20 evaluate robustness to dropping portions of the sample.

Inclusion of control variables does not significantly affect coefficients of interest in any case. Indeed, while these variables explain population or built area growth, they are at most only weakly correlated with bedrock depth (correlation ≤ 0.1). Moreover, there is no systematic pattern of bias that appears when adding the controls and their squares interacted with log

[17] Correcting standard errors for arbitrary spatial autocorrelation using a triangular kernel out to 200 km or 400 km, or clustering at the administrative level, barely increases standard errors. The built area equation coefficients are more sensitive to these standard error adjustments but remain significant in all cases (not shown).

1975 population. We consider proximity to coasts or lake shores (measured by both logged Euclidean distances and dummies for whether the city is located within 10 km of the geographic feature), altitude (its mean within the city boundary), ruggedness (Ibid.), earthquake risk (Ibid.), agricultural suitability (Ibid.), and wind speed (Ibid.).[18] Since subway construction can be affected by bedrock depth, we consider dummies for whether the city had a subway and the log number of subway stations in 1975 (or 1975 and 2015).[19] We consider market access, for city i the total sum of the 1975 population of other cities j in the same country weighted by the inverse of Euclidean distance between cities i and j. Lastly, we simultaneously consider the log Euclidean distance from a mine ca. 2010 and the log Euclidean distance from an offshore or onshore oil or gas field ca. 2000. Overall, individually or simultaneously adding these controls may increase or decrease magnitudes of estimates, and this response often (but not always) goes in opposite directions for the population and built area outcomes.[20]

Figure 5: Robustness Checks

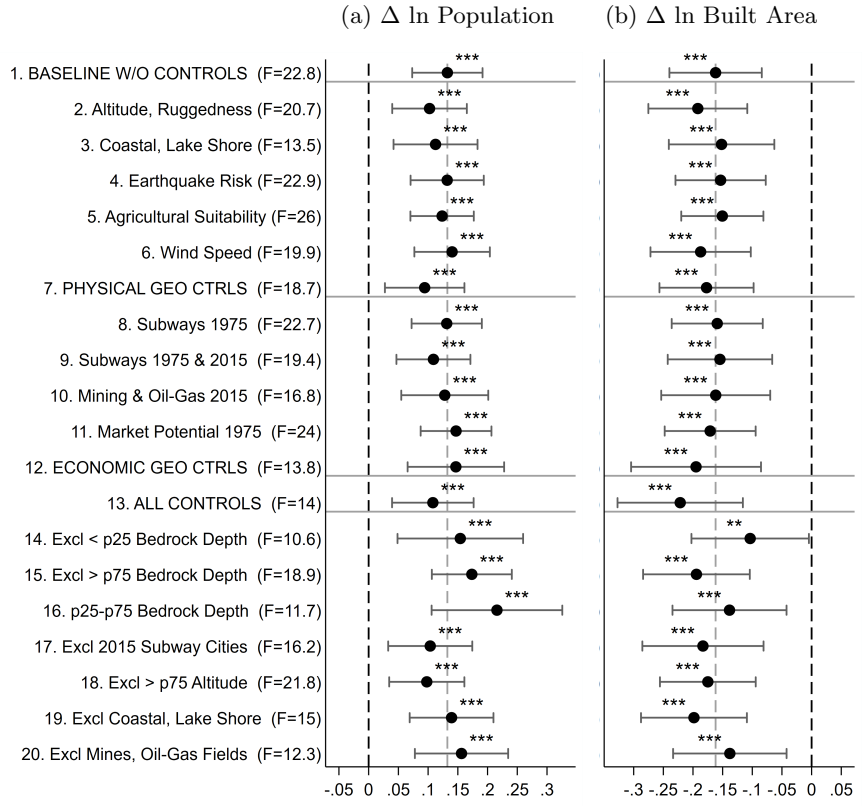

Notes: Rows 2-13: Each row graphs estimated IV coefficients on Δ ln (Heights+1) in regressions with the same specification as in Table 3 with the addition of a quadratic in the control(s) indicated in the row header and interactions of this quadratic with 1975 ln city population. These 4 additional variables per control mimics the functional form used for bedrock depth. Rows 14-20: Cities with indicated attributes are excluded from the sample. 95% confidence intervals.

Excluding quartiles of the bedrock depth distribution (rows 14-16) has no effect. For example, row 14 excludes cities whose mean bedrock depth is shallower than the 25th percentile value in the data (5 m). This excludes cities with exposed bedrock, i.e., more mountainous cities and addresses the potential worry that shallow bedrock may interfere with utilities or roads (highway subbases are less than 1 meter), or may be related to agricultural productivity (only the first 1-2

[18]Results are insensitive to using 5, 10 or 25 km to define coastal and lake shore cities.

[19]The log number of subway stations is very highly correlated (> 0.90) with the log of the total length of the subway network for a global subsample of cities for which there is data on both (not shown).

[20]The R-squared of the second-stage regressions increases by 21%-23% when including all the controls, thus confirming that they have a significant impact on population and built area growth.

meters of soil matter). To our knowledge, subways are the only types of urban infrastructure that can go beyond 5 m in depth but results hold when controlling for subways (rows 9-10) or dropping all subway cities (row 17).[21] Finally, excluding high altitude or coastal cities, which tend to be higher amenity, has no significant effect on the estimates, nor does excluding cities within 50 km of natural resource extraction sites (mines and oil & gas fields) (rows 18-20).

As tall buildings have less usable floor space on higher stories, differences in total heights across cities may not accurately reflect differences in real estate services provided. We use building volume data, which we observe worldwide at the 90x90 m pixel level ca. 2015 (Esch et al., 2023), to construct an alternative measure of real estate services.[22] To measure tall building volumes, we aggregate pixels with an average building height of least 40 m, with this cut-off set sufficiently low so as to capture 55m+ buildings that share pixels with smaller neighboring buildings. The elasticity of this measure to the 2015 sum of heights is 0.93*** (se=0.24). Using log(Building Volume+1) ca. 2015 as the instrumented variable thus returns similar elasticities of 0.13*** (se=0.03) for population and -0.16*** (se=0.05) for built-up area (Table A7).[23]

One potential concern is that short buildings (<55m) are correlated with tall buildings (≥55m). However, more tall building heights actually predicts both more tall building volumes and *lower* total building volumes, meaning that favorable bedrock depth induces a more than 1 for 1 substitution away from floorspace in short buildings to that in tall buildings. That is, evidence using the volumes data corroborates our result that lower costs of height lead to more compact cities. Second, controlling for short building volume does not affect estimated impacts of tall buildings. We think this is a reasonable test, as the construction cost of short buildings should not be influenced by bedrock depth, especially beyond 5 m, to which we show our results are robust (Rankine's Theory implies foundations of less than 5 m for short buildings).

3.2 Additional Considerations

IV vs. OLS: OLS estimates of β in Eq. (7), reported in Table 3 Panel B above, are muted relative to IV estimates, at 0.08 for population and -0.02 for built area. As demand side threats to identification should bias both OLS coefficients in the same direction, we conclude that these smaller magnitudes reflect some combination of measurement error in heights and endogenous supply side forces. If unobserved demand factors, like productivity or amenity shocks correlated with intermediate bedrock depth conditional on 1975 population, were a central endogeneity concern, the OLS population and built area elasticities would both be biased upwards. IV estimates that correct this endogeneity problem would thus be smaller (or more negative) than OLS estimates for both population and built area. Instead, we have attenuation bias. Greater restrictions on tall building construction in growing cities, as has been found in the US (Hsieh and Moretti, 2019), China (Brueckner et al., 2017), and India (Brueckner and Sridhar, 2012), can explain our results. Moreover, local officials in many lagging Chinese cities offer discounted land

[21] Dropping subway countries, not just subway cities, returns similar elasticities with higher standard errors.

[22] Esch et al. (2023) use synthetic aperture radar (SAR) data to create the data. SAR is a satellite sensor system that transmits microwave signals and receives the signals that are reflected back from the Earth's surface. The speed at which a signal "returns" is then used to infer the height of any object on Earth.

[23] The first-stage F statistic (8.34) is lower than before. If we set the cut-off to 55 m instead of 40 m, the F statistic increases (51.45). The estimated elasticities are now lower (and highly significant) but only because the elasticity of volume with respect to heights increases. We verify that the elasticity of population (or area) with respect to tall building heights is equal to the product of the elasticity of population (or area) with respect to tall building volumes and of the elasticity of tall building volumes with respect to tall building heights.

to commercial skyscraper developers (Wang et al., 2023). Greater impediments to construction in more dynamic cities along with the public subsidization of infrastructure construction in lagging cities have been similarly observed for highways in the US (Duranton and Turner, 2012), explaining similar gaps between IV and OLS estimates in that context. IV estimates for built and urban area outcomes are very similar, whereas OLS estimates are not and have opposite signs. The IV estimates correct these implausibly divergent OLS estimates, which may reflect unobservables correlated with heights growth, like transport infrastructure, that are also correlated with growth in undeveloped urbanized land.

Additionally, about one-third of the gaps between OLS and IV estimates can be explained by the fact that they capture different local average treatment effects. Variation across cities within countries with more variation in city size interacted with bedrock depth identifies IV coefficients. In contrast, within-country variation in heights for all countries identifies corresponding OLS coefficients. In developing countries with at least 5 cities and a Gini index of the distribution of mean bedrock depth across cities above the 75th percentile, IV-OLS gaps are one-third smaller.

Functional Forms: Results are not qualitatively sensitive to measures of heights growth that impose different magnitudes for extensive margin comparisons of cities with and without tall buildings in 2015. Chen and Roth (2024) highlights the difficulty of interpreting treatment effect estimates that combine extensive and intensive margin responses and the perils of arbitrary scaling. We view a scaling factor of 1 meter (Δln(Heights+1)) as an upper bound on the treatment distance between cities with and without tall buildings and a scaling factor of 55 m as a lower bound. We have two types of treatments: one for having any tall buildings, and one for the amount of tall buildings conditional on having tall buildings. It is complicated to empirically separate out estimates of intensive margin effects because doing so introduces selection challenges, reduces statistical power over the lower part of the support of the 1975 population distribution, and requires an additional source of identifying variation.

Estimated extensive margin treatment effects, which measure heights growth as a dummy variable for any city 1975-2015 tall building construction, are 1.16*** for population (se=0.32) and -1.43*** for built area (se=0.42). Relative to our baseline results, we show robustness to the following alternative treatments of the extensive margin: i) using a building height cutoff of 100 m rather than 55 m, ii) excluding cities with 1975 populations of less than 150,000,[24] iii) using Δ ln(Heights+55) as the treatment variable, and iv) using asinh(Heights) or asinh(Heights/1000) as the treatment. Results are in Table A4. The use of intensive margin comparisons that are closer to the base, by using a base of 55 rather than 1 for example, grows coefficient magnitudes and reduces first stage power. Focusing on larger cities only (increasing weighting of intensive margin comparisons) reduces estimated treatment effects, though they remain highly significant. Standardized coefficients are more stable across specifications and samples. Ultimately, the scaling factor, of 1 versus 55 for example, is immaterial for welfare implications.[25]

Our IV strategy respects monotonicity conditions (Table A5). We replace the bedrock depth polynomial with a piece-wise linear spline function, in which one kink captures the "optimal" bedrock depth and a second kink captures the point beyond which bedrock depth no longer affects the cost of height. The first-stage F-statistic is maximized with the first kink at a bedrock depth of 20 m and the second kink at the maximum depth observed in the data of

[24] In our data, tall buildings only significantly appear in cities with populations above 150,000.

[25] The simulated method of moments procedure used to fit the model in Section 4 adjusts appropriately.

158 m (results insensitive to using 80-158 m). This specification allows us to demonstrate that variation in bedrock depth on both sides of the optimal depth each contributes to identification. When including the spline as two separate instruments, first stage coefficients on distance to the kink are 0.043*** (se=0.006) on the deep bedrock side of 20 m and 0.033*** (se=0.008) on its shallow bedrock side, yielding population and built area elasticities of 0.16*** (se=0.03) and -0.22*** (se=0.04), respectively (F=26.6). Only using variation within shallow bedrock depths and controlling for 1975 log city population interacted with bedrock depth greater than 20 m, population and built area elasticities are 0.17*** (se=0.05) and -0.35*** (se=0.09), respectively. Conversely, using only deep bedrock depths, we find 0.16*** (se=0.03) and -0.23*** (se=0.04), respectively. These deeper bedrock comparisons allay potential concerns that shallow bedrock depths are correlated with above-ground factors that may drive the outcomes of interest.[26]

In our main city population growth regression, log city population in 1975 appears in the dependent variable, as a component of the instrument, and as a control variable. Table A6 shows results are robust to various strategies for controlling for base year urban demand conditions if we: (i) also include log built area in 1975 as a control, which is especially relevant for the built area regressions; (ii) carry out the analysis for 1990-2015 while continuing to use log city population in 1975 to construct the instruments and as a control; and (iii) use log population 2015 as the outcome and log heights 2015 as the instrumented variable.

Interpretation: Our estimated elasticities primarily capture migration of people from rural areas to cities rather than displacement between cities. Borusyak et al. (2022) demonstrates the econometric challenges associated with endogenous migration flows between regions in the empirical setting in which local outcomes are regressed on exogenous location-specific shocks. As our data does not include rural units, our analysis is not subject to these biases provided that city growth in response to exogenous heights draws from the hinterland rather than from other cities. With an average UN measured urban share of ∼25% and very few tall buildings in 1975, our context is one of primarily rural-to-urban migration. This setting matches that of developed economies in history and our finding, discussed below, of similar population elasticities in the developed world for periods starting in 1850 as those for developing economies in 1975-2015.

We carry out three types of exercises to evaluate the prevalence of displacement in our data. First, we explore robustness to different levels of regional and sub-national fixed effects. As migration occurs at higher rates more locally, we expect there to be greater displacement between cities within fixed effects covering smaller regions. If coefficient estimates do not grow with the use of more local fixed effects, that is evidence that our estimated elasticities reflect rural-urban migration. Second, we explore robustness to a sub-sample that only includes countries with UN measured urbanization rates below 20% in 1975, in which case the vast majority of migrants to cities must have come from rural areas. Finally, in the spirit of Borusyak et al. (2022), we control for height changes in alternative cities that are likely to be viewed by migrants as substitutes.[27]

Table A8 shows the results of the first two exercises. IV estimates for population grow by at most 0.03 when including finer fixed effects (e.g., regions or districts) and decline by 0.03 when using world sub-region rather than country fixed effects. Table A8 also shows results for the sample restricted to countries that were less than 20% urban in 1975. The population elasticity

[26] Results also hold if we add the bedrock variables as excluded instruments instead (Table A6).

[27] Fully carrying out the proposed fix in Borusyak et al. (2022) requires observing migration flows in a base period; unfortunately, this information is unavailable for most countries in our global data.

remains stable at 0.13. Built area elasticities are somewhat more sensitive to the inclusion of various levels of fixed effects and sample. These estimates grow in magnitude to as much as -0.25 with alternative fixed effects. However, the elasticity shrinks to -0.08 for rural countries. None of these estimates are statistically different from our primary built area elasticity of -0.16.

For the third exercise, we calculate market potential (MP) terms that summarize accessibility of each city a in country c to other population centers and their heights in year t:

$$\text{MP}^H_{act} = \sum_{a' \in C(a), \neq a} \frac{\text{Heights}_{a'ct} \ \text{Pop}_{a'c75}}{\text{Pop}_{ac75} \ \text{Distance}(a, a')^{\alpha}}. \tag{8}$$

That is, we sum over heights in all other cities in the country of city a, scaling by relative city size and discounting by the distance between city a and a' raised to the power α, which we vary between $\frac{1}{3}$ and 3. From these measures in 1975 and 2015, we build the control variable $\Delta \ln \text{MP}^H_{act}$. With this specification, heights in MP^H_{act} are scaled to be of comparable magnitudes to heights in city a itself. A given percentage increase in heights on a small base will have the potential to redirect fewer migrants as a share of city a's 1975 population than on a large base.

As heights in other cities may be endogenous to trends in demand factors in city ac, we build an instrument for $\Delta \ln \text{MP}^H_{act}$ that follows the same logic as our instruments used in the main analysis. These instruments replace $\text{Heights}_{a'c75}$ in Eq. (8) with $\text{Pop}_{a'c75}\text{Bedrock}_{a'c}$ and $\text{Pop}_{a'c75}\text{Bedrock}^2_{a'c}$. As in Eq. (7), we also control for three additional terms capturing the discounted sums of 1975 city populations and bedrock depths by replacing Heights_{ac75} in Eq. (8) with $\text{Pop}_{a'c75}$, Bedrock_{ac}, or Bedrock^2_{ac} and taking logs. Lastly, since MP^H in Eq. (8) also directly includes $\frac{\text{Pop}_{a'c75}}{\text{Pop}_{ac75}}$, we create an additional MP term based on these relative 1975 city populations only.

Table A9 shows the results with these MP controls. We find no evidence that displacement effects between cities are driving elasticity estimates. We show OLS results for $\alpha = 0.33, \alpha = 0.5$ and $\alpha = 1$, and both OLS and IV results for $\alpha = 2$ and $\alpha = 3$. As bedrock depth tends to be spatially correlated, we need strong spatial decay in order for instruments to be able to separate out height growth in other cities from that in city ac. But whether instrumenting for $\Delta \ln \text{MP}^H$ or not, estimated population and built area elasticities remain very stable. We come to the same conclusion when separately considering the largest 10 cities and the other cities in the country in MP terms (and assuming a lower distance decay parameter for larger cities) or when controlling separately for height growth in each of these cities (unreported). The coefficient on the height MP control is zero or positive when instrumented, which may reflect a growth effect of improved access to markets. The lack of movement in our elasticity estimates of interest suggests that MP terms are conditionally uncorrelated with our instruments for height growth in city ac.

Implied Aggregate Impacts of Tall Buildings: While model-based counterfactuals reported in Section 4 are best suited for determining magnitudes by which reductions in the cost of height have influenced urbanization and land savings, here we provide a rough sense of the magnitudes implied by reduced form estimates. Taking observed 1975-2015 tall building construction as given, IV estimates imply that 18% of 2015 urban population in developing economies is accommodated and 15% of 2015 urban built up land (and 10% of urbanized land) remains as open space or rural because of this construction. As cities over 1 million residents in 1975 constructed 82% of developing world heights over the 1975-2015 period, large cities account for the majority of these changes. In these cities, 47% of the 2015 population is accommodated

because of tall buildings, absent which 2015 built area would be 28% greater.

For each city with 1975-2015 height growth, we allocate predicted land savings to a buffer around each city boundary obtained from the predicted built-up area change. Aggregating ca. 1982 land uses within these buffers, we find that 12% of land saved is tree canopy and 73% is non-tree vegetation (including cropland). This analysis uses the satellite-based 1982-2015 ≈5X5 km pixel resolution *Global Land Change Database* (Hansen and Song, 2018).[28]

3.3 Estimated Heterogeneity

Regional: Column (1) of Table 4 presents population and built area growth coefficients for all developing economy cities in Asia except the Middle East of 0.17 and -0.20, respectively. Other cities in the developing world generate similar estimates of 0.15 and -0.26, though these are slightly underpowered (F-stat. = 7.9; (2)). (3) presents results for developing economies that have relatively lax building restrictions. We defer the discussion of these results to Section 3.5.

Table 4: IV Results by World Region and Time Period

	(1)-(3) Developing Economies (1975-2015)			(4)-(6) Developed Economies		
	Asia (no Middle-East)	Other Countries	Unconstrained Countries	1975-2015 All	1850-1975 (Historical) 55 Developed	39 European
			Panel A: Δ ln Population			
Δ ln(Heights+1)	0.17***	0.15**	0.21***	0.00	0.14**	0.20**
	[0.03]	[0.07]	[0.04]	[0.03]	[0.06]	[0.10]
			Panel B: Δ ln Built Area			
Δ ln(Heights+1)	-0.20***	-0.26***	-0.39***	-0.04	-	-
	[0.04]	[0.09]	[0.09]	[0.03]	-	-
First Stage F	20.92	7.88	11.36	14.28	10.94	5.51
Observations	6,990	4,267	5,315	1,592	918	1,095

Notes: Each entry is from a separate IV regression using data from cities in world regions indicated in column headers over the indicated time period. "Asia (no Middle-East)" refers to developing economies in Asia except the Middle East (as of 2015). "Unconstrained" refers to 38 countries with no history of communism and with below median regulatory environments. Section 3.5 explains in more detail how this sample is selected. "55 Developed" refers to 918 cities in 55 developed countries (as of 2015) during the period 1850-1975 (source: Buringh and Hub (2013)). "39 European" refers to 1,095 cities in 39 European countries from Portugal to Russia (source: Bairoch (1988)). (5)-(6) The instrumental variables are the interactions of ln 1850 city population with bedrock and bedrock^2. We also control for country fixed effects, ln 1850 city population, and a quadratic in city mean bedrock depth. Robust SEs in brackets.

Estimates for developed economies (4) are subject to more complicated interpretation, as large cities in developed economies had significant heights in 1975. Moreover, these countries had largely completed their rural-to-urban transitions by 1975. While we find no overall average impact of heights in developed economies for the 1975-2015 period, estimated coefficients are quite large in magnitude, though under-powered, for cities in the USA and Canada (unreported).
Historical: To further understand why estimates differ for developing and developed economies, we look back in time to 1850-1975 for two separate samples of developed economy cities. During this period, they experienced similar phases of development as in many developing economies in 1975-2015. The specifications are the same as above except for the different base year. We

[28]Regressions similar to those in Table 3 but with changes in various land use measures *within* urbanized areas as dependent variables reveals that an approximate doubling of heights increased urbanization of 2015 UC land by 21% on a base average of 21 percent between 1982 and 2015 (not shown). Tall building construction caused about equal amounts of this newly urbanized land to be converted from tree cover and short vegetation. Total amounts of short vegetation and forested land at the edges of cities saved by tall building construction is about twice the total amount of vegetated land lost inside urbanized regions.

find population elasticities of 0.14** for the world (5) and 0.20** for Europe (6), though the Europe estimate is underpowered. Estimates for developing economies in the modern era are reassuringly in line with those for the currently developed world in its own period of development.

Building Use: While we observe building use in the Emporis data, we do not have separate instruments for commercial versus residential heights. Instead, we exploit the fact that country-specific industrial structure and land use planning regimes influence the extent to which tall buildings host residential or commercial tenants. For example, Egypt and Pakistan have ∼50% of their tall buildings dedicated to commercial uses whereas Brazil and India have >90% of tall buildings in residential use. Because the residential share of tall buildings is in part driven by country-specific factors, we can learn about impacts of the construction of residential versus commercial heights by restricting the sample to only countries with at least some baseline share of tall buildings in residential use. Figure A5 shows estimates by country residential share of tall buildings. Cities in countries that built more residential heights accommodated more population and saved more land. Population elasticities rise from 0.13 to 0.21 when moving from the sample of developing world countries with at least 50% of tall buildings residential to those with at least 90% residential. The residential impact is even greater for built area as built area elasticities decline from -0.13 to -0.50. As residential real estate is much more space intensive than offices per-capita, it is not surprising that residential buildings have bigger effects. The model developed in the following section is parameterized to respect this observation.

3.4 City Height Gaps

One aim of the model is to quantify the implications of allowing unrestricted heights in cities worldwide. This calculation requires measures of the extent to which each city constrains tall building construction. To this end, our "height gap" measure is the fraction of potential heights in each city justified by fundamental supply and demand conditions that has not been realized.

We follow Barr and Jedwab (2023) to determine each city's potential heights under no height constraints. Their regression model predicts city log heights using fundamental demand and supply factors across cities (excluding land use regulation). They consider 12,755 GHS-UCDB cities worldwide for the years 1995, 2000, 2005, 2010, 2015, and 2020. Predictors in this regression are measures of city lights at night and city population category interacted with quadratics in national per-capita GDP, as well as city population category interacted with quadratics in mean bedrock depth, earthquake risk, elevation and ruggedness, country population and area, all additionally interacted with year fixed effects. (See Appendix B for details.) The R-squared is 0.64. Resulting 2015 predicted heights are measures of the heights justified by each city's fundamental demand and cost factors (including bedrock itself) absent local regulation.

After ordering cities by their *predicted* log heights in 2015, we calculate the 95$^{\text{th}}$ percentile (3rd ranked city) of *actual* log height in 2015 for the moving window of 51 cities centered on each city in the data (except the top and bottom ranked 24 cities). This accommodates the possibility that one or two cities in each group of 51 has built particularly tall for idiosyncratic reasons that do not carry over to other cities. We smooth this 95$^{\text{th}}$ percentile function using local polynomial regression. The resulting function of predicted log heights, $h^{95}(\cdot)$ describes our inferred "unconstrained" heights. We also consider the 75th percentile function in robustness analysis.[29] The height gap measure for city ac follows as

[29] Brueckner et al. (2017) use land lease data to measure the stringency of land use regulation for 200 Chinese

$$\text{Gap}_{ac} = \max\left(1 - \frac{\text{Heights}_{ac2015}}{H^{95}(\widehat{\text{LHEIGHTS}}_{ac2015})}, 0\right), \tag{9}$$

where $H^{95}(\cdot) = \exp[h^{95}(\cdot)]$ and $\widehat{\text{LHEIGHTS}}_{ac2015}$ is predicted log heights for city ac in 2015. Gap_{ac} is between 0% and 100%. We emphasize that while this measure is reasonable on average conditional on observables and is plausible for most cities, it will not accurately measure building constraints in every city worldwide.[30] At the regional level, the population weighted height gaps are larger in developed economies in Oceania (90%), Europe (85%), and North America (77%), and smaller in developing economies in Asia (41%), Africa (48%), and Latin America (63%). These magnitudes reflect the greater real estate demand in developed economies along with the fact that Asian cities have expanded their stock of heights the most in the developing world.

3.5 Model-Relevant Estimates

Under its baseline parameterization, the model developed in the next section describes an environment in which fundamental supply and demand forces determine a city's equilibrium heights, population, and area. As such, we estimate the model under a baseline parameterization without height limits. Model quantification thus requires elasticity estimates for a sub-sample of cities that are unregulated. In order to maintain the same specification and identification assumptions as for the empirical analysis on the broader sample, we select this unconstrained city sample to include all cities in the most unregulated countries (with the lowest height gaps).

We use the same 2015 city-level residuals used in the first step of constructing city height gaps (Section 3.4). We aggregate these to the country level with 2015 city population weights. We then select all cities in developing countries without a history of Communism with an aggregated residual above 0, yielding a sample of 5,315 cities in 38 economies. The elasticity estimates for this sample, reported in Column (3) of Table 4, are larger than our broader average estimates reported in Table 3. We find an unconstrained population elasticity of 0.21*** (se=0.04) and an unconstrained built area elasticity of -0.39*** (se=0.09). We find similar estimates when further restricting the sample to exclude cities constrained by water and/or mountains (unreported).

4 Theoretical Analysis and Quantification

This section develops a theory that facilitates conceptual and quantitative analyses of the role of tall buildings in economic development. Comparative statics of city population and land area with respect to the cost of height clarify the mechanisms through which reductions in the cost of height promote densification and growth. Examination of model counterfactuals facilitates quantifications of the benefits of reducing the cost of height and removing height restrictions. The model follows in the tradition of Muth (1969)'s monocentric city land use model with endogenous housing supply. This setup draws from Ahlfeldt and Barr (2022), incorporating an expanded version of the real estate development technology in Section 2.2. It adds migration frictions through heterogeneity in tastes for urban life (McFadden, 1974), incorporating ideas from Harris

cities in 2002-11. Using their cleaner "matched" sample, we find a stronger correlation between their measure and height gaps calculated based on the 95th percentile (0.66) than the 75th percentile (0.41).

[30] As examples, gaps are 0% for Chicago, Kuala Lumpur, Sao Paulo, Seoul and Shanghai (within their predicted heights bin, they are cities at, or above, the 95th percentile value in actual heights), 11% for Guangzhou, 26% for NYC, 45% for Miami, 51% for Jakarta, 66% for London and Mexico City, 68% for Bogota, 70% for Boston, 75% for Houston, 80% for Buenos Aires, 82% for L.A., 86% for Washington DC, 91% for Karachi, and 93% for Cairo.

and Todaro (1970), Bryan and Morten (2018) and Desmet et al. (2018) to accommodate rural-urban migration. Imperfect mobility means that urban population *and* the utility of urban residents are endogenous objects. This "representative city" model is intended to be flexible enough to capture forces that link tall building construction to urban growth and change that are common to cities of different shapes, sizes, and stages of development.

The model incorporates standard features that facilitate quantification of the economic benefits of building tall. The higher population and employment densities in cities with more heights are associated with greater agglomeration forces in production and reduced commuting costs. Additional agglomeration benefits accrue through the greater overall city populations in taller cities. Of course, there may be additional benefits of heights beyond those in the model. These include enhanced city reputation and reduced environmental costs (Glaeser and Kahn, 2010). Our model also does not accommodate many of the potential negative externalities associated with tall buildings (Gyourko and McCulloch, 2024). These may include light pollution, the casting of shadows on nearby properties, congestion disamenities, loss of historical character, and disruptions associated with construction. Since we focus on the economic benefits of tall buildings, our analysis provides estimates against which these potential social and environmental costs of tall buildings can be compared.

4.1 Model Setup

We expand on the standard urban model with endogenous heights (Duranton and Puga, 2015; Albouy et al., 2020) by allowing rural residents the discrete choice of entering the city, following Ahlfeldt et al. (2022)'s approach to modeling labor market entry. Thus, we obtain an *imperfectly* open city which nests the conventional closed-city and open-city versions of the monocentric model as special cases. The model generates a positive (finite) height elasticity of population and a negative height elasticity of area, as observed in the data, through a floor space supply channel. These responses strike a balance between the zero population and large negative area elasticities in a closed-city model (Alonso, 1964) and the large population and small *positive* area elasticities in an open-city model with agglomeration forces (Ahlfeldt and Barr, 2022).

Environment: We consider a circular city of endogenous radius. The city is embedded in a region of $\bar{N}$ workers, which also has a rural hinterland. $\mathcal{L}(x) = 2\ell\pi x$ units of land are available for development at each distance x from an exogenously located historic city center, where $\ell = [0, 1]$ is the fraction of land that is developable. The area beyond the endogenous city margin at $x = x_1$ is the rural hinterland.

Workers: All workers are ex-ante identical and choose to live inside or outside the city. The utility of worker ν is described by:

$$U(\nu) = \max_{o}[U^o \exp(a^o(\nu))], \tag{10}$$

where $o \in \{inside, outside\}$ and $a^o(\nu)$ is an idiosyncratic taste shock for living in location o. Workers living in the agricultural hinterland receive an exogenous subsistence utility $U^{o=outside} = \widetilde{U}^{1/\zeta}$. All workers choosing to live in the city enjoy the same endogenous utility $U^{o=inside} = \bar{U}$. The idiosyncratic shocks $a^o(\nu)$ are drawn from the same Gumbel distribution with distribution function

$$G(a^o(\nu)) = \exp[-\exp(-\zeta a^o(\nu) - \Gamma)]. \tag{11}$$

$\zeta > 0$ is the taste dispersion parameter and Γ is the Euler-Mascheroni constant, included so that the Gumbel shocks are mean zero.

Utility maximization delivers the urban population N as share μ of region population $\bar{N}$.[31]

$$N = \mu\overline{N} = \frac{\overline{U}^{\zeta}}{\overline{U}^{\zeta} + \widetilde{U}}\overline{N} \tag{12}$$

The elasticity of urban population with respect to urban utility (the migration elasticity) is $\zeta(1-\mu)$, with $1-\mu$ reflecting the stock of available rural residents at risk of moving to the city.

City utility depends on a local amenity A, tradeable goods consumption g, and residential floor space f^R. Each worker's choice of residential location, on floor s in a building located at CBD distance x, must deliver the same utility level $U(x,s) = \bar{U}$ in equilibrium. Utility is Cobb-Douglas with a floor space expenditure share of $0 < (1-\alpha^R) < 1$. Put together,

$$U(x,s) = A^R(x,s)\Big(\frac{g}{\alpha^R}\Big)^{\alpha^R}\Big(\frac{f^R(x,s)}{1-\alpha^R}\Big)^{1-\alpha^R}. \tag{13}$$

The local amenity decays with distance from the center and rises with height:

$$A^R(x,s) = \bar{a}^R e^{-(\tau^R \max(0, x-\underline{x}^R))} s^{\tilde{\omega}^R}.$$

$\tilde{\omega}^R > 0$ is the height elasticity of the residential amenity (from better views or less exposure to noise). $\tau^R > 0$ determines the rate at which utility declines in distance from the edge of a central district located at $x = \underline{x}^R$, with $\bar{a}^R$ the amenity within this district. $\tau^R > 0$ generates the centripetal force of rising residential demand nearer to the center and can be interpreted as the utility cost of commuting an additional unit distance. A change in average population-weighted $A^R(x,s)$ can thus be viewed as measuring the (negative) change in commuting cost.

Workers face the budget constraint

$$y = p^R(x,s)f^R(x,s) + g,$$

in which the endogenous wage y can be spent on housing, with endogenous unit price $p^R(x,s)$, and the numeraire tradeable good.

Utility maximization and imposing $U(x,s) = \bar{U}$ yields the residential floor space bid rent for location (x,s) of

$$p^R(x,s) = A^R(x,s)^{\frac{1}{1-\alpha^R}} y^{\frac{1}{1-\alpha^R}} \bar{U}^{-\frac{1}{1-\alpha^R}}. \tag{14}$$

Averaging across all floors of a residential building of height $S^R(x)$ at every location delivers the horizontal residential bid rent

$$\bar{p}^R(x) = \frac{1}{1+\omega^R}\left[\frac{\bar{a}^R y}{\bar{U}} e^{-(\tau^R \max(0, x-\underline{x}^R))}\right]^{\frac{1}{1-\alpha^R}} S^R(x)^{\omega^R}, \tag{15}$$

where $\omega^R = \frac{\tilde{\omega}^R}{1-\alpha^R}$ is the height elasticity of residential rent. This follows the form asserted in Section 2.2. $\bar{p}^R(x)$ is declining in distance to the center x both because of declining amenities, as captured by $\tau^R > 0$, and declining equilibrium building heights $S^R(x)$.

The mass of residents at each location in the residential zone, in which residential use outbids commercial and agricultural use, is

[31] See Ahlfeldt et al. (2022) for a formal derivation. This is almost isomorphic to using Frechet random utility draws with dispersion parameter ζ, with the advantage that this formulation justifies cases in which $0 < \zeta < 1$.

$$n(x) = \frac{\mathcal{L}(x)S^R(x)}{y^R}\frac{\bar{p}^R(x)}{1-\alpha^R}. \tag{16}$$

In this expression, higher housing costs are associated with higher population densities.

Firms: Atomistic perfectly competitive firms produce the tradeable good using labor l and commercial floor space f^C with the Cobb-Douglas production function

$$g(x,s) = A^C(x,s)\left(\frac{l}{\alpha^C}\right)^{\alpha^C}\left(\frac{f^C(x,s)}{1-\alpha^C}\right)^{1-\alpha^C}. \tag{17}$$

Productivity at each location is shifted by

$$A^C(x,s) = \bar{a}^C N^\beta e^{-(\tau^C \max(0, x-\underline{x}^C))} s^{\tilde{\omega}^C}.$$

$\tilde{\omega}^C > 0$ is the height elasticity of productivity, capturing benefits such as signaling and workplace amenity effects. The agglomeration elasticity $\beta > 0$ describes how productivity increases in city employment N. $\tau^C > 0$ determines the rate at which productivity declines in distance from the edge of a central urban core at $\underline{x}^C$, with $\bar{a}^C$ the exogenous productivity within this core.[32] Profit maximization and zero profits delivers the commercial bid rent

$$p^C(x,s) = A^C(x,s)^{\frac{1}{1-\alpha^C}} y^{\frac{\alpha^C}{\alpha^C-1}}. \tag{18}$$

Averaging across all floors of a commercial building with height $S^C(x)$ at each location x delivers the horizontal commercial bid rent

$$\bar{p}^C(x) = \frac{1}{1+\omega^C}\left[\bar{a}^C N^\beta e^{-(\tau^C \max(0, x-\underline{x}^C))}\right]^{\frac{1}{1-\alpha^C}} y^{\frac{\alpha^C}{\alpha^C-1}} S^C(x)^{\omega^C}, \tag{19}$$

where $\omega^C = \frac{\tilde{\omega}^C}{1-\alpha^C}$ is the height elasticity of commercial rent. This form resembles Eq. (15).

Labor demand at each location in the central commercial zone is

$$L(x) = \frac{\alpha^C}{1-\alpha^C}\frac{\bar{p}^C(x)}{y^C}\mathcal{L}(x)S^C(x). \tag{20}$$

This expression reflects the unitary elasticity of substitution between labor and floor space embodied in the Cobb-Douglas production technology.

Developers: We extend the representative developer's problem laid out in Section 2.2 to index by type of use, commercial (C) or residential (R). Using Eq. (15) for residents and Eq. (19) for firms, the use-specific profit-maximizing building height matches Eq. (3), indexing all parameters by use.[33]

The developer may be subject to a height limit $\bar{S}^U$ imposed by the planning system. Conditional on building type U, the developer's resulting choice of height is thus

$$\tilde{S}^U(x) = \min(S^{*U}(x), \bar{S}^U). \tag{21}$$

Inserting into Eq. (2) and imposing zero profits, we obtain the use-specific bid rent for land[34]

$$r^U(x) = a^U(x)\left[\tilde{S}^U(x)\right]^{1+\omega^U} - c^U\left[\tilde{S}^U(x)\right]^{1+\theta^U}. \tag{22}$$

[32] By flattening the amenity and productivity in the central urban core, we avoid the peaking of bid-rents and profit-maximizing heights at unrealistically high levels at the most central point in the city.

[33] We require $\theta^U > \omega^U$ and $p^U(x) > c^U(1+\theta^U)$ for the solution to be well-behaved.

[34] $a^C(x) \equiv \frac{1}{1+\omega^C}[\bar{a}^C N^\beta e^{-(\tau^C \times \max(0, x-\underline{x}^C))}]^{\frac{1}{1-\alpha^C}} y^{\frac{\alpha^C}{\alpha^C-1}}$ and $a^R(x) \equiv \frac{1}{1+\omega^R}[\frac{\bar{a}^R y}{U} e^{-(\tau^R \max(0, x-\underline{x}^R))}]^{\frac{1}{1-\alpha^R}}$.

If planning restrictions do not bind, this function is declining in distance from the center x.

Spatial Equilibrium: For given values of the city-wide endogenous objects $\{y, N, \bar{U}\}$, all location-specific endogenous variables are uniquely determined. We obtain floor space rents from Eqs. (15) and (19), heights from Eq. (21), and use-specific land rents from Eq. (22). Land use then goes to the highest bidder at each location x given agricultural bid-rent r^A. Under the restriction that the commercial rent gradient is steeper than the residential rent gradient, which is consistent with plausible parameter values and empirical evidence, there is a distance x_0 at which commercial and residential land rents equate: $r^C(x_0) = r^R(x_0)$. At shorter distances, commercial developers outbid residential developers when competing for land; thus x_0 defines the boundary of the central business district (CBD).[35] Similarly, there is a distance x_1 at which residential and agricultural land rents intersect, $r^R(x_1) = r^A$, and the city ends.

General equilibrium: Aggregating labor supply in Eq. (16) and labor demand in Eq. (20) across the city, the labor market must clear at the city population N.

$$N = \int_{x_0}^{x_1} n(x)dx = \int_0^{x_0} L(x)dx \tag{23}$$

This implies an equilibrium wage of

$$y = \frac{\alpha^C}{1-\alpha^C} \frac{\int_0^{x_1} \bar{p}^C(x)\mathcal{L}(x)S^C(x)dx}{N}. \tag{24}$$

Aggregate housing market clearing is then

$$(1-\alpha^R)yN = \int_{x_0}^{x_1} \bar{p}^R(x)\mathcal{L}(x)S^R(x)dx. \tag{25}$$

Inserting Eq. (15) into Eq. (25) delivers equilibrium urban utility

$$\bar{U} = \left[\frac{\frac{1}{1+\omega^R} y^{\frac{1}{1-\alpha^R}} \int_{x_0}^{x_1} \tilde{A}(x)^{\frac{1}{1-\alpha^R}} (S^R(x))^{(1+\omega^R)} \mathcal{L}(x)d(x)}{(1-\alpha^R)yN} \right]^{1-\alpha^R}. \tag{26}$$

Eqs. (12), (24), and (26) constitute the exactly identified system of equations that determines the general-equilibrium constants $\{y\,(\text{wage}), \bar{U}\,(\text{reservation utility}), N\,(\text{urban population})\}$.

Welfare: Expected utility across all workers living inside and outside of the city is[36]

$$\mathcal{V} = \left(\widetilde{U} + \overline{U}^{\zeta} \right)^{\frac{1}{\zeta}}. \tag{27}$$

The aggregate land rent is

$$\mathcal{R} = \int_0^{x_0} r^C(x)\mathcal{L}(x)dx + \int_{x_0}^{x_1} r^R(x)\mathcal{L}(x)dx + \int_{x_1}^{\bar{x}} r^A\mathcal{L}(x)dx. \tag{28}$$

These rents are paid by urban firms, urban resident-workers, and rural resident-workers, respectively, to absentee landlords.

4.2 Comparative Statics

Here we discuss how equilibrium population, built area, heights, and expected utility change with a reduction in the cost of height θ. As rural utility is exogenous, the welfare consequences of any such shock can be determined by assessing the resulting change in urban utility $\bar{U}$.

[35] In our quantification, two parameter restrictions together ensure a commercial center surrounded by a residential area. The housing share in production is smaller than the housing share in consumption and $\tau^C > \tau^R$.

[36] See Ahlfeldt et al. (2022) for a formal derivation.

Differentiating the indirect utility function derived from Eq. (13), urban utility can change because of changes in wages y, housing rents $\bar{p}^R$, and/or commuting costs (here implicitly captured by local amenities $\bar{A}^R$) according to the following decomposition:

$$\mathrm{d}\ln \bar{U} = \mathrm{d}\ln y - (1-\alpha^R)\mathrm{d}\ln \bar{p}^R + \mathrm{d}\ln \bar{A}^R \tag{29}$$

Rents $\bar{p}^R$ and local amenities $\bar{A}^R$ can be measured as a population-weighted average across all locations in the city or at any one location. In simulations below, we quantify the importance of each of these three forces. Here we briefly summarize the logic of each one.

The wage changes for five reasons. First, localized agglomeration forces A^C change as firms operate in taller buildings. Second, there are stronger citywide agglomeration forces N^β. Third, there is substitution away from labor as property prices decline, shifting labor demand inwards (assuming factors are substitutable). Fourth, given the fixed output price, a scale effect shifts labor demand outwards. Finally, an outward shift in labor supply depresses the wage, as taller buildings facilitate higher residential amenities. In simulations below, these sum to a positive impact of reductions in the cost of height on the wage.

Residential rents change for three reasons. First, the supply effect reduces rents conditional on location and urban population. Second, a location effect centralizes the population, affecting average rents. Third, the migration effect bids up rents. In simulations below, rents hardly change, as real wage increases draw in enough population to counteract the supply effect.

Finally, average local amenities increase (commuting costs decline) with lower costs of height. This comes from centralization of the population into higher densities.

Revealed preference indicates that urban utility must increase with reductions in the cost of height given a finite migration elasticity. City population growth in response to a reduction in the cost of height reflects the urban welfare benefits of heights in the model.

Table 5: Baseline Parameterization

	Parameter	Value	Source
$1-\alpha^C$	Share of floor space in production	0.15	Lucas and Rossi-Hansberg (2002)
$1-\alpha^R$	Share of floor space in consumption	0.33	Combes et al. (2019)
β	Agglomeration elasticity in production	0.03	Combes and Gobillon (2015)
θ^C	Commercial height elasticity of construction cost	0.5	Ahlfeldt and McMillen (2018)
θ^R	Residential height elasticity of construction cost	0.55	Ahlfeldt and McMillen (2018)
ω^C	Commercial height elasticity of rent	0.03	Liu et al. (2018)
ω^R	Residential height elasticity of rent	0.07	Danton and Himbert (2018)
τ^C	Production amenity decay	0.014	See text and Appendix Section C.2
τ^R	Residential amenity decay	0.016	See text and Appendix Section C.2
ζ	Preference heterogeneity	3.3	See text and Appendix Section C.2

Notes: We set the scale parameters to $\bar{a}^C = \bar{a}^R = 2, c^C = c^R = 150$, $r^A = 50$, $\bar{N} = 6$ million, $\ell = 0.5$, $\bar{x} = 100$ km and invert $\tilde{U}$ so that $\mu = 0.5$. In the baseline parameterization, height limits are not binding ($\bar{S}^C = \bar{S}^R = \infty$).

4.3 Quantification

Given parameters $\{\alpha^U, \beta, \omega^U, \theta^U, \tau^U, \underline{x}^U, \bar{a}^U, c^U, \bar{S}^U, r^A, \zeta, \ell, \tilde{U}\}$ and endowments $\{\bar{N}, \bar{x}\}$, we solve for the endogenous objects $\{y, N, \bar{U}\}$ and the functions $\{L(x), n(x), \bar{p}^U(x), r^U(x), \tilde{S}^U(x)\}$ using the numerical procedure described in Appendix C.1. Table 5 lists parameter values associated with our baseline analysis for a city of 3 million with brief rationales below. See Appendix C.2 for details. After showing how changes in the construction cost of height affect this baseline city, we consider separate parameterizations for each city in our data.

While values for $\{\alpha^U, \beta, \theta^U, \omega^U\}$ can be taken from the literature, remaining parameters apply more specifically to our inquiry. These involve the spatial organization of the city and the interaction between the city and the rural hinterland. We set the radius of the urban core $\underline{x}^C = \underline{x}^R$ to 1 km. We set the share of built-up land ℓ to 0.5, which is approximately the observed mean ratio of built-up area over total land area across all cities in our data. Targeting a city of 3 million as a baseline, we set the total city plus rural population to $\bar{N} = 6$ million and the extent of the hinterland from the city center $\bar{x}$ to 100 km. Together, this generates a national population density of about 191 workers per km^2 and urban fraction μ of 0.5.

The amenity decay parameters τ^U must rationalize urban height, population, and rent gradients. We set these parameters to reflect commercial and residential log building height CBD distance gradients of -0.20 and -0.10, respectively, estimated using 2022 property assessment data in CoreLogic for Chicago. Chicago is in the middle of estimated gradients using building volumes data for 50 large unconstrained world cities (Appendix Section C.2.1).

Figure 6: Model Simulated Height Elasticities by Preference Heterogeneity (ζ)

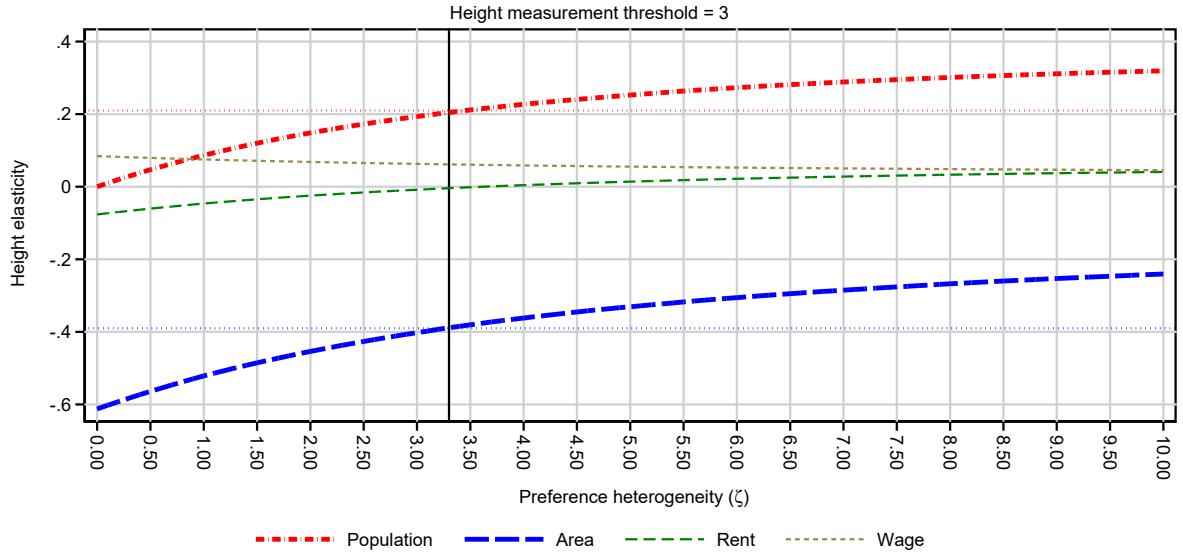

Note: Dotted red and blue horizontal lines are our estimates of the height elasticities of population and built up area for cities located in developing economies unconstrained by height regulation. These are moments matched to model counterparts. To generate model moments, indicated by the four dashed lines, we set one value of ζ and then solve the model under varying values of θ^U. We then regress each indicated log outcome on model generated log heights greater than or equal to $\mathcal{T}$. As such, manipulated variation in heights and the four outcomes originate exclusively from construction supply shocks.

Finally, ζ is a central parameter, as it governs the migration response to any shock that affects the attractiveness of the city. The larger is ζ, the more city population grows and the less city land area shrinks in response to a positive shock to the supply of tall buildings. With ζ sufficiently large, the city expands both vertically and horizontally. These relationships are depicted in Figure 6, which shows elasticities of population, area, rent and wages with respect to aggregate height as a function of ζ. Solving the model varying θ^U for each value of ζ delivers variation in aggregate tall building height which mimics that coming from the bedrock depth induced variation in the cost of height in our empirical analysis. At left is a closed city, in which ζ is 0. In this environment, a reduction in the cost of height does not draw in any population but instead makes the city more compact. The associated supply shock lowers rents. The greater spatial concentration of production raises the wage through an agglomeration force, in that employment becomes more spatially concentrated. Moving to the right in Figure 6, in-migration becomes easier, resulting in higher population, area, and rent elasticities with respect to height.

At $\zeta = 3.5$, the effect of lowering the cost of height gets balanced by the general equilibrium migration response such that rents do not respond to heights. For greater values of ζ, where population elasticities are very large, rent elasticities are slightly positive. As ζ increases, wage elasticities with respect to heights remain positive but fall slightly. We use a simulated method of moments (SMM) estimator to identify ζ, matching the model generated height elasticities of population and area depicted in Figure 6 to those in the data.[37]

Differences in land use and building patterns between the data and the model require attention when matching moments. As our building heights data is bottom-coded at 55 m, model generated heights must also be bottom-coded. However, unlike in the model, the data also exhibit variation in building heights at each CBD distance and buildings that tend to taper toward the top. Moreover, about half of land near CBDs in the data is not built up. For these reasons, the threshold above which to measure heights in the model should be well below 55 m ($\approx$ 14 stories). As it is unclear which height threshold $\mathcal{T}$ to use in the model, we treat $\mathcal{T}$ as an additional parameter to be estimated through SMM, thereby rendering model parameters just identified. In the counterfactual exercises below, $\mathcal{T}$ also serves as our minimum tall building height. Under $\mathcal{T} = 3$ and $\zeta = 3.3$, we exactly match the population and area elasticities. As long as $\mathcal{T} \geq 3$, we obtain a ζ value around 3.3.[38] We note that matching to IV estimates for the sample of height unconstrained cities in developing economies is key. While both estimated population and built area elasticities used in the SMM procedure deliver an identical ζ estimate of 3.3, the use of corresponding OLS estimates of 0.08 for population and -0.02 for built area would yield conflicting estimates of ζ. The use of the full developing country sample IV estimates of 0.13 and -0.16 would yield only slightly less conflicting estimates. Lastly, ζ estimates remain within the 3.0-4.5 range for all city populations above one million (not shown).

The implied labor supply (migration) elasticity to the city $\zeta(1-\mu)$ of 1.65 should be viewed as a broad-based long-run average that integrates over different environments. As our estimate applies to a 40 year time horizon, it is sensible that it exceeds estimates in the literature based on similar modeling frameworks applied to annual frequencies. Moreover, our look at changes in stocks rather than migration flows, as has been typical in the migration literature, will tend to increase elasticity estimates by incorporating fertility and death rate responses to real estate supply shocks. Using flow data, Caliendo et al. (2019) and Caliendo et al. (2021) find annual elasticities of 0.5 for the US and Europe, respectively. Tombe and Zhu (2019) finds 1.5-2.5 between provinces in China over worker life-cycles and Bryan and Morten (2018) finds 2.7 for Indonesia. Using more reduced form methods, Beaudry et al. (2014) finds a decadal labor supply elasticity to US metro areas of 2.0.

4.4 Illustrative Examples

We depict equilibrium floorspace rent, building height, and land rent under the baseline parameterization from Table 5 in the first row of Figure 7 below. Slopes of use-specific floor space bid-rent functions are co-determined with height gradients and bid-rent functions for land. The resulting land use pattern has a commercial district in the center surrounded by a residential

[37] As rent responses are predicted to be indeterminate in sign and near 0, an additional empirical analysis of rent responses would not be very informative. Historical rent data is also lacking for most developing countries.

[38] We see $\mathcal{T} = 3$ as a reasonable magnitude. Using CoreLogic data from Chicago, the CBD distance ring of 750 to 1000 meters has total residential and office building floorspace that is 3.7 times the land area and average building heights of 12.8 stories, or about 55 m. If floorspace in these buildings was reallocated to cover all of this land area at an equal height, the building height would be 12.8/3.7 = 3.5 stories, close to our $\mathcal{T}$ estimate of 3.

district and then rural land. The small discontinuities in floor space rents and heights at the commercial-residential land use boundary x_1 arise endogenously as a result of a net-cost of height $\theta^U - \omega^U$ that is smaller for commercial than residential developments.[39]

Figure 7: Urban Spatial Structure, Cost of Height, and Regulation

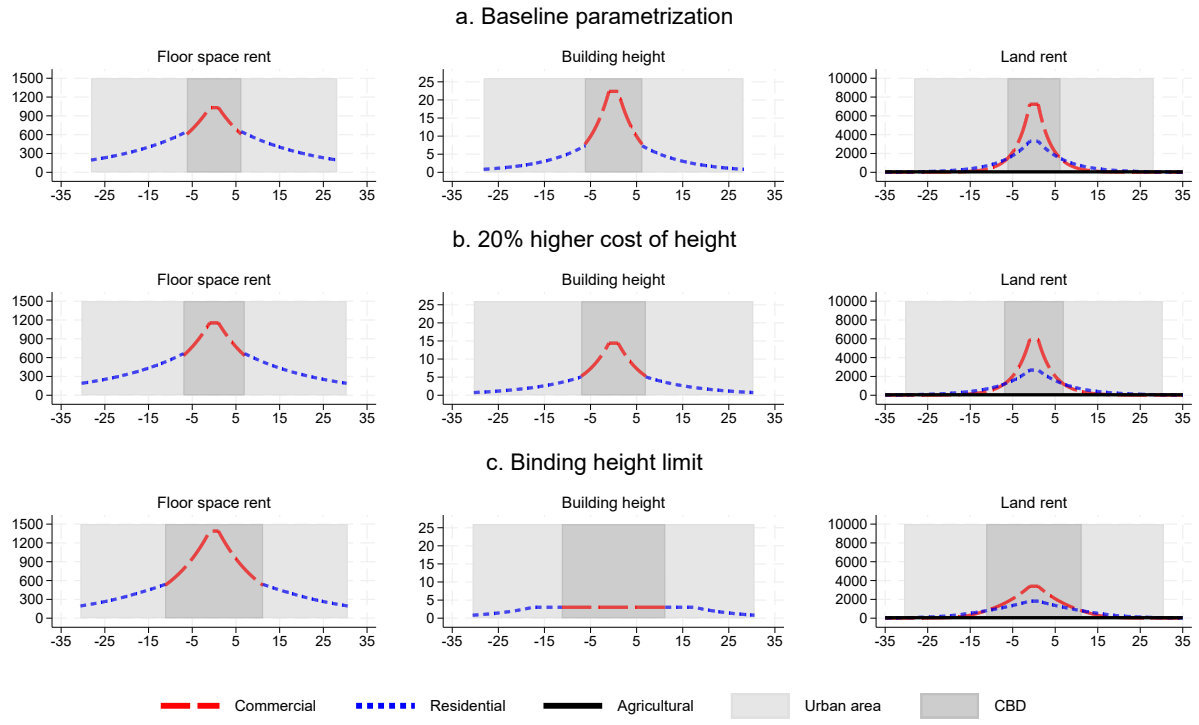

Note: Figure illustrates the solution to the model under the parameter values from Table 5 (upper panels), a counterfactual where we increase the cost of height to $\theta^C = 0.6, \theta^R = 0.65$ (middle panels), and a counterfactual in which we introduce a height limit of $\bar{S}^C = \bar{S}^R = \mathcal{T} = 3$. Table A10 reports impacts of the greater cost of height and a binding height limit on aggregate outcomes.

The second row of Figure 7 uses the same parameterization except that the costs of height are increased by 20% to emulate an environment with less favorable bedrock depth. Building heights fall and the city area expands by 16%. The relocation of firms and residents to more peripheral locations increases commuting costs (or, equivalently, reduces residential amenities) by 2.6% and lowers productivity (commercial amenities) by 0.9%. Due to the reduction in floor space supply, average commercial rents increase by 8%. Lower productivity and higher commuting costs make the city less attractive, thereby reducing housing demand and leading to slightly lower average residential rents, despite the reduction in residential floor space. Lower productivity and higher commercial rents reduce labor demand; reduced accessibility to the center reduces labor supply. The result is a reduction of 2.5% in the equilibrium wage. Due to the lower wage and greater commuting costs, city utility $\bar{U}$ falls by 5.3%. Since living in the city has become less attractive, the population falls by 8.7%. Expected utility across all workers inside and outside the city, $\mathcal{V}$, falls by 2.6%. Aggregate land values fall by 0.7%. Owners of land in the city center are worse off, as this is where the intensity of land use falls. Owners of land near the city periphery are better off, as this land is now more urbanized.

In the third row, we revert to the same parameters as in the first row but impose the height cap $\bar{S}^C = \bar{S}^R = \mathcal{T} = 3$ such that there are no (model-defined) tall buildings. This scenario corresponds to a city "height gap" of 100%. Relative to an unconstrained city, this height cap

[39] For example, residential towers need stronger water pumps. The flat rent and height functions at the center are artifacts of the imposition of the constant productive amenity value a for locations $x < \underline{x}^C$.

results in a substantial horizontal expansion of the CBD. Although we have imposed a tighter constraint on vertical growth, the horizontal area of the city increases only slightly more (at 18%) than in the cost counterfactual, rationalized through a larger population decline of 18%. The more pronounced horizontal expansion of the CBD results in an 8% increased average commuting cost and 5% reduction in average productivity. With a 7% decline, the wage falls more than in the cost counterfactual. The result is a reduction in housing demand that is so large that, despite the negative shock to residential floor space supply, residential rents fall substantially by 14%. The increase in commuting costs and the lower wage, however, dominate the effect of rents on indirect utility in the city, which decreases by 10%, leading to a decline in expected utility $\mathcal{V}$ of 5%. Driven by the conversion of rural into residential and residential into commercial land use, aggregate land values increase by 11%. The height limit redistributes income from the mobile labor factor to the immobile land factor. A major cost of height limits arises from the induced spatial misallocation of firms away from central locations at which they are most productive.

Figure 8: Heterogeneity in Welfare Costs of Height Limits

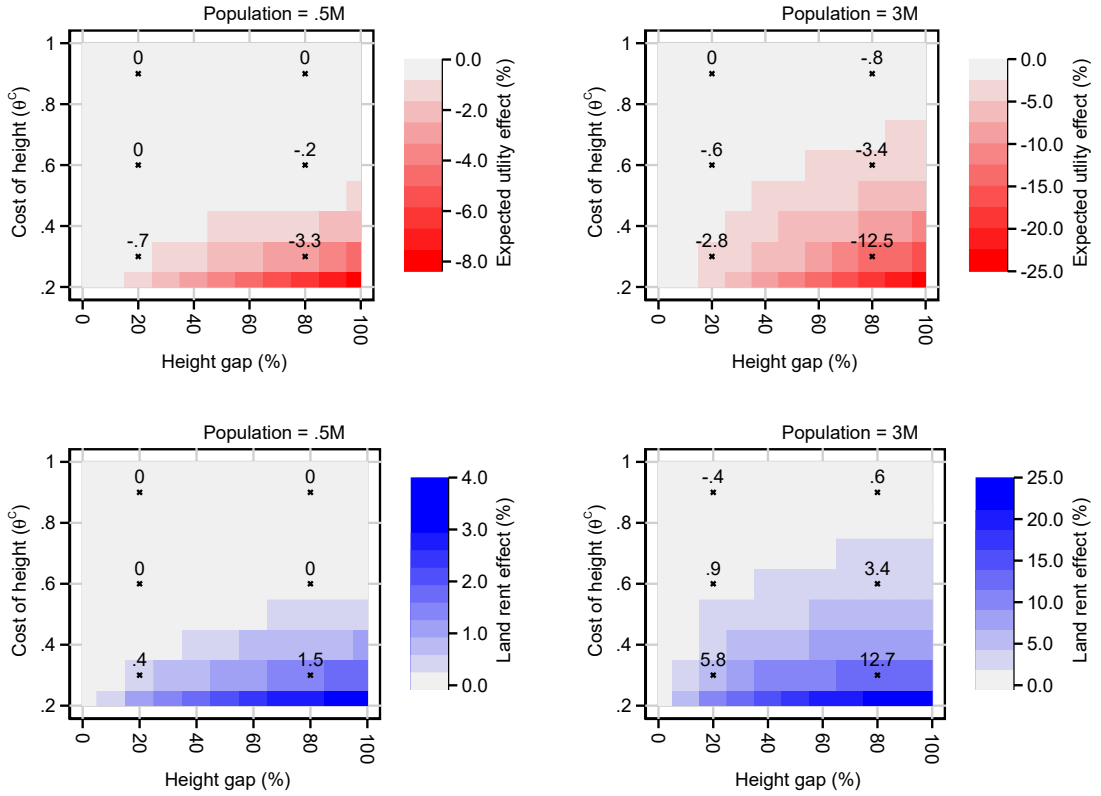

Note: We solve the model under different values of $\{\theta^C\}$, setting $\theta^R = \theta^C + 0.05$, finding values of $\{\bar{S}, \tilde{U}\}$ to rationalize a given combination of population and height gap, conditional on each value of θ^U. We adjust the regional population to ensure an urbanization rate of 0.5 and hold all other parameter values constant at the value described in Table 5. The height gap is the fraction of free-market total tall-building height that is not developed due to a height limit.

Figure 8 illustrates how the effect of a height limit depends on population and the cost of height. To generate this figure, we solve the model varying the height cost (θ^U), height limit ($\bar{S}^U$), and rural utility $\tilde{U}$. We exploit that there is a unique mapping from urban and rural utility to population in Eq. (12) to find $\{\bar{S}^U, \tilde{U}\}$ values that rationalize any given combination of population and height gap using the procedure described in Algorithm 4. We use this procedure to compute welfare effects for all combinations of cost of height $\{0.2, 0.3, ..., 1\}$ and height gap $\{0\%, 10\%, ..., 100\%\}$. We show results for cities of half a million and three million residents.[40]

[40]For each given cost of height and height gap, we engineer the model to generate larger population cities by

Figure 8 confirms that constraining heights results in greater welfare losses if the cost of height is low (e.g. due to favorable bedrock). A cost of height of 0.3 rather than 0.6 approximately triples the welfare loss at each height gap in a city with a population of three million (top right panel). Demand conditions also matter. Holding the cost of height constant, we observe greater effects in larger cities. Height limits are more costly in cities with fundamentals that increase the demand for and/or the supply of height. As vertical compression leads to horizontal expansion, binding height limits increase land values. Impacts on aggregate land rent are much greater in cities with lower costs of height, where the loss of heights are particularly large. This primarily reflects redistribution of production and residences to more peripheral locations.

4.5 The Welfare Costs of Limiting Heights

We use the model to evaluate the welfare consequences of limiting heights for each of the 12,877 cities in the full GHS sample. As before, we invert the model to rationalize observed populations and height gaps conditional on the observed construction cost of height for each city in our data (Algorithm 4). We set the population of the region, including the rural population, to the city population scaled by the inverse of the 2015 country-specific urbanization rate.[41] We obtain city-specific estimates of the cost of height using mean bedrock depths and the non-parametric estimated relationship between bedrock depth and the cost of height illustrated in Figure A4.

Table 6 below considers two counterfactuals. Relative to current height-constrained equilibria, we first calculate losses associated with banning all equilibrium tall buildings ("no tall building"), capturing the economic benefits of the tall building technology as it is currently used in each city. Second, we calculate the benefits associated with fully relaxing existing height gaps ("no height limit"). We include all rural potential migrants in our welfare calculations.

For developing economies, imposing a height restriction of no tall buildings reduces worker welfare by 1.8%. As fully relaxing current height constraints increases worker welfare by 5.3%, only about one-quarter of the potential welfare gains from building tall have been realized.

Mechanisms driving welfare effects are indicated below the top row. Relaxing height restrictions leads to higher wages, higher average property rents, and lower commuting costs (or equivalently, higher amenities). The wage response comes from greater productivity associated with lower office costs and increased commercial density through agglomeration economies. The commuting cost response comes from the greater urban compactness, which facilitates shorter commutes. The positive rent response, which comes through general equilibrium population gain effects, is smaller than the other two positive influences on welfare.

Aggregating these three forces using Eq. (29), urban utility in developing economy cities falls by 4.2% absent any tall buildings and rises by 8.0% relaxing current height limits. As the overall losses reported in the first row of Table 6 include rural residents, they are smaller than urban utility responses. The wage component accounts for about 60% of total welfare effects in developing economies. The commuting cost/amenity component accounts for about 70%, reflecting the fact that tall buildings facilitate urban compactness and shorter commutes. The rent component then accounts for ∼-30% of the total. Lastly, if we combine the commuting cost/amenity and rent components, the resulting adjusted rent component accounts for ∼40%.

reducing rural utility $\tilde{U}$, thereby also generating greater demand for height in the city.

[41] This implicit partitioning of rural areas into multiple city-specific hinterlands is empirically justified with our evidence in Tables A8 and A9 of minimal heights-driven growth spillovers across cities.

City population, the cost of height, and the height gap all influence the magnitude of welfare benefits associated with relaxing height limits. With height gaps larger in the developed world (averaging 76% against 45% in developing economies), in part because of a greater share of its urban population in large cities and a lower cost of height due to better bedrock depths, its welfare costs of height limits are greater than that for the developing world, at -3.1% for imposing a height ban and 11.6% for relaxing all height restrictions. The respective contributions of the wage and adjusted rent components are similar in both groups of countries. Aggregating across developing and developed economies, worldwide welfare costs associated with no tall buildings and benefits of relaxing existing height limits are 2.0% and 6.4% of current welfare, respectively.[42]

Table 6: Welfare Costs of Limiting Tall Building Construction

	City characteristics			Expected utility $\mathcal{V}$		Agg land rent $\mathcal{R}$	
World region	In cities >1 mill.	Cost of height θ (bedrock)	Est. height gap	No tall building	No height limit	No tall building	No height limit
Developing Economies	43.3%	0.54	44.8%	–1.8%	5.3%	–1.0%	–4.8%
	• *Wage in City* (A):			–2.5%	4.7%		
	• *Rent in City* (B):			–3.5%	6.9%		
	• *Commute Cost in City* (C):			2.9%	–5.6%		
	Urban Utility (A-0.33*B-C)			–4.2%	8.0%		
	Share Adjusted Rent (-0.33*B-C)			0.41	0.41		
Developed Economies	59.6%	0.39	75.9%	–3.1%	11.6%	–2.1%	–11.0%
	• *Wage in City* (A):			–3.0%	9.4%		
	• *Rent in City* (B):			–2.1%	12.7%		
	• *Commute Cost in City* (C):			3.7%	–10.2%		
	Urban Utility (A-0.33*B-C)			–6.0%	15.4%		
	Share Adjusted Rent (-0.33*B-C)			0.50	0.39		
All Economies	46.3%	0.51	50.5%	–2.0%	6.4%	–1.2%	–6.0%
	- Cost of height 20% lower			–2.2%	8.4%	–1.7%	–7.9%
	- Floorspace production share 33% lower			–1.7%	4.7%	–0.5%	–5.9%
	- No citywide agglomeration economies			–1.0%	2.4%	0.3%	–2.8%

Notes: Entries are population-weighted averages across cities and hinterlands in each indicated region. City-specific welfare effects are from counterfactual analysis within the model, in each case using a parameterization that matches a real-world city in terms of urban population, rural population, cost of height, and height gap. City height gaps are estimated as described in Section 3.4. To compute hinterland populations, we combine the city population with the country-specific 2015 urbanization rate. Results in "No tall building" and "No height limit" columns report average changes in expected utilities and aggregate land rents relative to city constrained equilibria under existing height gaps. "No tall building" imposes a height limit of model defined $\mathcal{T}$ floors. "No height limit" sets each city height gap to 0. Associated population-weighted changes in wages, rents and commuting costs (negative residential amenities) are indicated, along with average urban utility responses (using a housing expenditure share of 0.33). Each of the three rows at the bottom of the table show welfare and aggregate land rent changes under the same two counterfactual scenarios but given the indicated alternative parameter value. In these scenarios ζ and $\mathcal{T}$ are re-estimated to match empirical moments. Additional sensitivity analysis is in Table A12.

[42] As cities in developed areas of Asia are large, this region's opportunities for welfare gains from eliminating existing height limits are large at 17.8% (Table A11). North America and Europe are at 10.5% and 7.9%, respectively. Opportunities are greater in the former region because its cities are larger, despite Europe's tighter land use regulations and more favorable bedrock. In the developing world, Africa and Latin America have the most to gain from relaxing height limits, at 7.0% and 7.8%, as their cities' average costs of height are low. Relaxing inferred height restrictions in developing Asian economies would lead to welfare gains of 4.1%.

The final two columns of Table 6 show the aggregate land rent changes associated with moving from current height constrained equilibria to either a full height cap or no height constraints. For both developing and developed economies, departures from current equilibria generate reduced land values. Further constraining heights reduces central land values through reduced densities in city centers. Relaxing current height limits reduces land values by making cities more compact. Height constraints decentralize urban land use into less accessible lower property rent areas. This composition effect drives down average property rents but comes with a size effect that increases aggregate urban land values. The fact that the land rent responses are negative under both counterfactuals reflects the fact that declines in central land values offset increases in land values at the fringe once more severe height constraints are imposed. Relaxing current height constraints would reduce aggregate land values by 4.8% in developing economies and 11.0% in developed economies. The positive aggregate land value responses to height constraints rationalize the political economy of height and density restrictions seen in many countries, as articulated in Duranton and Puga (2023). They also confirm that height limits redistribute income from the mobile labor factor to the immobile land factor. As such, relaxing height limits potentially contributes to reducing aggregate inequality. In general equilibrium, tall building construction disproportionately benefits workers.

4.6 Additional Results and Sensitivity Analyses

The welfare costs of height limits are likely to grow over time. Extant estimates suggest that the cost-of-height parameter, θ, has declined by $\sim$2% per year over the past 50 years (Ahlfeldt and Barr, 2022). Even if cities adjust to keep the relative bite of height regulation constant, a 20% reduction in the cost of height will come with an implicit welfare cost that increases by about one-third, from 6.4% to 8.4% (bottom of Table 6), assuming no world population growth.

Next, we evaluate the consequences of reducing the share of floorspace in production by one-third (from 0.15 to 0.10), capturing the move toward work from home since the COVID-19 pandemic. Under this alternative parameterization, welfare consequences of limiting heights decline from 6.4% to 4.7% (bottom of Table 6). While firms' smaller space requirements reduce the importance of tall buildings for enhancing productivity, they also reduce adjusted rents by increasing housing supply (the contribution of the adjusted rent channel is 55% vs. 41% in the baseline).[43] Conversely, Table A12 shows that increasing the share of floorspace to 0.20, as in developing country cities where urban production may be more space-intensive (Tsivanidis, 2022), does not substantially increase the loss associated with height restrictions. (The associated contribution of the adjusted rent channel decreases to 31%.)

Evidence in the final row of Table 6 shows the role of citywide agglomeration economies in driving welfare and land value responses. Shutting down agglomeration economies ($\beta = 0$) significantly reduces the wage growth effects of heights. There are some benefits from commuting cost reductions, as lower incomes induce urban residents to live on less space thereby raising urban residential densities and giving people better access to the CBD. Conversely, doubling the agglomeration elasticity to 0.06, as sometimes observed in developing country contexts (Combes and Gobillon, 2015; Chauvin et al., 2016), strongly increases the losses associated with height limits (Table A12). Because they help workers save on commuting costs, tall buildings allow

[43] Even if firms require less space to produce, workers still commute to the CBD. The lower demand for commercial space in central areas makes way for more residential towers, thereby reducing commuting costs.

high-agglomeration cities to absorb more workers, promoting economic growth.

Additional sensitivity analyses with respect to residential and production decay parameters τ, the preference heterogeneity parameter ζ, and the height gap percentile cutoff are in Table A12. Increasing or lowering τ^C and τ^R by 10% only modestly changes welfare conclusions. Reducing the ζ to 0.1 (or increasing it to 10) also does not substantially changes welfare conclusions, though land values are substantially affected. Given the model's lack of a rural production sector, one could be concerned that our analysis does not consider the impact of rural-to-urban migration on rural production and wages. Our approach follows the dual-sector model of Lewis et al. (1954) whereby surplus labor from the rural sector is absorbed by the urban sector. China did not reach its Lewis turning point before the 2010s and India still has not reached it. Regardless, a low ζ implies that potential migrants respond relatively less to changes in urban conditions. The fact that results do not significantly depend on the ζ suggests that assuming a Lewisian or post-Lewisian world should not matter much for the results.[44]

5 Conclusion

The Skyscraper Revolution has allowed cities around the world to accommodate greater populations on less land. Using bedrock depth induced variation across cities in 1975-2015 reductions in the cost of building tall, estimated elasticities of city population and built land area with respect to aggregate city building heights are 0.13 and -0.16, respectively. As heights respond more to variation in the cost of height in higher demand locations, aggregate responses to reductions in the cost of building taller appear disproportionately in the world's largest cities.

By revealed preference, this evidence demonstrates that there are benefits associated with the heights that result from lower construction costs. Quantification using a land use model reveals that the enhanced urban compactness facilitated by the lower costs of building tall results in both productivity gains and reduced urban travel costs. Migration responses mute potential housing affordability benefits. Given the gap between actual and potential building heights calculated for each city in our data, we find that only about one-quarter of the potential welfare gains from heights have been realized. Economic gains of 11.6% and 5.3% are available by eliminating existing height regulations in developed and developing economies, respectively. As the cost of building tall declines with technical progress, and as the global population keeps growing, such potential for welfare gains will increase into the future.

With the losses in land values that would come with relaxing height limits, it is perhaps not surprising that so many cities restrict tall building construction. The political economy of such deregulation is fraught. Even though aggregate gains associated with allowing more tall building are to be found, in many areas these gains are distributed disproportionately to potential urban residents that do not own property in the city. Given the potential negative amenity and productivity responses from the congestion associated with increased urban density, tall building construction may also be regressive and costly in the short run, even if it expands real estate supply to the benefit of all renters in the long run. Tall buildings are also often seen as environmentally wasteful and can destroy historical character. A priority for future research should be to develop a better understanding of the extent to which each of these potential reasons for the opposition to densification hold up empirically, and to devise potential policy remedies.

[44] Across all analyses, we find similar results separately for developing and developed economies (not shown). We also verify that the SMM-estimated parameters ζ and $\mathcal{T}$ are unaffected in most cases (Table A12).

References

Ades, Alberto F and Edward L Glaeser, "Trade and circuses: explaining urban giants," *The Quarterly Journal of Economics*, 1995, *110* (1), 195–227.

Ahlfeldt, Gabriel M. and Daniel P. McMillen, "Tall buildings and land values: Height and construction cost elasticities in Chicago, 1870-2010," *Review of Economics and Statistics*, 2018, *100* (5), 861–875.

_ **and Jason Barr**, "Viewing urban spatial history from tall buildings," *Regional Science and Urban Economics*, 11 2020, p. 103618.

_ **and** _ , "The economics of skyscrapers: A synthesis," *Journal of Urban Economics*, 5 2022, *129*, 103419.

_ **, Duncan Roth, and Tobias Seidel**, "Optimal minimum wages," *CEPR Discussion Paper 17026*, 2022.

Albouy, David, Mauricio Arango, and Minchul Shin, "Crowning the metropolis: skylines, land values, and urban population," *Working paper*, 2020.

Alonso, William, *Location and Land Use*, Cambridge, MA: Harvard Univ. Press, 1964.

Anagol, Santosh, Fernando Vendramel Ferreira, and Jonah M Rexer, "Estimating the economic value of zoning reform," Technical Report, mimeo 2024.

Bairoch, Paul, *Cities and economic development: from the dawn of history to the present*, University of Chicago Press, 1988.

Balboni, Clare, "In harm's way? infrastructure investments and the persistence of coastal cities." PhD dissertation, London School of Economics and Political Science 2019.

_ **, Gharad Bryan, Melanie Morten, and Bilal Siddiqi**, "Could Gentrification Stop the Poor from Benefiting from Urban Improvements?," in "AEA Papers and Proceedings," Vol. 111 American Economic Association 2014 Broadway, Suite 305, Nashville, TN 37203 2021, pp. 532–537.

Barr, Jason and Remi Jedwab, "Exciting, boring, and nonexistent skylines: Vertical building gaps in global perspective," *Real Estate Economics*, 2023.

_ **, Troy Tassier, and Rossen Trendafilov**, "Depth to Bedrock and the Formation of the Manhattan Skyline, 1890–1915," *The Journal of Economic History*, 2011, *71* (4), 1060–1077.

Barro, Robert J and Xavier Sala i Martin, "Convergence," *Journal of political Economy*, 1992, *100* (2), 223–251.

Baum-Snow, Nathaniel, "Did Highways Cause Suburbanization?," *Quarterly Journal of Economics*, 2007, *122* (2), 775–805.

_ **, Loren Brandt, J Vernon Henderson, Matthew A Turner, and Qinghua Zhang**, "Roads, Railroads, and Decentralization of Chinese Cities," *The Review of Economics and Statistics*, 1 2017, *99* (3), 435–448.

Beaudry, Paul, David A. Green, and Benjamin M. Sand, "Spatial equilibrium with unemployment and wage bargaining: Theory and estimation," *Journal of Urban Economics*, 2014, *79*, 2–19. Spatial Dimensions of Labor Markets.

Bertaud, Alain and Jan Brueckner, "Analyzing building-height restrictions: predicted impacts and welfare costs," *Regional Science and Urban Economics*, 2005, *35* (2), 109–125.

Borusyak, Kirill, Rafael Dix-Carneiro, and Brian Kovak, "Understanding migration responses to local shocks," *Available at SSRN 4086847*, 2022.

Brueckner, Jan and Kala Seetharam Sridhar, "Measuring welfare gains from relaxation of land-use restrictions: The case of India's building-height limits," *Regional Science and Urban Economics*, 2012, *42* (6), 1061–1067.

Brueckner, Jan K., "The structure of urban equilibria: A unified treatment of the muth-mills model," *Handbook of Regional and Urban Economics*, 1987, *2*, 821–845.

Brueckner, Jan K and David A Fansler, "The economics of urban sprawl: Theory and evidence on the spatial sizes of cities," *The review of Economics and Statistics*, 1983, pp. 479–482.

Brueckner, Jan, Shihe Fu, Yizhen Gu, and Junfu Zhang, "Measuring the stringency of land use regulation: The case of China's building height limits," *Review of Economics and Statistics*, 2017, *99* (4), 663–677.

Bryan, Gharad and Melanie Morten, "The Aggregate Productivity Effects of Internal Migration: Evidence from Indonesia," *Journal of Political Economy*, 12 2018.

_ , Edward Glaeser, and Nick Tsivanidis, "Cities in the developing world," *Annual Review of Economics*, 2020, *12* (1), 273–297.

Burchfield, Marcy, Henry G Overman, Diego Puga, and Matthew A Turner, "Causes of sprawl: A portrait from space," *The Quarterly Journal of Economics*, 2006, *121* (2), 587–633.

Buringh, Eltjo and Urbanization Hub, "The Clio-infra database on urban settlement sizes: 1500–2000," 2013.

Caliendo, Lorenzo, Luca David Opromolla, Fernando Parro, and Alessandro Sforza, "Goods and factor market integration: A quantitative assessment of the EU enlargement," *Journal of Political Economy*, 2021, *129* (12), 3491–3545.

_ , Maximiliano Dvorkin, and Fernando Parro, "Trade and Labor Market Dynamics: General Equilibrium Analysis of the China Trade Shock," *Econometrica*, 5 2019, *87* (3), 741–835.

Campante, Filipe and David Yanagizawa-Drott, "Long-range growth: economic development in the global network of air links," *The Quarterly Journal of Economics*, 2018, *133* (3), 1395–1458.

Chauvin, Juan Pablo, Edward L. Glaeser, Yueran Ma, and Kristina Tobio, "What is different about urbanization in rich and poor countries? Cities in Brazil, China, India and the United States," *Journal of Urban Economics*, 2016, pp. 1–33.

Chen, Jiafeng and Jonathan Roth, "Logs with zeros? Some problems and solutions," *The Quarterly Journal of Economics*, 2024, *139* (2), 891–936.

Chiovelli, Giorgio, Stelios Michalopoulos, and Elias Papaioannou, "Landmines and spatial development," Technical Report, National Bureau of Economic Research 2018.

Civelli, Andrea, Arya Gaduh, Alexander D Rothenberg, and Yao Wang, "Urban sprawl and social capital: Evidence from Indonesian cities," *The Economic Journal*, 2023, *133* (654), 2110–2146.

Combes, Pierre-Philippe and Laurent Gobillon, "The Empirics of Agglomeration Economies," in Gilles Duranton, J Vernon Henderson, William C B T Handbook of Regional Strange, and Urban Economics, eds., *Handbook of Regional and Urban Economics*, Vol. 5, Elsevier, 2015, pp. 247–348.

_ , Gilles Duranton, and Laurent Gobillon, "The Costs of Agglomeration: House and Land Prices in French Cities," *The Review of Economic Studies*, 10 2019, *86* (4), 1556–1589.

Council on Tall Buildings and Urban Habitat, "Data set: Buildings over 80 meters tall," Technical Report 2022.

Coury, Michael, Toru Kitagawa, Allison Shertzer, and Matthew Turner, "The value of piped water and sewers: Evidence from 19th century chicago," Technical Report, National Bureau of Economic Research 2022.

Curci, Federico, "The taller the better? Agglomeration determinants and urban structure," *Working paper*, 2020.

D'Amico, Leonardo, Edward L Glaeser, Joseph Gyourko, William R Kerr, and Giacomo AM Ponzetto, "Why Has Construction Productivity Stagnated? The Role of Land-Use Regulation," Technical Report, National Bureau of Economic Research 2024.

Danton, Jayson and Alexander Himbert, "Residential vertical rent curves," *Journal of Urban Economics*, 2018, *107*, 89–100.

Desmet, Klaus, Dávid Krisztián Nagy, and Esteban Rossi-Hansberg, "The Geography of Development," *Journal of Political Economy*, 1 2018, *126* (3), 903–983.

Ducruet, César, Réka Juhász, Dávid Krisztián Nagy, and Claudia Steinwender, "All aboard: The effects of port development," Technical Report, National Bureau of Economic Research 2020.

Duranton, Gilles and Diego Puga, "Urban Land Use," in Gilles Duranton, J. Vernon Henderson, and William C. Strange, eds., *Handbook of Regional and Urban Economics*, Vol. 5, Elsevier, 2015, chapter 8, pp. 467–560.

_ and _, "Urban growth and its aggregate implications," *Econometrica*, 2023, *91* (6), 2219–2259.

_ and Matthew A. Turner, "Urban Growth and Transportation," *The Review of Economic Studies*, 2012, *79* (4), 1407–1440.

Emporis, *Emporis* 2022.

Esch, Thomas, Klaus Deininger, Remi Jedwab, and Daniela Palacios-Lopez, "Outward and Upward Construction: A 3D Analysis of the Global Building Stock," Working Papers 2023-09, The George Washington University, Institute for International Economic Policy September 2023.

Faber, Benjamin, "Trade Integration, Market Size, and Industrialization: Evidence from China's National Trunk Highway System," *The Review of Economic Studies*, 7 2014, *81* (3), 1046–1070.

Florczyk, A., M. Melchiorri, C. Corban, M. Schiavina, L. Maffenini, M. Pesaresi, P. Politis, F. Sabo, S. Carneiro Freire, D. Ehrlich, T. Kemper, P. Tommasi, D. Airaghi, and L. Zanchetta, "Description of the GHS Urban Centre Database 2015," *Publications Office of the European Union*, 2019.

Gechter, Michael and Nick Tsivanidis, "Spatial spillovers from high-rise developments: Evidence from the Mumbai Mills," *Unpublished manuscript*, 2023.

Glaeser, Edward, *Triumph of the City: How Our Greatest Invention Makes Us Richer, Smarter, Greener, Healthier, and Happier* 2012.

_ and Joseph Gyourko, "The economic implications of housing supply," *Journal of economic perspectives*, 2018, *32* (1), 3–30.

Glaeser, Edward L and Matthew E Kahn, "The greenness of cities: Carbon dioxide emissions and urban development," *Journal of urban economics*, 2010, *67* (3), 404–418.

_ , Hedi D Kallal, Jose A Scheinkman, and Andrei Shleifer, "Growth in Cities," *Journal of Political Economy*, 5 1992, *100* (6), 1126–1152.

Gollin, Douglas, Casper Worm Hansen, and Asger Mose Wingender, "Two Blades of Grass: The Impact of the Green Revolution," *Journal of Political Economy*, 2021, *129* (8), 2344–2384.

Gonzalez-Navarro, Marco and Matthew A. Turner, "Subways and urban growth: Evidence from earth," *Journal of Urban Economics*, 11 2018, *108*, 85–106.

Gyourko, Joseph and Raven Molloy, "Regulation and housing supply," in "Handbook of regional and urban economics," Vol. 5, Elsevier, 2015, pp. 1289–1337.

_ and Sean E McCulloch, "The Distaste for Housing Density," Technical Report, National Bureau of Economic Research 2024.

Hansen, M. and X. Song, *Vegetation Continuous Fields (VCF) Yearly Global 0.05 Deg.* 2018.

Harari, Mariaflavia, "Cities in bad shape: Urban geometry in India," *American Economic Review*, 2020, *110* (8), 2377–2421.

_ and Maisy Wong, "Slum upgrading and long-run urban development: Evidence from Indonesia," *Working paper*, 2019.

Harris, John R and Michael P Todaro, "Migration, Unemployment and Development: A Two-Sector Analysis," *The American Economic Review*, 2 1970, *60* (1), 126–142.

Heblich, Stephan, Stephen J Redding, and Daniel M Sturm, "The Making of the Modern Metropolis: Evidence from London," *The Quarterly Journal of Economics*, 11 2020, *135* (4), 2059–2133.

Henderson, J Vernon, Tanner Regan, and Anthony Venables, "Building the city: from slums to a modern metropolis," *The Review of Economic Studies*, 2021, *88* (3), 1157–1192.

_ , **Tim Squires, Adam Storeygard, and David Weil**, "The global distribution of economic activity: nature, history, and the role of trade," *The Quarterly Journal of Economics*, 2018, *133* (1), 357–406.

Henderson, Vernon, Ari Kuncoro, and Matt Turner, "Industrial Development in Cities," *Journal of Political Economy*, 5 1995, *103* (5), 1067–1090.

Hsieh, Chang-Tai and Enrico Moretti, "Housing Constraints and Spatial Misallocation," *American Economic Journal: Macroeconomics*, 2019, *11* (2), 1–39.

Knoll, Katharina, Moritz Schularick, and Thomas Steger, "No price like home: Global house prices, 1870–2012," *American Economic Review*, 2017, *107* (2), 331–353.

Lewis, William Arthur et al., "Economic development with unlimited supplies of labour," 1954.

Liu, Crocker, Stuart S Rosenthal, and William C Strange, "The Vertical City: Rent Gradients and Spatial Structure," *Journal of Urban Economics*, 2018, *106*, 101–122.

_ **,** _ **, and** _ , "Employment Density and Agglomeration Economies in Tall Buildings," *Regional Science and Urban Economics*, 2020, *84*.

Lucas, Robert E Jr. and Esteban Rossi-Hansberg, "On the Internal Structure of Cities Author," *Econometrica*, 2002, *70* (4), 1445–1476.

McFadden, Daniel, "The measurement of urban travel demand," *Journal of Public Economics*, 1974, *3* (4), 303–328.

Mills, Edwin S, "An Aggregative Model of Resource Allocation in a Metropolitan Area," *The American Economic Review*, 1967, *57* (2), 197–210.

Morten, Melanie and Jaqueline Oliveira, "The effects of roads on trade and migration: Evidence from a planned capital city," *American Economic Journal: Applied Economics*, 2024, *16* (2), 389–421.

Muth, R, *Cities and Housing*, Chicago: Chicago University Press, 1969.

NGDC, *Global Radiance Calibrated Nighttime Lights* 2015.

Ortalo-Magné, François and Andrea Prat, "On the political economy of urban growth: Homeownership versus affordability," *American Economic Journal: Microeconomics*, 2014, *6* (1), 154–181.

Redding, Stephen J. and Esteban Rossi-Hansberg, "Quantitative Spatial Economics," *Annual Review of Economics*, 2017, *9* (1), 21–58.

Saiz, Albert, "The geographic determinants of housing supply," *The Quarterly Journal of Economics*, 2010, *125*, 1253–1296.

Schleier, Merill, *The Skyscraper in American Art, 1890–1931* 1986.

Shangguan, Wei, Tomislav Hengl, Jorge Mendes de Jesus, Hua Yuan, and Yongjiu Dai, "Mapping the global depth to bedrock for land surface modeling," *Journal of Advances in Modeling Earth Systems*, 2017, *9* (1), 65–88.

Tombe, Trevor and Xiaodong Zhu, "Trade, migration, and productivity: A quantitative analysis of china," *American Economic Review*, 2019, *109* (5), 1843–1872.

Tsivanidis, Nick, "Evaluating the impact of urban transit infrastructure: Evidence from bogota's transmilenio," *Unpublished manuscript*, 2022, *18*.

UN COMTRADE, "UN COMTRADE," 2020.

United Nations, *World Urbanization Prospects: The 2018 Revision* 2018.

USGS, "Mineral Industry Surveys 1960-2020," 2020.

Wang, Jin, Ting Chen, Ziyang Chen, and Yatang Lin, "Building Tall, Falling Short: An Empirical Assessment of Chinese Skyscrapers," *Falling Short: An Empirical Assessment of Chinese Skyscrapers*, 2023.

World Bank, *World Development Indicators* 2022.

WEB APPENDIX NOT FOR PUBLICATION

A Data and stylized facts

A.1 Additional Data Sources

The following data sources are used to construct robustness results reported in Figure 5.

Elevation data comes from GMTED (2010) (resolution: 15 arc-seconds, or 500 m close to the equator). We use the mean of elevation ("altitude") and standard deviation of elevation ("ruggedness") within city boundaries (measured in m). Data on the location of coastal and lake shorelines comes from Wessel and Smith (1996). Giardini et al. (1999) reports peak ground acceleration (PGA; m per s^2) at the 0.0833*0.0833° level (≈ 9 x 9 km). PGA takes into account the probability of strong earthquakes in each pixel as well as the probability of diffusion over space. Since land-use regulations related to earthquake risk tend to be adopted based on fuzzily defined local conditions, we consider buffers of 0.05 decimal degrees (5.55 km) around each city. We then obtain the mean PGA for each city/buffer. Data on agricultural suitability comes from Schneider et al. (2022). We rely on their measure of "historic 1980-2008 suitability with current irrigation patterns" and use mean suitability within the city's boundary. Wind speed data comes from Davis et al. (2023). We obtain mean wind speed within each city's boundary. Data on the location of mines circa 2005 comes from USGS (2023). Data on the location of oil and gas fields circa 2009 comes from Lujala et al. (2007). Data on subway stations and network length comes from Gonzalez-Navarro and Turner (2018) and Gendron-Carrier et al. (2022).

A.2 Construction Cost Index

This index nets out factors that contribute to construction costs but are unrelated to height and bedrock depth (e.g. labor costs, construction materials prices, and exchange rate differences). To build the index, we residualize construction cost $C_{i,a(i),c(i),t}$ per unit of floor area $F_{i,a(i),c(i),t}$ of each building i, constructed in city a in country c during decade t using the following regression:

$$\ln C_{i,a(i),c(i),t} - \ln F_{i,a(i),c(i),t} = \mu_{a(i)} + \eta_{c(i),t} + \varepsilon^{C}_{i,a(i),c(i),t},$$

where $\mu_{a(i)}$ is a time-invariant fixed effect controlling for arbitrary demand and supply shifters at the city level and $\eta_{c(i),t}$ is a country by decade effect. We recover the residual, $\varepsilon^{C}_{i,a(i),c(i),t}$, as a relative cost measure that describes log deviations from country-trend-adjusted city averages.

Summary statistics about the Emporis cost data are in the notes to Figures A1 and A3.

A.3 Temporal and Cross-Sectional Variation in the Cost of Height

To evaluate relationships between the construction cost index, building height, and year or bedrock depth non-parametrically, we employ a locally weighted regressions approach using a bivariate kernel. Using building level data, we grid the two observables $\{s^1, s^2\}$ that determine our construction cost index. These observables are building height and year for Figure A1 or building height and bedrock depth for Figure A3. For each combination of grid values along those dimensions $\tilde{s}^1 \in \tilde{S}^1, \tilde{s}^2 \in \tilde{S}^2$ we run the locally weighted regression

$$\varepsilon^{C}_{i} = \bar{\varepsilon}^{\tilde{s}^1,\tilde{s}^2} + \tilde{\varepsilon}^{\tilde{s}^1,\tilde{s}^2}_{i}$$

using the Gaussian kernel weight

$$
\begin{aligned}
W_i^{\tilde{s}^1,\tilde{s}^2} &= \frac{w_i^{\tilde{s}^1,\tilde{s}^2}}{\sum_{j=i}^{J} w_j^{\tilde{s}^1,\tilde{s}^2}}, \text{where} \\
w_i^{\tilde{s}^1,\tilde{s}^2} &= \prod_{s=\in\{s^1,s2\}} \frac{1}{\kappa^s\sqrt{\pi}} \exp\left[-\frac{1}{2}\left(\frac{s_i-\tilde{s}}{\kappa^s}\right)^2\right].
\end{aligned} \tag{30}
$$

κ^s are bandwidth parameters.

Hence, we run $\tilde{S}^1 \times \tilde{S}^2$ locally weighted regressions to recover $\tilde{S}^1 \times \tilde{S}^2$ parameters $\bar{\varepsilon}^{\tilde{s}^1,\tilde{s}^2}$ which are local means that we plot on the height-year plane in FigureA1 and the height-bedrock plane in Figure A3. This amounts to 112 (years) $\times$ 195 (height values) = 21,840 regressions in FigureA1 and 35 (bedrock depth values) $\times$ 195 (height values) = 6,825 regressions in Figure A3.

Figure A1 provides evidence on reductions in the cost of height over time. Our index of construction cost per floor area is mean 0 (by construction) in each year. Therefore, this figure speaks only to the changes in construction costs in taller relative to shorter buildings. Evident in Figure A1 are steep declines in the cost of height over the past century that continued throughout our study period of 1975-2015. In 1975, buildings of 200 m were on average 3.7% higher cost to build per square m than 125 m tall buildings. By 2015, that gap had fallen to 1.3% greater.

Figure A3 depicts both the non-monotonicity of construction costs in bedrock depth conditional on height and the rate at which construction costs increase in height. The descriptive evidence is that the cost-minimizing bedrock depth for 125 m tall buildings is 18 m (blue lines), while that for 200 m tall buildings is 25 m (red lines). Constructing a 125 m tall building at the optimal bedrock depth saves more than 5% in cost per sq m relative to building on surface level or very deep bedrock. The cost savings are much larger for 200 m tall buildings. Moreover, Figure A3 shows that unit costs increase in building height more rapidly where bedrock is deep.

A.4 The cost of Height and Bedrock Depth

Eq. (1) defines θ as the elasticity of per-unit construction cost with respect to height. The engineering literature and stylized evidence discussed in Section 2 suggests that this elasticity should by U-shaped in bedrock depth. To empirically substantiate this notion, we use a instrumental variables locally weighted regression (LWR-IV) approach to estimate how bedrock depth influences unit cost responses to building heights. For implementation, we require a demand-side IV to remove the effect of supply-side factors such as ruggedness that could be correlated with sub-soil geology. We use distance from the CBD as an IV for building heights since it affects building heights via demand side forces and has been shown to be a strong predictor of height (Ahlfeldt and Barr, 2022). If the city has buildings exceeding 100 m in heights, the city center is defined as the median coordinate of these buildings. Otherwise, the city center is defined to be the location of the tallest building ever built in the city.

Concretely, we estimate the first stage

$$
\ln h_{i.a(i),c(i),t} = \alpha^{\tilde{b}} \ln DCBD_{i,a(i)} + \tilde{\mu}^{\tilde{b}}_{a(i)} + \tilde{\eta}^{\tilde{b}}_{c(i),t} + \tilde{\varepsilon}^{\tilde{b}}_{i,a(i),c(i),t} \tag{31}
$$

and second stage

$$
\ln C_{i,a(i),c(i),t} - \ln F_{i,a(i),c(i),t} = \theta^{\tilde{b}} \widehat{\ln h}_{i.a(i),c(i),t} + \mu^{\tilde{b}}_{a(i)} + \eta^{\tilde{b}}_{c(i),t} + \varepsilon^{\tilde{b}}_{i,a(i),c(i),t} \tag{32}
$$

for each LWR $\tilde{b} \in \tilde{B}$ using a weighted 2SLS estimator. $h_{i,a(i),c(i),t}$ is the height of building i,

constructed in city a in country c during decade t, $DCBD_{i,a(i)}$ is building i's distance from the center of city $a(i)$, $\ln C_{i,a(i),c(i),t} - \ln F_{i,a(i),c(i),t}$ is the log cost per unit of floor area, $\{\mu^{\tilde{b}}_{m(i)}, \mu^{b}_{a(i)}\}$ are city fixed effects, and $\{\eta^{\tilde{b}}_{c(i),t}, \eta^{b}_{c(i),t}\}$ are country by decade fixed effects.

In each LWR $\tilde{b} \in \tilde{B}$ we weight observations by the Gaussian kernel weight

$$\begin{aligned} W_i^{\tilde{b}} &= \frac{w_i^{\tilde{b}}}{\sum_{j=i}^{J} w_j^{\tilde{b}}}, \text{where} \\ w_i^{\tilde{b}} &= \frac{1}{\kappa^{\tilde{b}}\sqrt{\pi}} \exp\left[-\frac{1}{2}\left(\frac{b_i - \tilde{b}}{\kappa^{\tilde{b}}}\right)^2\right]. \end{aligned} \tag{33}$$

Eq. (33) uses a univariate version of the same kernel as in Eq. (30), except that we employ a LWR-specific bandwidth. This is because we wish to allow for a more flexible fit via a smaller bandwidth in the more populated part of the bedrock distribution, where we also expect more variation in θ. In the right tail of the bedrock distribution that is more sparsely populated and where we expect less variation in θ, the larger bandwidth reduces standard errors. To this end, we use a variant of Scott's rule of thumb for bandwidth selection and define

$$\kappa^{\tilde{b}} = \mathcal{M}\frac{3.49\hat{\sigma}^{\tilde{b}}}{\left(N^{\tilde{b}}\right)^{\frac{1}{3}}},$$

where the standard deviation $\hat{\sigma}^{\tilde{b}}$ and the number of observations $N^{\tilde{b}}$ are computed for rolling subsamples that satisfy $|b_i - \tilde{b}| \leq \mathcal{B} = 10$. We scale the rule-of-thumb bandwidth by a factor of $\mathcal{M} = 2$ since the non-parametric estimation of derivatives generally requires larger bandwidths than the estimation of levels (Henderson and Parmeter, 2015, Section 5.9).

Figure A4 supports the engineering-based hypothesis that bedrock at intermediate depths reduces the construction cost of tall buildings. Within the sample of buildings for which we observe height, construction cost, and floor area, the elasticity of cost with respect to height is minimized at a bedrock depth of ∼15 m. At depths less than about 5 m or greater than ∼25 m, the cost of height is significantly larger. This range is roughly consistent with the descriptive evidence from Figures A3, given an average building height of 109 m in our sample. Figure A4 supports the idea that as demand for height increases over time, cities with bedrock within an intermediate range will have a greater ease of accommodating that demand.

B Details of Height Gap Calculations

We adopt the regression specification to predict city heights used in Barr and Jedwab (2023, eq. (6)). The analysis uses 12,755 GHS-UCDB cities, a, in 163 countries, c, in the years $t = \{1995, 2000, 2005, 2010, 2015, 2020\}$ (N = 76,530). In each year, these cities are classified into 10 categories, indexed by p, as determined by population at time t: 0-100K, 100-250K, 250-500K, 500-750K, 750-1,000K, 1,000-2,500K, 2,500-5,000K, 5,000-7,500K, 7,500-10,000K, 10,000K+. Since city population is only available in 1990, 2000, and 2015, population categories are defined using year 2015 population data for 2010-2020 and 2000 data for 1995-2005.

The estimation equation is

$$\begin{aligned} \text{LHEIGHTS}_{act} &= \rho_1 \text{LDMSP}_{act(d)} + \rho_2 \text{LVIIRS}_{act(v)} \\ +\Sigma_{p=1}^{10}\gamma_{p,t}\mathbb{1}(\text{CAT}_{act}=p) &+ \Sigma_{p=1}^{10}\mathbb{1}(\text{CAT}_{act}=p)X_{ct}\beta_{p,t} \\ &+\Sigma_{p=1}^{10}\mathbb{1}(\text{CAT}_{act}=p)X_{ac}\delta_{p,t} + \nu_{act}. \end{aligned} \tag{34}$$

ρ_1, ρ_2, and $\gamma_{p,t}$ are scalars. $\beta_{p,t}$ and $\delta_{p,t}$ are vectors to reflect that X_{ct} and X_{ac} are matrices that include the variables described below. LHEIGHTS_{act} is the log of (total sum of tall building heights + 1) in city a, country c, and year t. Population size dummies (CAT_{act}) are fully interacted with year fixed effects to control for differing levels and trends in real estate demand and construction costs across cities of different sizes. Remaining controls for other demand and supply factors include country-level controls (X_{ct}) and time invariant city-level controls (X_{ac}), which are interacted with the population size dummies and year fixed effects, allowing their impacts to vary by city size over time. The objective is to estimate residuals ν_{ac2015}, which proxy for land-use regulations and height restrictions in city ac in 2015.

The first two variables in the regression denote city total night lights and proxy for city income in different years. The log of (total sum of DMSP lights + 1) can be calculated for years $t(d)$ 1995, 2000, 2005 and 2010.[45] The log of (total sum of VIIRS lights + 1) can be calculated for years $t(v)$ 2010, 2015 and 2020.[46] Other demand side factors (X_{ct}) are accounted for with city population and year interacted with quadratics in national per-capita GDP,[47] national population, and national land area.[48] More populated countries tend to have larger large cities, which naturally have more demand for heights and tall buildings. Likewise, countries with more available (lower cost) land tend to have less vertical cities. Time-invariant city-level controls (X_{ac}) (interacted with city size dummies and year fixed effects) account for various demand and supply factors. On the supply side are city mean bedrock depth, earthquake risk, and quadratics in the mean and standard deviation of city elevation. Elevation range also controls for some demand side factors, as cities surrounded by more mountainous land have less scope for horizontal expansion, thereby increasing the demand for heights.

The estimated adjusted R-squared of 0.64 suggests that fundamental demand and supply factors may account for almost two thirds of the international variation in city heights. Assuming the other 0.36 can be attributed to land-use regulation, the residuals ν_{act} capture the extent to which each city has more or less heights than other cities with similar observable characteristics.

Using estimated parameters in (34), we predict each city's 2015 stock of heights were it to have among the most heights for cities with similar observables. We view this prediction as the amount of heights the city would have were it unconstrained by regulation. Comparisons of actual heights to this prediction of unconstrained heights delivers each city's height gap.

To build up to the determination of each city's counterfactual unconstrained heights, we begin by predicting the log sum of heights in 2015 for each city using parameter estimates in (34). We then select the 25 cities with the most similar predicted heights above and below each city's prediction. For each city's group of 51, we obtain the 95th percentile ("p95"), or 3rd

[45] Night lights data corresponding to the DMSP satellites are provided by NGDC (2015). The radiance calibrated version of this data, which is available for select years between 1996 and 2011, is used to avoid top-coding complications. The data are available at a 30 arc second ($\approx$ 1km at the equator) spatial resolution.

[46] Night lights data from VIIRS satellites are provided by Elvidge et al. (2021). The data is not top-coded and are available at a 15 arc second ($\approx$ 500m at the equator) spatial resolution.

[47] Annual per-capita GDP (PPP, constant international 2011 $) is obtained from Maddison (2008) and Bolt and van Zanden (2020) To avoid short-term fluctuations in income, data in year t reflects a 7 year moving-average.

[48] The main sources for land area and total population are United Nations (2018) and World Bank (2022).

ranked city-level residual. High p95 values indicate that the city's group includes cities that are well above the world's conditional average.[49] By construction, cities that are predicted to have little heights belong to groups where the least constrained cities do not have measurably more heights than the world's conditional average. Cities that are predicted to have a lot of heights also belong to relatively homogeneous groups in terms of heights. Cities with the largest height fundamentals all have similar height stocks, *ceteris paribus*, meaning that their height gaps are relatively low. Larger differences can be observed for cities with intermediate height predictions. Such cities disproportionately belong to developing economies, where more varied patterns of vertical development can be observed within a group of otherwise similar cities.[50]

We calculate the height gap (%) for city ac in the year 2015 using both the actual heights (unlogged) and the counterfactual log heights:

$$Gap_{ac} = \max\left(1 - \frac{Heights_{ac2015}}{\exp(\widehat{LHEIGHTS}_{ac2015})}, 0\right),$$

where $\widehat{LHEIGHTS}_{ac2015}$ is predicted log heights for city ac in 2015. A gap of 20% means that the city has built 80% of what the p95 city in the city's group has built despite sharing similar economic conditions. Cities with residuals above the p95 value have their gaps set to 0%. The median gap is 0%, reflecting the many small cities in our data whose fundamentals do not justify tall buildings. However, the distribution has a thick right tail driven by larger cities. The mean and standard deviation are 24% and 41%, respectively. Weighting by city population, the median is 66%, the mean 50%, and the standard deviation 45%.

Among the 100 largest cities in the world, we obtain gaps of 0% for cities including Chicago, Kuala Lumpur, Sao Paulo, Seoul, and Shanghai, and gaps of 11% for Guangzhou, 26% for New York, 37% for Ho Chi Minh City, and 45% for Miami. We obtain larger gaps of 66% for Bangkok, Paris, London, and Mexico City, 73% for Beijing, 80% for Buenos Aires, 91% for Karachi, and 93% for Cairo. Sensible differences are obtained within the US. Lower-gap large cities include Chicago (0%), New York (26%) and Miami (45%). Higher-gap large cities include Boston (70%), Los Angeles (82%), Washington DC (86%) and San Francisco (94%). Lastly, to compute global or regional gaps, we use 2015 city populations as weights. We find a global gap of 50%.

C Model

C.1 Equilibrium solver

Values of endogenous objects $\{y, \bar{U}\}$, parameters $\{\alpha^U, \beta, \omega^U, \theta^U, \tau^U, \underline{x}^U, \bar{a}^U, \tilde{c}^U, \bar{S}^U, r^a, \zeta, \ell, \tilde{U}\}$, and the endowment $\bar{N}$ deliver a unique mapping to all other endogenous objects. To solve for these equilibrium values, we implement Algorithm 1.

[49] We use p95 instead of the max or p99 to allow for the possibility that 2 cities in each group may have a lot of heights due to idiosyncratic city-specific factors rather than laissez-faire planning regulations. For example, they may have a large government sector or developers with interests in marquee skyscrapers that are not justified by city fundamentals.

[50] Similar relationships are obtained when excluding Chinese and Middle Eastern cities (unreported).

Algorithm 1: Equilibrium solver

Data: Given values for primitives $\{\alpha^U, \beta, \omega^U, \theta^U, \tau^U, \underline{x}^U, \bar{a}^U, \tilde{c}^U, \bar{S}^U, r^a, \zeta, \ell, \bar{N}, \tilde{U}\}$
Guesses of equilibrium values of $\{\bar{U}, y\}$

while $\bar{U} \neq \widehat{\bar{U}}$ *or* $y \neq \hat{y}$ **do**
- Compute N using Eq. (12)
- Compute $\bar{p}^U(x)$ using Eqs. (15) & (19)
- Compute $\tilde{S}^U(x)$ using Eq. (21)
- Compute $r^U(x)$ using Eq. (22)
- Allocate land to use with the highest land rent
- Compute market-clearing wage $\hat{y}$ using Eqs. (20) and (23)
- Compute endogenous city-utility $\widehat{\bar{U}}$ using Eq. (26)
- Update guesses to weighted combination of old guesses and $\{\widehat{\bar{U}}, \hat{y}\}$

Result: Equilibrium values of $\{\bar{U}, y\}$

C.2 Quantification

C.2.1 Amenity decay (τ^U)

In the absence of binding height limits, we can use equations (3) and (14) or (18) to obtain the structural equation for building height by use at each location $x > \underline{x}^U$:

$$\ln S^U(x) = \frac{1}{(1-\alpha^U)(\theta^U - \omega^U)} k^U - \frac{1}{\theta^U - \omega^U} \ln\left[c^U(1+\theta^U)\right] - \frac{\tau^U}{(1-\alpha^U)(\theta^U - \omega^U)} x,$$

where $k^R = \ln \frac{\alpha \bar{R} y}{\bar{U}}$ and $k^C = \ln \frac{\bar{\alpha}^C N^\beta}{y^{\alpha^C}}$. This equation motivates the following reduced form building type-specific log-linear regression specification that has been used to estimate various price and density gradients:

$$\ln S^U_{ib} = \mathcal{G}^U_0 + \mathcal{G}^U_1 DIST_{ib} + \mathcal{E}^U_{ib}$$

$DIST_{ib}$ is the distance from building i in distance ring b to the city center and $\mathcal{E}^U_{ib}$ is a residual term that captures deviations in observed height from a smooth gradient. It is straightforward to recover the amenity decay from an estimate of the reduced-form parameters $\mathcal{G}^U$:

$$\tau^U = -\mathcal{G}^U(1-\alpha^U)(\theta^U - \omega^U)$$

To estimate $\mathcal{G}^U$, we use the number of stories for all commercial or residential buildings within 10 km of the Chicago city center, excluding industrial and government buildings. We define the city center as the average location of the tallest 5 commercial buildings in the city. We use the CoreLogic property assessment data set from 2021/22. We weight by the inverse of the number of observations in each 250 m wide distance ring bin b, giving each bin equal weight in the regressions. We choose Chicago as our case in point because it is arguably the stereotype of an unconstrained, monocentric city that conforms to our land-use model. From the unreported height gradient estimates, we infer the values of our structural parameters $\tau^C = 0.014$ and $\tau^R = 0.016$.

Since we are interested in the degree to which the height gradients estimated for Chicago generalize to other cities, we also examine urban structure in a broader set of height unconstrained global cities. We thus make use of a global 80X80 m raster data set of remote-

sensed building volumes (Esch et al., 2023). We include cities with height gaps below 50% (see Section 3.4 for calculation of height gaps) and with populations of at least 1 million in 2015. This gives us 39 cities in developing economies and 11 cities in developed economies (incl. Chicago).

Since the volume data does not distinguish between commercial and residential uses, we exploit our model's prediction of a change in the slope of the height gradient at the border between the commercial and the residential zones. Therefore, for each of the 50 selected cities, we estimate the following piece-wise linear spline specification with one endogenous knot:

$$\ln FAR_b = \mathcal{B}_0 + \mathcal{B}_1 DIST_b + (\mathcal{B}_2 - \mathcal{B}_1)(DIST_b - \mathcal{K}_1)\mathbb{1}(DIST_b \geq \mathcal{K}_1) + \mathcal{E}_b$$

FAR_b is the total building volume divided by land area across all 80X80 m pixels in city center distance ring b out to 10 km. Each distance $DIST_b$ is 250 m wide. Therefore, the outcome measure is close to a floor area ratio (FAR) measure of building density, though the denominator includes area of land in all uses (including roads and parks). For each of the 50 cities, we identify the city center location using information on lights at night and the tallest buildings in each city. $\mathcal{K}_1$ gives the distance from the endogenous knot to the city center, $\mathcal{B}_1$ is the height gradient for $DIST_b < \mathcal{K}_1$ and $\mathcal{B}_2$ is the gradient when $DIST_b \geq \mathcal{K}_1$. We use non-linear least squares to estimate $\{\mathcal{B}_0, \mathcal{B}_1, \mathcal{B}_2, \mathcal{K}_1\}$ for each city. Chicago's internal structure is not an outlier. Within the building volume data, Chicago's overall gradient, knot location and location-specific gradients are close to the mean and the mode across these 50 cities (unreported).

C.2.2 Rural utility

We treat rural utility, $\tilde{U}$, as a fundamental that we can invert for given values of other primitives and an observed or user-specified urban population share, μ, using Algorithm 2.

Algorithm 2: $\tilde{U}$ inverter

Data: Given values of primitives $\{\alpha^U, \beta, \omega^U, \theta^U, \tau^U, \underline{x}^U, \bar{a}^U, \tilde{c}^U, \bar{S}^U, r^a, \zeta, \ell, \bar{N}\}$
Guess of $\tilde{U}$
User-chosen μ

while $\tilde{U} \neq \widehat{\tilde{U}}$ **do**
- Compute $\bar{U}$ using Algorithm 1
- Compute rural utility, $\widehat{\tilde{U}}$, using Eq. (12)
- Update guess of $\tilde{U}$ to weighted combination of old guess and $\widehat{\tilde{U}}$

Result: $\tilde{U}$ that rationalizes given μ

C.2.3 Preference heterogeneity

We need the value of ζ under which the model generates our key empirical moments. These are estimates of the height elasticity of population, $\hat{\beta}^N$, and the height elasticity of area, $\hat{\beta}^{\mathcal{L}}$. Our identification strategy exploits subsoil geography to ensure that we identify these parameters from variation in the cost of height, holding demand factors constant. Since we have full control over the data-generating process, it is straightforward to mimic this source of variation in the model.

To this end, we solve the model multiple times for values of $\theta \in \Theta$, where $\theta^C = \theta$ and $\theta^R = \theta + 0.05$ to maintain the same difference between the commercial and residential height

elasticity as in the baseline specification in Table 5. We obtain differences in equilibrium outcomes that are solely driven by variations in the cost of height. To operationalize our SMM approach, we nest this loop over $\theta \in \Theta$ within a search over a parameter space defined by $\zeta \in \mathcal{Z}$ and $\mathcal{T} \in \mathcal{R}$. We invert $\tilde{U}$ each time we adjust ζ, setting $\mu = \bar{\mu}$ and all parameters to the values in Table 5 to keep the city population constant. For each combination of $\{\theta, \zeta, \mathcal{T}\}$, we solve the model and compute (the endogenous outcomes) city area

$$\mathcal{L}_\theta^{\zeta,\mathcal{T}} = \int_0^{(x_1)^{\theta,\zeta,\mathcal{T}}} \mathcal{L}(x)dx,$$

city population

$$N_\theta^{\zeta,\mathcal{T}} = \int_{(x_0)^{\theta,\zeta,\mathcal{T}}}^{(x_1)^{\theta,\zeta,\mathcal{T}}} (n(x))^{\theta,\zeta} dx,$$

and city tall building height

$$H_\theta^{\zeta,\mathcal{T}} = \int_0^{(x_1)^{\theta,\zeta,\mathcal{T}}} \mathcal{L}(x) \left((S^C(x))^{\theta,\zeta} - \mathcal{T} \right) dx + \int_{(x_0)^{\theta,\zeta,\mathcal{T}}}^{(x_1)^{\theta,\zeta,\mathcal{T}}} \mathcal{L}(x) \left((S^R(x))^{\theta,\zeta} - \mathcal{T} \right) dx. \tag{35}$$

For each combination of $\{\zeta, \mathcal{T}\}$, we run the following regressions on the model-based outcomes to recover our moments in the model $\{\tilde{\beta}^N, \tilde{\beta}^{\mathcal{L}}\}$:

$$\ln \mathcal{L}_\theta^{\zeta,\mathcal{T}} = c^{\mathcal{L},\zeta,\mathcal{T}} + \tilde{\beta}_{\zeta,\mathcal{T}}^{\mathcal{L}} \ln H_\theta^{\zeta,\mathcal{T}} + \tilde{\epsilon}_\theta^{\mathcal{L},\zeta,\mathcal{T}}$$
$$\ln N_\theta^{\zeta,\mathcal{T}} = c^{N,\zeta,\mathcal{T}} + \tilde{\beta}_{\zeta,\mathcal{T}}^{N} \ln H_\theta^{\zeta,\mathcal{T}} + \tilde{\epsilon}_\theta^{N,\zeta,\mathcal{T}}$$

We find our preferred combination of $\{\zeta, \mathcal{T}\}$ by minimizing the value of the residual sum of squares of the moments in model and data:

$$\zeta, \mathcal{T} = \arg \min_{\zeta \in \mathcal{Z}, \mathcal{T} \in \mathcal{R}} \sum_{o \in N, \mathcal{L}} \left(\hat{\beta}^o - \tilde{\beta}^o \right)^2 \tag{36}$$

We provide a compact summary of the procedure using pseudo code Algorithm 3.

Algorithm 3: Calibrating $\{\zeta, \mathcal{T}\}$

Data: Given values of primitives $\{\alpha^U, \beta, \omega^U, \theta^U, \tau^U, \underline{x}^U, \bar{a}^U, \tilde{c}^U, \bar{S}^U, r^a, \zeta, \ell, \bar{N}\}$
Moments in data $\{\widehat{\beta}^N, \widehat{\beta}^{\mathcal{L}}\}$
User-chosen μ

foreach $\zeta \in \mathcal{Z}$ **do**
  Use Algorithm 2 to invert $\tilde{U}$ so to match $\mu = 0.5 (\Rightarrow) N = \mu \bar{N} = 3M)$ under baseline values of $\{\theta^C = 0.5, \theta^R = 0.55\}$
  foreach $\mathcal{T} \in \mathcal{R}$ **do**
    foreach $\theta \in \Theta$ **do**
      Use Algorithm 1 to solve for equilibrium outcomes of $\{\mathcal{L}_\theta^{\zeta,\mathcal{T}}, N_\theta^{\zeta,\mathcal{T}}, H_\theta^{\zeta,\mathcal{T}}\}$
    foreach $o \in N, \mathcal{L}$ **do**
      Regress $\ln o_\theta^{\zeta,\mathcal{T}}$ against $\ln H_\theta^{\zeta,\mathcal{T}}$ to obtain model moment $\tilde{\beta}^o$
Use moments in data $\{\widehat{\beta}^N, \widehat{\beta}^{\mathcal{L}}\}$ and model $\{\tilde{\beta}^N, \tilde{\beta}^{\mathcal{T}}\}$ in Eq. (36) to find $\{\zeta, \mathcal{T}\}$

Result: $\{\zeta, \mathcal{L}\}$ values that match moments in model and data

Guided by Figure A4, we define a grid of height costs $\Theta = \{0.2, 0.3, ..., 1\}$ and set $\bar{\mu} = 0.5$. For the moments in the data, we use $\hat{\beta}^N = 0.21$ and $\hat{\beta}^{\mathcal{L}} = -0.38$ estimated from a subset of cities that are relatively unconstrained by height regulation (col. (3) of Table 4). Under $\zeta = 3.3$ and $\mathcal{T} = 3.0$, we almost exactly match the moments. There is a clearly defined minimum in the objective function at our identified value of ζ (not shown). In contrast, the choice of $\mathcal{T}$ is less consequential. As long as $\mathcal{T} \geq 3.0$, the model generates height elasticities that are close to those estimated from data.

It is plausible that we obtain the best fit under a value of $\mathcal{T} = 3$ ($\sim$ 15 m) that is smaller than the bottom-coding in the data (55 m). To see this, consider that the model generates an average height of 14 floors (55 m). Setting $\mathcal{T} = 15$, we would generate a tall building height measure in the model of $H = 0$. In reality, we would most likely observe a positive value for H because the mean height of 55 m would be generated by a mix of taller and shorter buildings.

C.3 Welfare calculations

Algorithm 4 describes the numerical procedure used to compute welfare effects for cities of a given cost of height, population, and height gap.

Algorithm 4: Welfare effects

Data: Given values of primitives $\{\alpha^U, \beta, \omega^U, \tau^U, \underline{x}^U, \bar{a}^U, \tilde{c}^U, \bar{S}^U, r^a, \zeta, \ell, \bar{N}, \mathcal{T}\}$
City population, Pop_a, observed in data
Height gap, HG_a, observed in data
Bedrock depth, MBD_a, observed in data

Use MBA_a and non-linear mapping in Figure A4 to obtain cost of height, θ_a^C
Set $\theta_A^R = \theta_a^C + 0.05$
Set height limit in model to $\bar{S}^U = \mathcal{T}$
while *Height gap in model,* $\tilde{HG} < HG_a$ **do**
    Use Algorithm 2 to invert rural utility, $\tilde{U}$, that satisfies $\mu\bar{N} = Pop_a$
    Use Eq. (35) to compute constrained tall building height H
    Use Algorithm 1 to solve for counterfactual under no height limit, $\bar{S} = \infty$
    Use Eq. (35) to compute unconstrained tall building height H^*
    Compute $\tilde{HG} = \frac{H}{H^*} - 1$
    Marginally increase height limit in model, $\bar{S}$
Use Algorithm 1 to solve for $\mathcal{W}^{actual}$, where $\mathcal{W} \in \{\mathcal{V}, \mathcal{R}\}$, under calibrated height limit $\bar{S}$
Use Algorithm 1 to solve for welfare $\mathcal{W}^{ban}$ under counterfactual height limit $\bar{S} = \mathcal{T}$
Use Algorithm 1 to solve for welfare $\mathcal{W}^{market}$ under counterfactual height limit $\bar{S} = \infty$
Compute welfare effect of existing tall buildings $\hat{\mathcal{W}}^{actual} = \frac{\mathcal{W}^{actual}}{\mathcal{W}^{ban}} - 1$
Compute welfare potential of tall buildings $\hat{\mathcal{W}}^{potential} = \frac{\mathcal{V}^{market}}{\mathcal{W}^{ban}} - 1$
Compute welfare effect of existing height regulation $\hat{\mathcal{W}}^{regulation} = \frac{\mathcal{V}^{actual}}{\mathcal{W}^{market}} - 1$

Result: Effects of existing tall buildings, all potential tall buildings, and height limits on expected utility $\{\hat{\mathcal{V}}_a^{actual}, \hat{\mathcal{V}}_a^{potential}, \hat{\mathcal{V}}_a^{regulation}\}$ and land rent $\{\hat{\mathcal{R}}_a^{actual}, \hat{\mathcal{R}}_a^{potential}, \hat{\mathcal{R}}_a^{regulation}\}$ for city a

Appendix References

Ahlfeldt, Gabriel M. and Jason Barr, "The economics of skyscrapers: A synthesis," *Journal of Urban Economics*, 5 2022, *129*, 103419.

Barr, Jason and Remi Jedwab, "Exciting, boring, and nonexistent skylines: Vertical building gaps in global perspective," *Real Estate Economics*, 2023.

Bolt, Jutta and Jan Luiten van Zanden, *Maddison style estimates of the evolution of the world economy. A new 2020 update* 2020.

Davis, Neil N, Jake Badger, Andrea N Hahmann, Brian O Hansen, Niels G Mortensen, Mark Kelly, Xiaoli G Larsén, Bjarke T Olsen, Rogier Floors, Gil Lizcano et al., "The Global Wind Atlas: A high-resolution dataset of climatologies and associated web-based application," *Bulletin of the American Meteorological Society*, 2023, *104* (8), E1507–E1525.

Elvidge, Christopher D., Mikhail Zhizhin, Tilottama Ghosh, Feng-Chi Hsu, and Jay Taneja, "Annual Time Series of Global VIIRS Nighttime Lights Derived from Monthly Averages: 2012 to 2019," *Remote Sensing*, 2021, *13* (5).

Esch, Thomas, Klaus Deininger, Remi Jedwab, and Daniela Palacios-Lopez, "Outward and Upward Construction: A 3D Analysis of the Global Building Stock," Working Papers 2023-09, The George Washington University, Institute for International Economic Policy September 2023.

Gendron-Carrier, Nicolas, Marco Gonzalez-Navarro, Stefano Polloni, and Matthew A. Turner, "Subways and Urban Air Pollution," *American Economic Journal: Applied Economics*, January 2022, *14* (1), 164–196.

Giardini, D, G Grunthal, KM Shedlock, and Zhang P, "The GSHAP Global Seismic Hazard Map," *Ann. Geophys.*, 1999, *42* (6).

GMTED, *GMTED2010 Global Grids* 2010.

Gonzalez-Navarro, Marco and Matthew A Turner, "Subways and urban growth: Evidence from earth," *Journal of Urban Economics*, 2018, *108*, 85–106.

Henderson, Daniel J. and Christopher F. Parmeter, *Applied Nonparametric Re- gression* 2015.

Lujala, Päivi, Jan Ketil R d, and Nadja Thieme, "Fighting over oil: Introducing a new dataset," *Conflict Management and Peace Science*, 2007, *24* (3), 239–256.

Maddison, Angus, *Statistics on World Population, GDP and Per Capita GDP, 1-2008 AD* 2008.

NGDC, *Global Radiance Calibrated Nighttime Lights* 2015.

Schneider, Julia M, Florian Zabel, and Wolfram Mauser, "Global inventory of suitable, cultivable and available cropland under different scenarios and policies," *Scientific Data*, 2022, *9* (1), 527.

United Nations, *World Urbanization Prospects: The 2018 Revision* 2018.

USGS, "Major mineral deposits of the world," 2023.

Wessel, Pål and Walter HF Smith, "A global, self-consistent, hierarchical, high-resolution shoreline database," *Journal of Geophysical Research: Solid Earth*, 1996, *101* (B4), 8741–8743.

World Bank, *World Development Indicators* 2022.

Figure A1: Trends in Construction Costs by Height: U.S.

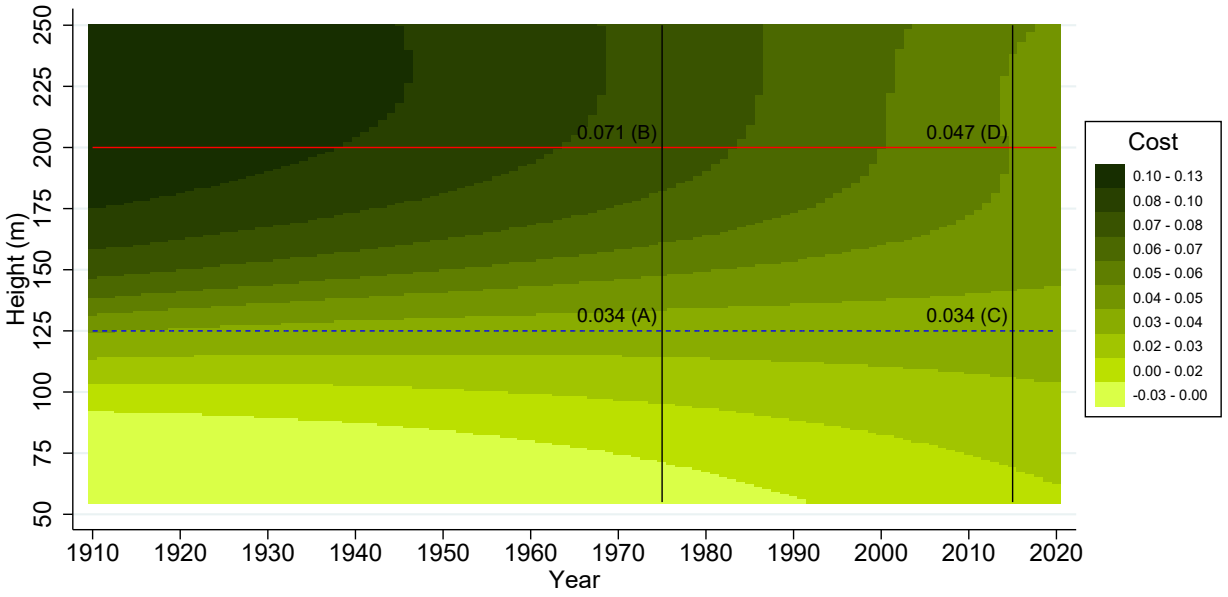

Notes: The sample includes 591 tall buildings in 93 U.S. cities built 1902-2021. The mean height is 102 m on a mean bedrock depth of 20 m. "Cost" is the log cost per floor area, residualized for city FE and decade of construction FE. It has a standard deviation of 0.53. Overall log construction cost has a mean of 7.05 and standard deviation of 1.20. We use locally weighted regressions with a bivariate Gaussian kernel to estimate local means of the residualized cost measure within the height-bedrock plane with a bandwidth parameter for both covariates of $\kappa = 50$. Regressing log construction cost per floor area on log height, year, and the interaction yields a coefficient on the interaction of -0.006.

Figure A2: Schematic Diagram of Bedrock Depth and Tall Building Foundations

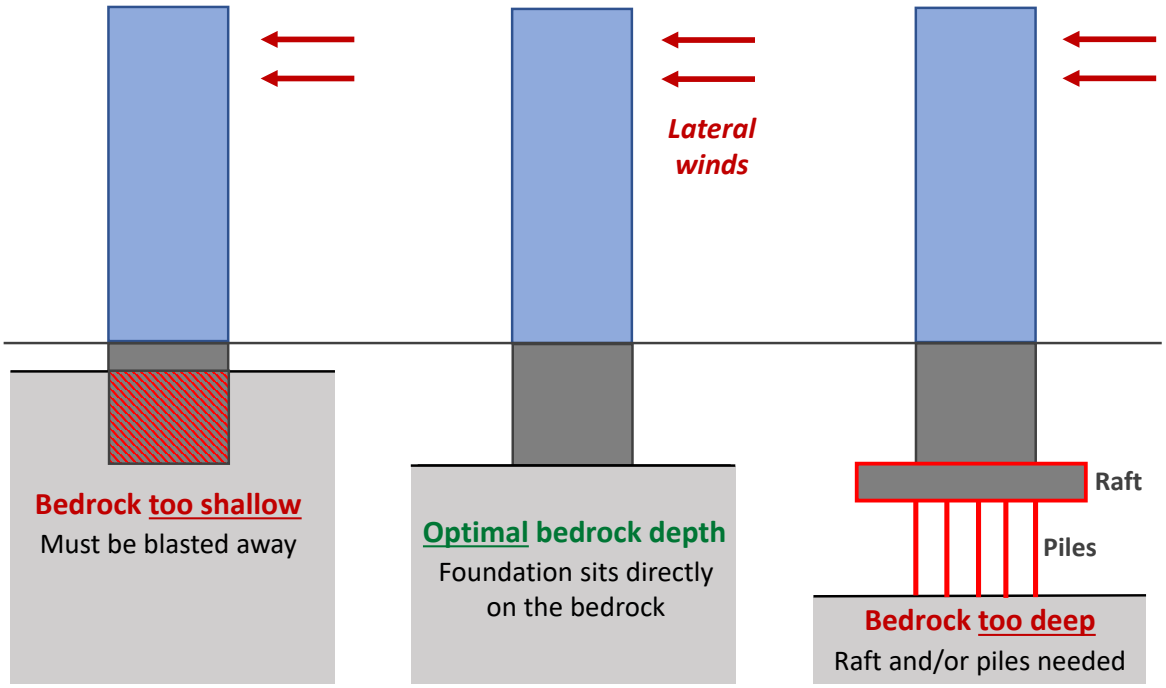

Figure A3: Construction Cost as a Function of Height and Bedrock Depth

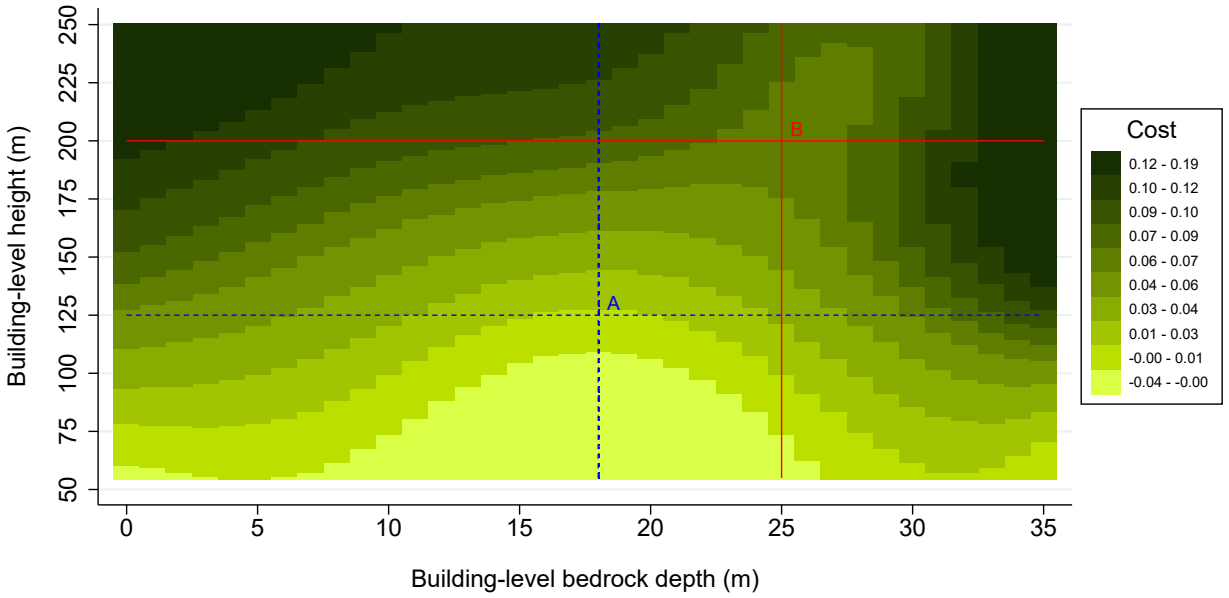

Notes: The sample includes 1,033 tall buildings in 206 world cities and 55 countries built through year 2021. The mean construction year is 1995, the mean height is 113 meters, and the mean bedrock depth is 20. Most are concrete buildings. "Cost" is the log cost per floor area residualized for city fixed effects and country-by-decade of construction fixed effects. It has a standard deviation of 0.85. The mean log construction cost is 7.12 with a standard deviation of 1.58. Locally weighted regressions with a bivariate Gaussian kernel are used to estimate local means of the residualized cost measure within the height-bedrock plane. We set the bandwidth parameter for bedrock, b, to $\kappa^b = 6$ and for building height, h, to $\kappa^h = 40$, which corresponds to about one third of the standard deviation of each respective covariate. We topcode height at the upper limit on the graph, so 250 m includes all buildings of at least 250 m.

Figure A4: Estimated Cost of Height as a Function of Bedrock Depth

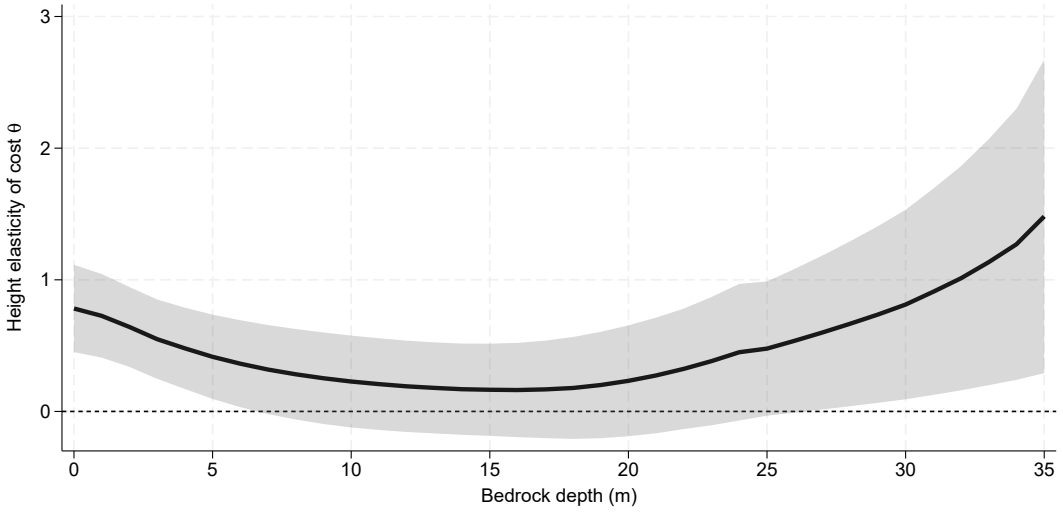

Notes: The plot shows non-parametric estimates of the cost of height using the LWR-IV approach explained in Section A.4. In each LWR, we estimate the height elasticity from a regression of the log of construction cost per floor area on building height, controlling for city fixed effects and country by decade of construction effects. The sample consists of 785 tall buildings in 118 cities and 6 countries. We drop countries with fewer than 25 observations to obtain more precise estimates. We use distance from the city center as an instrumental variable for height to remove the effects of unobserved factors that affect construction cost (such as ruggedness) that could be correlated with bedrock depth. The city center is defined as the median coordinate of buildings exceeding 100 meters, or the location of the tallest building if no building exceeds 100 meters. The median first-stage F-statistic is 10.4. We use a Gaussian kernel with a locally varying bandwidth that is inversely related to the density of observations. Confidence bands are at the 95% level.

Figure A5: Effects of Heights by Country Tall Building Residential Share

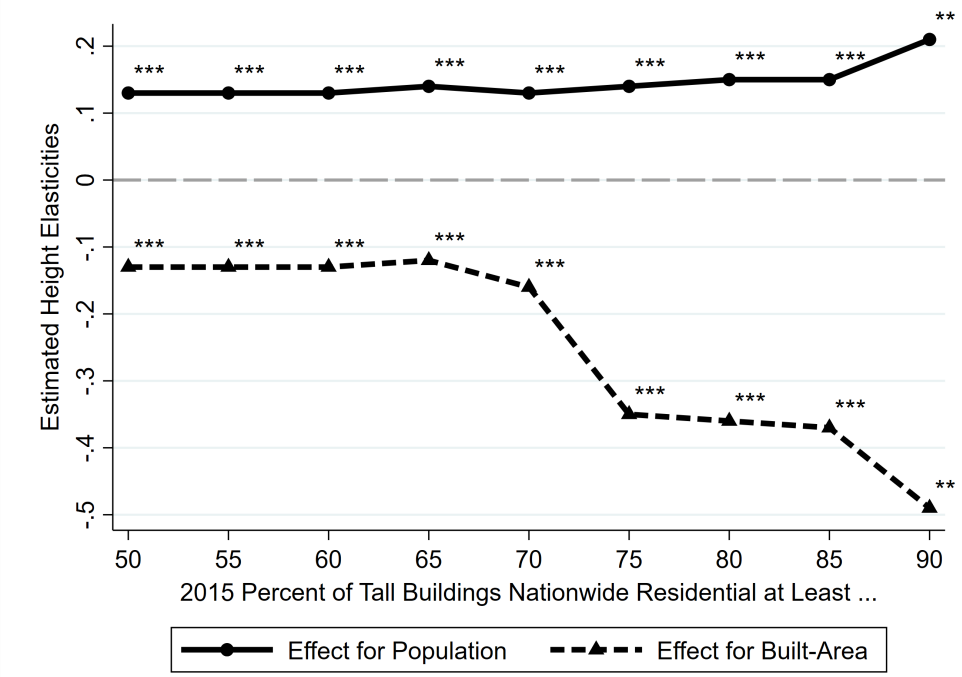

Notes: This figure shows two sets of estimated coefficients on the change in log heights in IV regressions of the form in (7). The top portion of the graph indicates coefficients for which the 1975-2015 change in log population is the outcome ("Effect for Population"). The outcome in the bottom half of the graph is 1975-2015 change in log city built area ("Effect for Built-Up Area"). Moving from left to right, the sample becomes increasingly constrained to include only developing economies with at least the fraction of tall buildings nationwide in 2015 residential use indicated on the horizontal axis.

Table A1: Summary Statistics

	All Developing Countries		Large Cities Only	
	Mean	Std Dev	Mean	Std Dev
ln pop 1975	11.63	0.65	14.50	0.61
Δ ln pop, 1975-2015	0.50	0.39	0.58	0.69
Δ ln built area, 1975-2015	0.58	0.51	0.67	0.52
Fraction with tall buildings, 1975	0.01	0.10	0.35	0.48
Δ Fraction 1975-2015	0.04	0.20	0.46	0.50
ln(Heights+1), 1975	0.05	0.56	2.10	3.03
Δ ln(Heights+1) 1975-2015	0.27	1.28	4.59	3.44
Mean Bedrock Depth	15.73	15.81	20.86	17.37

Notes: Means and standard deviations are shown for the 11,269 cities in developing countries that make up our primary sample. Also shown in the last two columns are summary statistics for the 168 "large" developing country cities with over 1 million inhabitants in 1975.

Table A2: First Stage Estimates: Remaining Coefficients

Period for Dep. Var.	1975-2015				1975	2015
	(1)		(2)	(3)	(4)	(5)
Interaction Variable =	1975 Large CityDummy	1975 Small CityDummy	1975 Large CityDummy	ln 1975 CityPop	ln 1975 CityPop	ln 1975 CityPop
M Variable =	1975 Small CityDummy	1975 Large CityDummy	-	-	-	-
			-	-	-	-
Bedrock*M Variable	-0.0012***	-0.0069**	-0.0013	-0.3064***	-0.0353	-0.3417***
	[0.0003]	[0.0028]	[0.0011]	[0.0638]	[0.0323]	[0.0687]
Bedrock^2*M Variable	0.0000***	0.0000**	0.0000	0.0020**	0.0005*	0.0025**
	[0.0000]	[0.0000]	[0.0000]	[0.0009]	[0.0003]	[0.0010]
Large City Dummy	3.4397***	-0.1948***	1.4148***			
	[0.4965]	[0.0523]	[0.5069]			
ln 1975 City Pop.			0.6086***	0.5208***	0.2998***	0.8206***
			[0.0365]	[0.0674]	[0.0477]	[0.0804]
1975 Large City Dummy	Yes	Yes	Yes	No	No	No
ln 1975 City Population	No	No	Yes	Yes	Yes	Yes
Bedrock, Bedrock^2	No	No	Yes	Yes	Yes	Yes
Country Fixed Effects	Yes	Yes	Yes	Yes	Yes	Yes

Notes: This table reports remaining first stage coefficients associated with each regression in Panel A of Table 1. The dependent variable in column ((1))) is Δ ln(Heights+1) interacted with the indicated interaction variable. The dependent variable in columns (2)-(3) is Δ ln(Heights+1). The dependent variables in the final two columns are ln(Heights+1) in 1975 and 2015, respectively. See the notes to Table 1 for further details about each specification.

Table A3: Main IV and OLS Results: Remaining Coefficients

Period s-t:	Δ ln Pop 1975-2015	Δ ln Built Area 1975-2015	Δ ln Urban. Area 1975-2015	Δ ln Pop Dens. 1975-2015	Δ ln Lights 1990-2015
			Panel A: IV Estimates		
ln Initial Pop s	-0.12***	0.24***	-0.68***	0.56***	-0.15***
	[0.03]	[0.03]	[0.06]	[0.04]	[0.04]
Bedrock Depth	0.00***	0.00***	0.02***	-0.02***	0.00**
	[0.00]	[0.00]	[0.00]	[0.00]	[0.00]
Bedrock Depth^2	-0.00	-0.00**	-0.00***	0.00***	-0.00
	[0.00]	[0.00]	[0.00]	[0.00]	[0.00]
			Panel B: OLS Estimates		
ln Initial Pop s	-0.10***	0.14***	-0.92***	0.82***	-0.09***
	[0.01]	[0.01]	[0.02]	[0.02]	[0.01]
Bedrock Depth	0.00***	0.00***	0.02***	-0.02***	0.00**
	[0.00]	[0.00]	[0.00]	[0.00]	[0.00]
Bedrock Depth^2	-0.00	-0.00***	-0.00***	0.00***	-0.00
	[0.00]	[0.00]	[0.00]	[0.00]	[0.00]
R-squared	0.08	0.04	0.24	0.23	0.01

Notes: This table shows coefficients on control variables for regressions in Table 3.

Table A4: Alternative Heights (H) Measures: IV Estimates

H Growth Measure	$1(\Delta H>0)$	Δln(H+1)		Δln(H+55)	Δasinh(H)		Δasinh(H/1000)	
				Panel A: Δ ln Pop				
Heights (H) Growth	1.16***	0.13***	0.09**	0.24***	0.12***	0.08**	0.40***	0.27***
	[0.32]	[0.03]	[0.04]	[0.05]	[0.03]	[0.04]	[0.09]	[0.10]
				Panel B: Δ ln Built Area				
Heights (H) Growth	-1.43***	-0.16***	-0.13***	-0.29***	-0.15***	-0.12***	-0.48***	-0.40***
	[0.42]	[0.04]	[0.05]	[0.07]	[0.04]	[0.04]	[0.12]	[0.14]
Observations	11,257	11,257	1,528	11,257	11,257	1,528	11,257	1,528
First Stage F	13.22	20.76	20.23	19.33	22.51	18.25	12.04	9.58
SD of H Growth	0.20	0.99	2.66	0.61	1.40	2.90	0.35	0.86
Min Pop 1975 (,000)	0	0	150	0	0	150	0	150
Min Height	55	100	55	55	55	55	55	55

Notes: Results are analogous to those in Table 3, except for the heights measure and sample. Equation (7) shows the regression specification used. Each column uses the measure of heights growth indicated in the top row. The first column shows extensive margin results. "H" and "Heights" in column headers both indicate city aggregate heights in meters.

Table A5: Bedrock Quality Instruments: Local Identification

	Δ ln(H+1)	Δ ln Pop 1975-2015			Δ ln Built Area 1975-2015		
Bedrock for IV:	Both	Both	Shallow	Deep	Both	Shallow	Deep
	(1)	(2)	(3)	(4)	(5)	(6)	(7)
Δ Log Height (H) 1975-2015		0.158***	0.172***	0.159***	-0.216***	-0.352***	-0.229***
		(0.029)	(0.048)	(0.029)	(0.042)	(0.090)	(0.042)
$Bedrock^{deep}$*ln Pop 1975	0.043***		-0.001			0.005*	
	(0.006)		(0.002)			(0.003)	
$Bedrock^{shallow}$*ln Pop 1975	0.033***			0.000			-0.004**
	(0.008)			(0.001)			(0.002)
First Stage F-stat	-	26.6	18.5	53.0	26.6	18.5	53.0

Notes: N = 11,269 observations. Specifications are analogous to those in Tables 1 and 3, except that the quadratic in mean bedrock depth is replaced by a linear spline in mean bedrock depth. Regression in (1) is the first stage for the IV regressions in (2) and (5). Regressions in (3) and (6) use variation within shallow bedrock (up to 20 meters) and those in (4) and (7) use variation within deep bedrock (beyond 20 meters) only for identification. Robust standard errors in parenthesis. The R-squared for the first stage regression in the first column is 0.30.

Table A6: Robustness Checks on Functional Form

	Δ ln Population (Pop)			ln Pop	Δ ln Built Area (BA)			ln BA
Period:	1975-2015	1975-2015	1990-2015	2015	1975-2015	1975-2015	1990-2015	2015
Test:	Bedrock Vars in IV	Built Area Ctrl 1975	Pop 1975 in IV	Cross Section	Bedrock Vars in IV	Built Area Ctrl 1975	Pop 1975 in IV	Cross Section
Δln(Heights+1)	0.13***	0.07***	0.09***		-0.16***	-0.11***	-0.23***	
	[0.03]	[0.03]	[0.03]		[0.04]	[0.04]	[0.05]	
$\ln(\text{Heights}+1)_{2015}$				0.13***				-0.12***
				[0.03]				[0.04]
First Stage F-Stat	18.53	18.92	14.57	19.91	18.53	18.92	14.57	16.31

Notes: Specifications match those in Table 3 except as indicated. (1) and (5) "Bedrock Vars in IV": Mean bedrock depths and its square enter as instruments instead of as controls. (2) and (6) "Built Area Ctrl 1975": Additional control for log city built area in 1975 (in addition to log city population in 1975). (3) and (7) "Pop 1975 in IV": 1990 is the base year though instruments are constructed using log city population in 1975. (4) and (8) "Cross Section ": Dependent variables and heights are for 2015 only. Instruments are constructed using log city population size in 1975. Column (8) includes an additional control for log city built area in 1975. Robust standard errors in brackets.

Table A7: Analysis of Building Volumes

Tall Building Volumes ≥ ..... (meters)	40	40	55	55	0
	Panel A: ln 2015 City Tall Building Volumes				
ln(2015 Heights+1) (α)	0.93***		2.87***		-0.26***
	[0.24]		[0.32]		[0.08]
First Stage F-Stat	19.91		19.91		19.91
	Panel B: ln 2015 City Population				
ln(2015 Tall Building Volumes+1) (β)	0.13***	0.13***	0.04***	0.05***	-0.46***
	[0.03]	[0.03]	[0.01]	[0.01]	[0.18]
ln(2015 Short Building Volumes+1)		0.01		0.07***	
		[0.02]		[0.01]	
Product of α and β	0.12	0.12	0.11	0.14	0.12
First Stage F-Stat	8.34	10.97	51.45	52.55	7.36
	Panel C: ln 2015 City Built Area				
ln(2015 Tall Building Volumes+1) (γ)	-0.16***	-0.11***	-0.06***	-0.04***	0.60***
	[0.05]	[0.03]	[0.01]	[0.01]	[0.15]
ln(2015 Short Building Volumes+1)		0.17***		0.12***	
		[0.02]		[0.01]	
Product of α and γ	-0.15	-0.10	-0.17	-0.11	-0.16
First Stage F-Stat	8.34	10.97	51.45	52.55	7.36

Notes: Each entry shows one coefficient and robust standard error from an IV regression of the variable indicated in the panel header on the variable indicated at left, ln 1975 city population, bedrock depth, bedrock depth squared, and country fixed effects, matching Table 1 Specification (5). Dependent variables in Panel A and predictor variables in Panels B and C are total 2015 city volumes for 80X80 meter pixels with heights of at least the threshold indicated in the top row (0, 40 or 55 meters). "Short Building Volumes" indicate the total volume of remaining pixels in the city. A quadratic in bedrock depth interacted with 1975 city population instruments for the predictor variable in all regressions. Robust standard errors in brackets.

Table A8: Displacement Effects: Robustness to Different Fixed Effects and Samples

	Panel A: Δ ln Population				
Δ ln Height	0.13***	0.10***	0.16***	0.14***	0.13***
	[0.03]	[0.03]	[0.03]	[0.02]	[0.04]
	Panel B: Δ ln Built Area				
Δ ln Height	-0.16***	-0.21***	-0.25***	-0.22***	-0.08
	[0.04]	[0.05]	[0.04]	[0.03]	[0.05]
Level of FE	Baseline	Subregion	Admin 1	Admin 2	Baseline
Sample	Full	Full	Full	Full	<20% Urb
Observations	11,257	11,269	10,606	7,439	4,594
IV F-stat	22.84	20.02	28.96	35.23	9.77

Notes: Results of variants of the baseline empirical specification in Table 3 with the following alternative fixed effects (FE). Subregion: 2018 United Nations Geoscheme, grouping countries into 20 world regions (e.g., South America, Central America, and North America). We do not include country FE. Admin 1: First-level administrative divisions that subdivide countries into large sub-national units (e.g., provinces for China) (1,584 divisions). Admin 2: Second-level administrative divisions that subdivide countries into smaller sub-national units (5,176 divisions). The final column only uses cities that were less than 20% urbanized in 1975 (source: World Urbanization Prospects database of the United Nations).

Table A9: Displacement Effects: Controls for Heights-Based Changes in Market Potential (MP)

	(1)-(5) Δ ln Population					(6)-(10) Δ ln Built Area				
	Panel A: IV for Δ ln(Hgt+1), OLS for Δ ln(MP^H)									
Δln(Hgt+1)	0.13***	0.13***	0.13***	0.13***	0.14***	-0.16***	-0.16***	-0.16***	-0.15***	-0.16***
	[0.03]	[0.03]	[0.03]	[0.03]	[0.03]	[0.04]	[0.04]	[0.04]	[0.04]	[0.04]
Δln(MP^H)	-0.01*	-0.01*	-0.01**	-0.00	0.04***	-0.01	-0.00	0.00	0.04***	0.08***
	[0.00]	[0.00]	[0.00]	[0.00]	[0.00]	[0.00]	[0.00]	[0.00]	[0.00]	[0.01]
1st Stage F	21.88	21.96	22.18	22.59	23.12	21.88	21.96	22.18	22.59	23.12
	Panel B: IV for Δ ln(Hgt+1), IV for Δ ln(MP^H)									
Δ ln(Hgt+1)			0.10***	0.09**	0.18***			-0.13**	-0.09**	-0.14***
			[0.03]	[0.04]	[0.04]			[0.05]	[0.04]	[0.04]
Δ ln(MP^H)			0.14***	0.02	0.08			0.35***	0.17***	0.19***
			[0.04]	[0.02]	[0.06]			[0.07]	[0.03]	[0.07]
1st Stage F			16.83	11.12	13.60			16.83	11.12	13.60
Decay Param	0.33	0.5	1	2	3	0.33	0.5	1	2	3
Country FE	Yes	Yes	Yes	Yes	Yes	Yes	Yes	Yes	Yes	Yes

Notes: Regressions have the same specification as in Table 3, except that we also include the log change in heights-based market potential 1975-2015 (Δ ln(MP^H)). We instrument Δ ln(MP^H) using similarly constructed instruments as for Δ ln(Hgt+1). See the text for details of MP calculation and included controls. Robust standard errors in brackets.

Table A10: Counterfactuals: Illustrative Examples

	20% higher cost of height	Binding height limit	Binding height limit under 20% higher cost of height
Total population	–8.7%	–17.5%	–12.3%
Total area	15.8%	17.7%	8.8%
Average commuting cost	2.6%	8.1%	5.2%
Average residential rent	–0.3%	–14.4%	–10.8%
Average commercial rent	7.7%	2.0%	–2.3%
Average productivity	–0.9%	–5.1%	–4.1%
Wage	–2.5%	–6.7%	–4.7%
Total land value	–0.7%	11.3%	7.8%
Urban utility ($\bar{U}$)	–5.3%	–10.3%	–6.7%
Expected utility ($\mathcal{V}$)	–2.6%	–4.8%	–2.9%

Notes: Scenarios in the first two columns directly correspond to the counterfactuals in the second and third rows of Figure 7. The scenario in the third column shows impacts of imposing a binding height limit on a simulated city that begins at a 20% greater cost of height than the baseline. Averages are weighted by the number of workers.

Table A11: Welfare Effects of Tall Buildings by World Region

World region	Urban pop. (BN)	City characteristics: In cities >1 mill.	City characteristics: Cost of height θ	City characteristics: Est. height gap	Expected utility ($\mathcal{V}$): No tall building	Expected utility ($\mathcal{V}$): No height limit	Agg. land rent ($\mathcal{R}$): No tall building	Agg. land rent ($\mathcal{R}$): No height limit
Africa, G	0.55	34.7%	0.43	47.0%	-0.8%	7.0%	-0.4%	-5.6%
Asia, G	1.95	44.5%	0.59	41.1%	-1.9%	4.1%	-1.2%	-3.6%
Europe, G	0.04	29.2%	0.47	50.7%	-0.9%	1.7%	0.2%	-1.1%
Latin America, G	0.33	52.9%	0.41	61.8%	-2.6%	7.8%	-1.9%	-7.3%
Mean, G	2.87	43.3%	0.54	44.8%	-1.8%	5.3%	-1.0%	-4.8%
Asia, D	0.19	77.2%	0.39	65.1%	-6.3%	17.8%	0.0%	-17.5%
Europe, D	0.25	41.4%	0.32	84.5%	-1.1%	7.9%	-2.9%	-6.5%
LAC, D	0.02	48.6%	0.91	61.8%	-0.7%	2.2%	0.3%	-1.6%
North America, D	0.17	67.4%	0.43	76.4%	-2.6%	10.5%	-3.6%	-9.7%
Oceania, D	0.01	64.2%	0.34	89.2%	-0.6%	11.7%	-0.3%	-7.7%
Mean, D	0.64	59.6%	0.39	75.9%	-3.1%	11.6%	-2.1%	-11.0%
Mean, all	3.51	46.3%	0.51	50.5%	-2.0%	6.4%	-1.2%	-6.0%

Notes: Entries are population-weighted averages across cities in each indicated world region (G = developing economies only; D = developed economies only). Results are analogous to those in Table 6, calculated by world region.

Table A12: Welfare Costs of Limiting Tall Building Construction: Sensitivity Analysis

	ζ	$\mathcal{T}$	Expected utility $\mathcal{V}$: No tall building	Expected utility $\mathcal{V}$: No height limit	Share adj. rent: No tall building	Share adj. rent: No height limit	Agg land rent $\mathcal{R}$: No tall building	Agg land rent $\mathcal{R}$: No height limit
Baseline parameterization	3.3	3.0	-2.0%	6.4%	0.44	0.41	-1.2%	-6.0%
Cost of height 20% lower	3.3	3.0	-2.2%	8.4%	0.45	0.41	-1.7%	-7.9%
Height gap cutoff 75^{th} pctile	3.3	3.0	-3.3%	3.4%	0.42	0.42	-0.4%	-3.6%
Floorspace prod share = 0.10	3.7	3.0	-1.7%	4.7%	0.56	0.55	-0.5%	-5.9%
Floorspace prod share = 0.20	3.1	2.7	-2.1%	5.4%	0.31	0.31	-0.9%	-3.0%
Citywide agglom elas = 0.00	3.6	4.3	-1.0%	2.4%	0.41	0.37	0.3%	-2.8%
Citywide agglom elas = 0.06	2.5	2.4	-3.0%	7.6%	0.43	0.44	-1.2%	-6.5%
Amenity decay 10% higher	3.2	3.2	-1.9%	5.1%	0.42	0.42	-0.6%	-4.5%
Amenity decay 10% lower	3.6	2.7	-1.8%	4.8%	0.41	0.40	-0.8%	-4.1%
Very low ζ (low mobility)	0.1	3.0	-2.9%	5.7%	0.54	0.47	4.6%	-12.2%
Very high ζ (high mobility)	10	3.0	-1.2%	6.7%	0.21	0.36	-4.6%	-2.5%

Notes: Entries are analogous to those in Table 6 for "All Economies" except using indicated alternative parameter values. Entries in "Share adj. rent" columns are fractions of changes in urban utility $\bar{U}$ accounted for through changes in rents and commuting costs.